# A MOLECULAR IMAGING PRIMER: MODALITIES, IMAGING AGENTS, AND APPLICATIONS

## Michelle L. James and Sanjiv S. Gambhir

Molecular Imaging Program at Stanford, Department of Radiology, Bio-X Program, and Departments of Bioengineering and Materials Science & Engineering, Stanford University, Palo Alto, California



**James ML, Gambhir SS.** A Molecular Imaging Primer: Modalities, Imaging Agents, and Applications. *Physiol Rev* 92: 897–965, 2012; doi:10.1152/physrev.00049.2010.— Molecular imaging is revolutionizing the way we study the inner workings of the human body, diagnose diseases, approach drug design, and assess therapies. The field as a whole is making possible the visualization of complex biochemical processes involved in

normal physiology and disease states, in real time, in living cells, tissues, and intact subjects. In this review, we focus specifically on molecular imaging of intact living subjects. We provide a basic primer for those who are new to molecular imaging, and a resource for those involved in the field. We begin by describing classical molecular imaging techniques together with their key strengths and limitations, after which we introduce some of the latest emerging imaging modalities. We provide an overview of the main classes of molecular imaging agents (i.e., small molecules, peptides, aptamers, engineered proteins, and nanoparticles) and cite examples of how molecular imaging is being applied in oncology, neuroscience, cardiology, gene therapy, cell tracking, and theranostics (therapy combined with diagnostics). A step-by-step guide to answering biological and/or clinical questions using the tools of molecular imaging is also provided. We conclude by discussing the grand challenges of the field, its future directions, and enormous potential for further impacting how we approach research and medicine.

I.	INTRODUCTION	897
II.	MOLECULAR IMAGING MODALITIES	899
III.	MOLECULAR IMAGING AGENTS	923
IV.	APPLICATIONS OF MOLECULAR IMAGING	937
V.	<b>GUIDE TO PERFORMING A MOLECULAR</b>	947
VI.	THE FUTURE OF MOLECULAR IMAGING	951
VII.	SUPPLEMENTARY MATERIAL	953

## I. INTRODUCTION

Molecular imaging is greatly enhancing the way researchers and clinicians visualize and investigate complex biochemical phenomena. One may define molecular imaging as the noninvasive, real-time visualization of biochemical events at the cellular and molecular level within living cells, tissues, and/or intact subjects (276, 318, 451, 452). Generally speaking, molecular imaging involves specialized instrumentation, used alone or in combination with targeted imaging agents, to visualize tissue characteristics and/or biochemical markers. The data generated from molecular imaging studies can be used to help understand biological phenomena, identify regions of pathology, and provide insight regarding the mechanisms of disease. Although still in its infancy, molecular imaging is showing enormous promise in the areas of diagnostics, therapy monitoring, drug discovery and development, and understanding nanoscale reactions such as protein-protein interactions and enzymatic conversion.

The words *molecular imaging* mean different things to various groups, and thus the areas of research and medicine that fall under the umbrella of molecular imaging are incredibly vast and varied. Due to space constraints, this review will focus on molecular imaging of intact living subjects. We will only make very brief mention of microscopybased imaging techniques used to visualize biochemical processes in live cells and tissues ex vivo (see sect. IIA5).

Molecular imaging in living subjects has strong ties to nuclear medicine (457). Since its advent, nuclear medicine has aimed to facilitate the noninvasive diagnosis and management of patients via imaging instrumentation and radionuclides (either alone or attached to molecules that specifically interact with one or more molecular targets). In the early days, researchers relied on hand-held Geiger Counters to crudely measure the biodistribution of radioactivity in a patient without forming an image. It was not until 1950 that the first instrument capable of imaging organs in the body, known as the rectilinear scanner, was designed and constructed by Benedict Cassen at the University of California Los Angeles (7, 48, 457). In 1956, a photographic component was fitted to the rectilinear scanner, creating the Photoscanner. While this modification improved the resolution and sensitivity of the instrument, the scans themselves were time consuming and contained motion artifacts. A few years later, the Photoscanner was superseded by the Gamma Camera, also known as the Scintillation Camera

(367). The Gamma Camera addressed many of the Photoscanner's issues due to its novel design containing vacuum photomultiplier tubes, enabling the spatial location of gamma rays to be calculated by analyzing resulting voltage signals. Later, the Gamma Camera was modified so that it could act as a rotating detection system used in conjunction with reconstruction algorithms and computers to generate tomographic images, an application known as single photon emission computed tomography (SPECT) (206). The first general purpose SPECT instrument was developed and implemented by John Keyes in 1976.

The development of SPECT, and other highly sensitive imaging modalities including positron emission tomography (PET), combined with the synthesis of novel radiolabeled molecules specific for different biochemical targets, launched the field of nuclear medicine into a new era of imaging. Over the last decade, the principle of injecting molecules into a living subject to target specific molecular processes has been generalized so that the signaling from such molecules is not restricted to only a radioactive atom. Techniques, using optical signaling, as well as signaling using magnetic resonance imaging (MRI), ultrasound (US), Raman, photoacoustics (PA), and computed tomography (CT), have also been steadily increasing. So although molecular imaging of living subjects can trace its roots back to nuclear medicine, many newer strategies are now possible (see sect. II for details on available molecular imaging modalities).

The field of molecular imaging is highly multidisciplinary, drawing from many areas of science, including, but not limited to, molecular biology, biochemistry, physiology, physics, engineering, genetics, mathematics, chemistry, pharmacology, immunology, and medicine. The areas of science currently driving the development and expansion of this relatively new field include bioengineering, nanotechnology, radio/bioconjugate chemistry, protein engineering, bioinformatics, systems biology, and the -omics (i.e., genomics, transcriptomics, metabolomics, and proteomics).

One of the main motivations of molecular imaging is to translate common in vitro bioassay strategies to an in vivo setting in an attempt to overcome existing limitations. While in vitro techniques have long provided valuable information and insight into the inner workings of cells and the biochemistry of disease, they are limited by 1) the inability to provide analyses of entire intact organisms over time, making it difficult to appreciate the "full picture" of disease states and/or biochemical process; 2) the required removal of cell, organ, or tissue samples from their natural environment and/or the need for preparing samples with fixatives, rendering results not true of physiological conditions; 3) the fact that samples (e.g., brain tissue slices) can often only be analyzed by one or two in vitro techniques due

to the sample being destroyed or irreversibly altered, meaning only limited information can be extracted from each sample; and 4) the necessary euthanasia of animals, making impossible the longitudinal study of the same animal, and creating issues with regards to both costs and ethics.

For these reasons (among others), there has been a great need for methods that allow one to visualize and study biochemical processes in intact living subjects, noninvasively, over time. The marriage of traditional in vitro molecular biology with in vivo imaging has begun to bridge many gaps across areas of science where in vitro and ex vivo techniques have previously fallen short.

Compared with traditional in vitro methods, molecular imaging approaches have a number of advantages.

- Molecular imaging permits the noninvasive study of cells in their natural microenvironment, without perturbing the system under investigation. Whereas traditional in vitro approaches require cells to be removed from their native surroundings and hence can only at best, provide information on a small part of the whole picture.
- Via different molecular imaging techniques, one can trace movement of cells and thus perceive dynamic biological processes [e.g., tracking the location of therapeutic cytolytic T cells in a patient with glioma using PET and a reporter gene system (473); see sect. IV, D and E]. Molecular imaging enables the researcher to observe cellular processes in their natural environments in real time, thereby greatly enhancing the value and veracity of research.
- Molecular imaging approaches enable investigation of intact, signaling and transduction pathways in real time, whereas in vitro studies provide a more static picture and do not allow signaling to be interrogated.
- Rapid information concerning pharmaceuticals (pharmacokinetics and pharmacodynamics) can be obtained, thereby reducing the amount of time it takes to evaluate the efficacy, metabolism, and safety profile of a potential therapeutic (462).
- Molecular imaging makes it possible to perform repeat studies in the same animal. Thus the collection of longitudinal data is possible, resulting in the use of fewer animals since each animal serves as its own control.
- Most available molecular imaging techniques may be conducted with adequate temporal and spatial resolution for studying intricate biological and physiological processes in living subjects (e.g., visualizing the formation of new neurons using optical imaging; Ref. 69).

Although the advantages associated with molecular imaging techniques are many, they also have their limitations (see sect. VIA). Subsequently at this stage, employing a com-

bination of traditional in vitro methodologies and molecular imaging is necessary and extremely valuable.

Overall molecular imaging is an exciting field of research with enormous potential and a wide range of applications, including, diagnostics, drug discovery and development, theranostics, and personalized medicine. It is emerging as an important means of exploring the inner workings of the body in both normal and disease states. This review aims to serve as a "how to" guide for newcomers to molecular imaging while simultaneously presenting some of the most recent advances in the field. Please refer to FIGURE 1 for a general scheme of a molecular imaging study. Specifically, we focus on imaging intact living subjects and the available tools for investigating biochemical processes in normal and disease states. We provide an introduction to the classical imaging modalities, including PET, SPECT, MRI, CT, optical imaging, and US, by reference to their relative advantages and limitations, and a description of newer emerging technologies. We then present an analysis of the characteristics, strengths, and limitations of different classes of imaging agents including small molecules, peptides, antibodies, aptamers, and nanoparticles. Applications of molecular imaging in the fields of oncology, neuroscience, gene therapy, cell tracking, and theranostics are provided, followed by a description of key steps and considerations involved in performing a molecular imaging study. Lastly, we discuss the likely future directions of molecular imaging, current limitations, and suggestions for the continued development, innovation, and progress of the discipline.

#### **II. MOLECULAR IMAGING MODALITIES**

There exist a range of different imaging modalities a researcher or clinician may use for a particular study (FIGURE 2). The selection of an appropriate imaging modality is dependent on the biochemical process(es) one wishes to visualize and the type of imaging data one wants to obtain. There are numerous factors and questions a researcher or clinician must consider to select an appropriate modality (or modalities, if relevant) including the following:

- What spatial resolution is required?
- What level of sensitivity is required? Sensitivity refers to the minimum concentration of imaging agent that can be detected. The issue of sensitivity will depend on the levels of your target(s).
- Is dynamic information needed?
- Is whole body/subject imaging required? Or only a small region?
- What temporal resolution is required, i.e., how quickly should the image be acquired?
- Is depth of penetration important?
- Is quantitative data needed?
- Will multiple, repeat studies be required?

- Are multiplexing capabilities needed/preferable? Multiplexing refers to the ability to image/visualize multiple molecular targets simultaneously.
- Is clinical translation the end goal?

# A. Overview of Classical Imaging Modalities

## 1. CT

CT is a technique that relies on differential levels of X-ray attenuation by tissues within the body to produce images reflecting anatomy.

A) BASIC PRINCIPLES OF CT. Unlike traditional X-ray examinations, CT employs tomography (imaging by sections) and thus results in a three-dimensional anatomic image of the subject being scanned. FIGURE 3A depicts the basic geometry of a CT scanner. The X-ray source/tube typically produces a fanbeam spanning the entire subject width. This X-ray source is linked to the detector array in such a way that both are able to rotate together around the subject. A large number of detectors are used to enable an adequate number of measurements to be obtained across the entire scan circle. Tissues or media that strongly absorb X-rays (e.g., bone) appear white while others that absorb poorly (e.g., air) appear black, creating a high-contrast image displaying detailed morphological information, and enabling delineation between various structures. Hounsfield units (HU) are numerical values (introduced by Nobel laureate, Godfrey N. Hounsfield) that reflect these differences in density and composition, and thus X-ray attenuation, between various tissue types (e.g., HU for bone = 1,000, blood = 40, cerebrospinal fluid = 15, water = 0, fat = -50 to -100, and air = -1,000). Radiologists use software that automatically assigns HUs (between -1,000 and 1,000) to every voxel of a CT scan to enable efficient scan interpretation.

Often, an iodinated contrast agent will be used during CT imaging to improve spatial resolution and soft tissue contrast. In the clinic, CT has proven invaluable in identifying and assessing tumors (442), brain injury (94), ischemia (269), pulmonary embolism (397), and a vast array of other conditions. It is truly the workhorse for modern-day clinical imaging.

In preclinical research, a miniaturized (small animal) version of a clinical CT scanner is used. Small animal CT is considered to be a cost effective, relatively rapid means of investigating live animal models of disease (200), allowing real-time assessment of certain pathologies (including cancer) and their associated response to therapies via the production of high-resolution anatomical images (see **FIGURE 3B** and Ref 215). Moreover, small animal CT can also provide quantitative, anatomical information about the microanatomy of various invertebrates in a fast and inexpensive manner, whereas standard in vitro procedures for retrieving

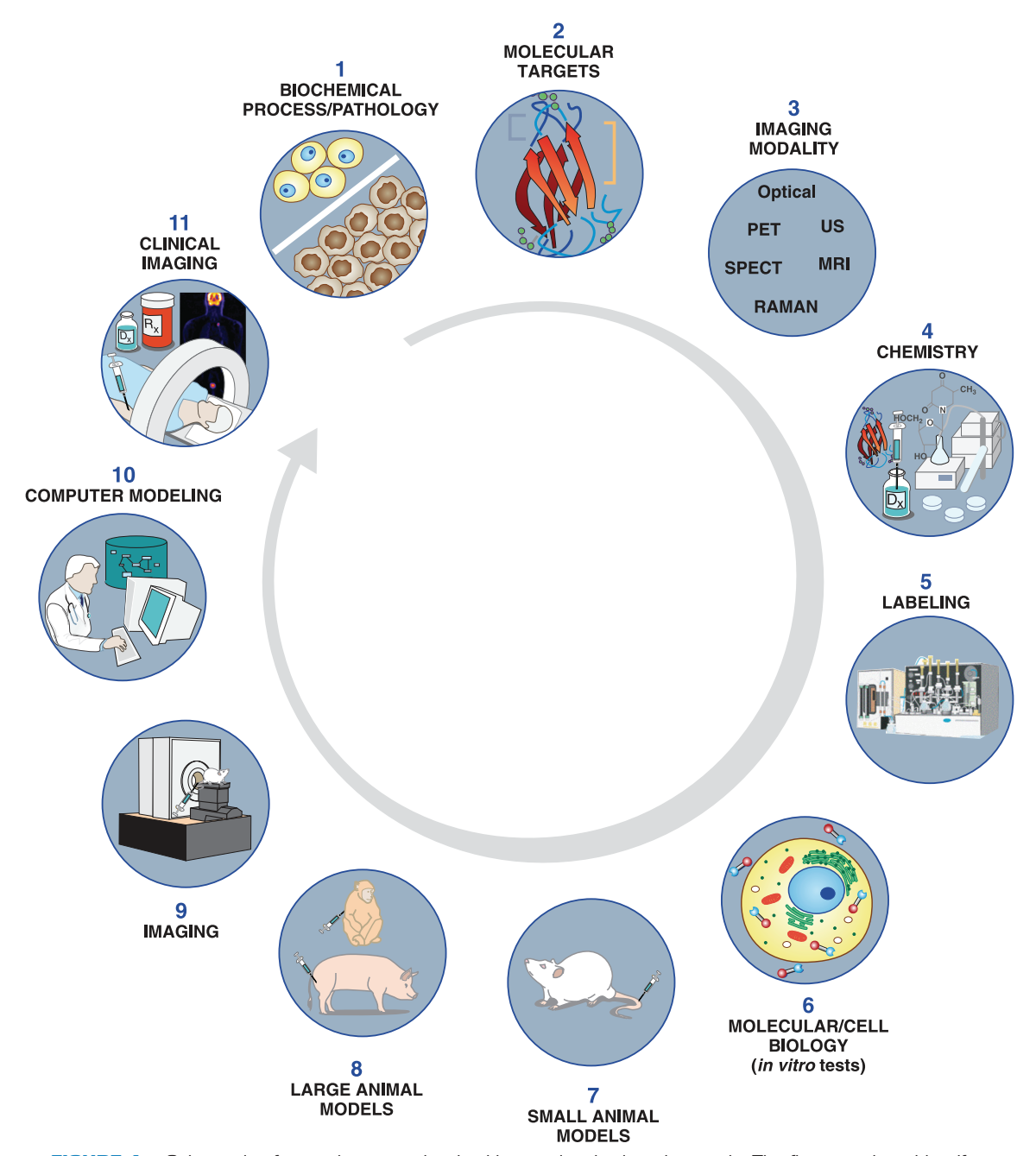
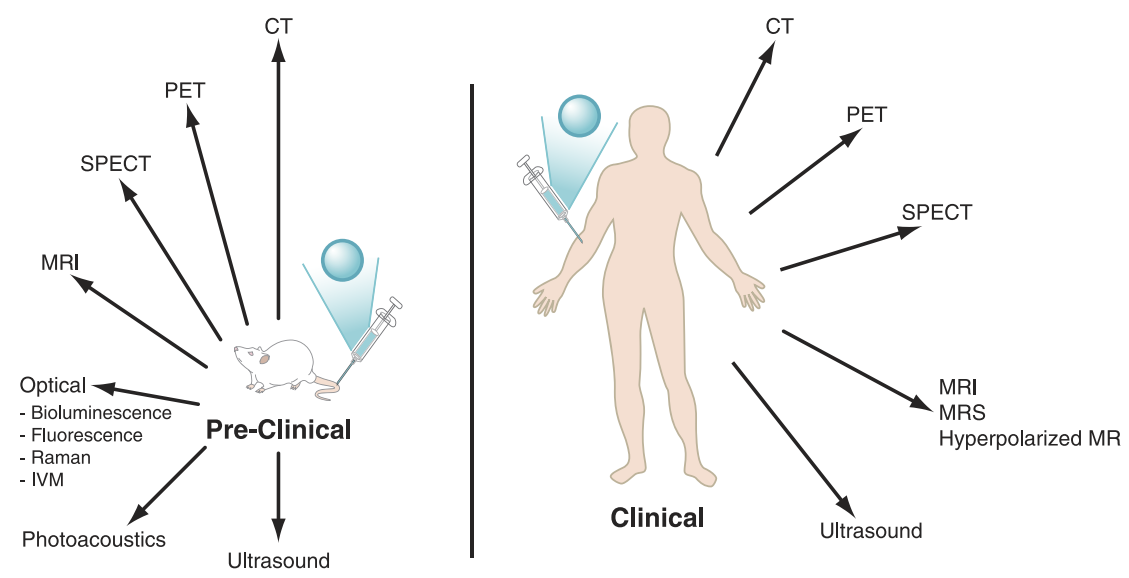


FIGURE 1. Schematic of some key steps involved in a molecular imaging study. The first step is to identify a biochemical process or pathology of interest, and to assess the significance of visualizing this process/pathology noninvasively via the tools of molecular imaging. The second step is to decide on a molecular target that will enable direct or indirect visualization of the phenomena of interest. This is usually followed by selection of an appropriate imaging modality (like those discussed in sect. II) and, if necessary, an imaging agent (discussed in sect. III). Typically, some chemistry and labeling are required to synthesize the imaging agent (so that it contains both a targeting and signaling component). A number of in vitro (molecular/cell biology-based) and in vivo (animal model-based) tests are required to evaluate the specificity and selectivity of the imaging method for visualizing the phenomena of interest. If clinical studies are the end goal, FDA approval is required, and certain mathematical models/algorithms might need to be developed so that meaningful data can be obtained from images. Please refer to section V for a step-by-step guide to performing a molecular imaging study. PET, positron emission tomography; US, ultrasound; SPECT, single photon emission computed tomography; MRI, magnetic resonance imaging; RAMAN, surface enhanced Raman spectroscopy.

this kind of structural data are costly and time-consuming. A recent study demonstrated the effective use of microCT to image the anatomy of the honeybee brain (352).

B) KEY STRENGTHS AND LIMITATIONS. Some advantages of CT include its fast acquisition time, high spatial resolution (preclinical = 0.05-0.2 mm, clinical = 0.5-1.0 mm), cost-ef-



**FIGURE 2.** Key molecular imaging modalities used for preclinical and/or clinical applications. CT, computed tomography; PET, positron emission tomography; SPECT, single photon emission computed tomography, MRI, magnetic resonance imaging; MRS, magnetic resonance spectroscopy; IVM, intravital microscopy. Blue circle, appropriate contrast agent or molecular imaging agent.

fectiveness, availability, clinical utility, and relative simplicity. Depth of penetration is a non-issue with this modality given the relatively high energy of X-rays and their ability to penetrate through the body.

One of the main limitations of CT is the high exposure to radiation, which often limits the number of scans that can

be performed in the same patient in a given time frame. It is important to note, however, that advances in X-ray detector sensitivity made in the last 5 years (and ongoing) will in the future afford significant dose reductions. Although the maturity of these technologies is not yet sufficient for widespread clinical translation, they are currently being employed in preclinical small animal systems. Another limita-

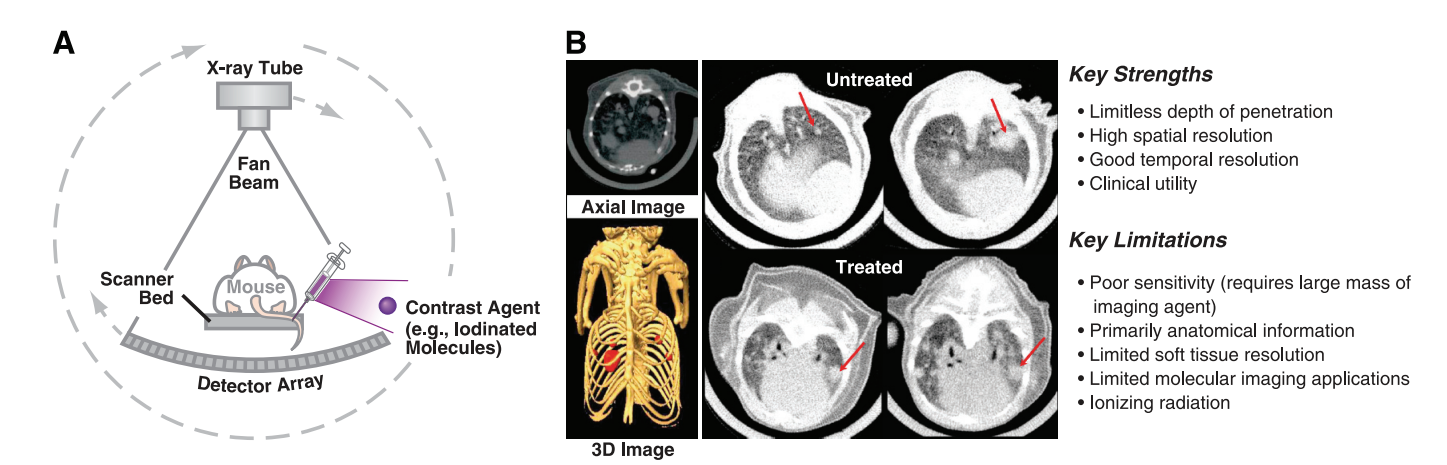


**FIGURE 3.** Small animal computed tomography (CT). A: schematic illustrating the principles of CT, i.e., first a suitable contrast/imaging agent may or may not be administered to a subject (in this example, a mouse). The X-ray source/tube typically produces a fanbeam spanning the entire subject width. The X-ray source is linked to the detector array in such a way that both are able to rotate together around the subject. X-rays will be differentially attenuated depending on the types of tissues or media with which they come in contact. Tissues or media that strongly absorb X-rays (e.g., bone) appear white while others that absorb poorly (e.g., air) appear black, creating a high-contrast image displaying detailed morphological information, and enabling delineation between various structures. B: small animal CT axial images and 3D representation of tumor volumes in a genetically engineered mouse model of non-small-cell lung cancer. The images on the *left* (axial and 3D) show that lung tumors can be detected via CT (shown in red on 3D depiction). The axial images on the *right* demonstrate the effects of treating one of these mice with radiation therapy. The tumors (highlighted by red arrows) in untreated mice continue to grow rapidly over 1 month, whereas the tumors of treated mice grow very slowly over the same time period (214). [From Kirsch et al. (214), with permission from Elsevier.]

tion is the low-quality soft tissue contrast CT affords compared with MRI, necessitating the use of iodinated contrast agents to enable more accurate discrimination between normal and disease-containing regions (276). These simple iodine-based contrast agents, although useful, are typically nonspecific and thus do not provide information on specific biochemical targets (340). Moreover, in the clinic, contrast agents can be problematic (due to renal toxicity) and cannot be given to all patients; for example, it is not advisable to administer contrast agents to elderly patients with high creatinine levels or to pregnant women.

c) MULTISLICE CT. One of the most significant technological advances for CT imaging was the introduction of helical scanning (37, 152) and multi-detector CT (MDCT) (171, 343). As its name implies, MDCT has multiple detector rows and is capable of acquiring numerous tomographic slices within a single (sub)second. Early prototypes of MDCT were capable of acquiring ~4 slices of varying widths per rotation (243) and were followed by the 8- and 16-slice detector row scanners (106). Most recently the 320-detector-row MDCT (320-MDCT) was introduced, capable of performing four-dimensional morphological and kinematic analyses of swallowing or cardiac function (114).

Compared with early CT, MDCT has the advantage of providing high temporal and axial (along the length of the body) spatial resolution. Since MDCT enables such rapid acquisition, it eliminates a large proportion of motion artifacts observed with regular CT when imaging patients (and regions of patients) prone to voluntary and/or involuntary movement, e.g., pediatrics, geriatrics, and thoracic/cardiac imaging studies. For this reason, and also due to the enhanced spatial resolution, MDCT has become the new standard for cardiac CT imaging. In fact, in many cases, MDCT is more suitable than invasive coronary angiography for locating and characterizing coronary plaques (403). MDCT is also being successfully used to predict coronary events and for long-term stent assessment (305). However, the high radiation dose may limit its use for this application.

While MDCT offers more rapid acquisition and improved axial resolution, it suffers from safety issues due to its high radiation dose. Work is currently underway to reduce the amount of radiation linked with this technique (403); however, caution needs to be taken due to concerns with radiation-induced malignancies. When lower cost and nonionizing radiation strategies are available, they need to be actively investigated as alternatives.

D) DUAL-ENERGY CT. Another important recent advance in CT technology is dual-energy CT (DECT), which has two separate X-ray tubes that can be operated at either the same energy (a technique called "dual source CT") or at two different energies (in this case it is referred to as DECT). DECT enables tissues to be delineated by their composition

as opposed to their attenuation only. This is possible due to the fact that attenuation of a particular tissue varies depending on the energy of X-rays used. DECT discriminates according to this difference in attenuation between two different energies. This technique is mainly used for discriminating between calcium and uric acid renal stones (342), assessing renal malignancies (134), imaging gout (189), and determining bone mineral density (70, 481).

E) MOLECULAR IMAGING WITH CT. Transforming CT into a modality capable of obtaining biochemical information is nontrivial due to the low sensitivity of CT-compatible contrast agents. Therefore, the primary limitation for CT in molecular imaging applications is the mass of imaging agent that needs to be injected in order for enough to reach the target site(s) for a change in X-ray attenuation. However, multiple examples of CT molecular imaging are beginning to emerge. Fayad and colleagues (174) reported the use of iodinated nanoparticles for cellular imaging of macrophage infiltration in atherosclerotic plaques in rabbits using MDCT. Also, a number of research groups have recently reported the use of targeted gold nanoparticles (known to induce strong X-ray attenuation) with CT for imaging cancer at the cellular and molecular levels (244, 340). For example, one group reported the synthesis and evaluation of CT-compatible gold nanoparticles functionalized with prostate specific membrane antigen (PSMA) RNA aptamers (210). The results demonstrated a fourfold higher uptake of PSMA-aptamer conjugated gold nanoparticles in the Ln-CaP (human prostate adenocarcinoma) cells overexpressing PSMA compared with the PC3 (another type of prostate epithelial) cells devoid of PSMA. In addition, a therapeutic drug against prostate cancer (doxorubicin) was loaded into the targeted nanoparticles, and it was shown that they were significantly more effective against the LnCaP cells compared with the negative control PC3 cells. While the results from these preliminary molecular imaging CT studies are promising, further work is needed to explore the possibilities of CT molecular imaging and its applications.

Overall, CT is an important clinical and preclinical imaging modality that is widely available, relatively cost effective, and highly efficient. Although the molecular imaging capabilities of CT are yet to be fully explored, it remains an extremely useful morphological tool. When combined with PET, SPECT, optical or MRI modalities, CT provides an anatomical reference frame for the biochemical and physiological findings that are afforded by these other imaging instruments.

#### 2. MRI

MRI is a highly versatile imaging modality (28) that uses a powerful magnet and radiofrequency (RF) energy to visualize the internal structure and soft tissue morphology of the body. The underlying principles of MRI are similar to those

for nuclear magnetic resonance (NMR) and allow imaging of atomic nuclei within the body.

A) BASIC PRINCIPLES OF MRI. Nuclear particles (protons and neutrons) are in constant motion and spin about their axes, which gives rise to angular momentum. Atoms with an equal number of protons and neutrons have a net angular momentum of zero, whereas atoms with an unequal number possess a specific spin angular momentum. Along with angular momentum, certain nuclei can also produce a small magnetic field (due to the mass, spin, and charge of protons). This magnetic field is termed magnetic moment and, like angular momentum, is a vector quantity. The ratio of angular momentum to magnetic moment is known as the gyromagnetic ratio and is unique for each magnetically active nucleus (102).

During an MRI scan, a living subject is placed inside a magnet (FIGURE 4A). As described above, certain atomic nuclei (in the body or elsewhere) have special spin characteristics and magnetic properties. When these nuclei are placed in an external magnetic field, they behave like magnetic dipoles and align either parallel or anti-parallel to the field. The MR signal is generated from the very small net difference in the number of magnetic dipoles that align parallel versus those that align anti-parallel. For example, a 1.5-T external magnetic field gives rise to a net difference in

parallel versus anti-parallel spins, or "polarization" of only 1 part per million at 37°C. As a result, MRI has an extremely weak signal and very poor sensitivity ( $\sim 10^{-3}$ - $10^{-5}$ M) (285), which is orders of magnitude lower than that of radionuclide ( $10^{-10}$ - $10^{-12}$ ) and optical ( $\sim 10^{-9}$ - $10^{-16}$ ) imaging (236). MRI signal is proportional to 1) concentration of nuclei, 2) gyromagnetic ratio (or "gamma factor," "g factor"), and 3) polarization. Additionally, MRI signal is dependent on the natural abundance of the "magnetically active" isotope of the element. For example, all <sup>1</sup>H nuclei are magnetically active, but only 1% of carbon exists in the form that is detectable by MRI (i.e., <sup>13</sup>C). Therefore, imaging of nuclei such as carbon often requires introduction of an exogenous contrast agent that has been enriched to 100% abundance (see below). For this reason, the most common nucleus for clinical MRI is <sup>1</sup>H. Anatomical images are formed using the hydrogen in tissue water, which is at a concentration of 80 M in the body. Other nuclei that can be imaged include <sup>31</sup>P and <sup>13</sup>C, and also <sup>23</sup>Na, <sup>19</sup>F, and <sup>17</sup>O<sub>2</sub>. Imaging of these nuclei (in particular <sup>13</sup>C) is usually achieved through magnetic resonance spectroscopy (MRS), in which there have been significant advances over the past decade with the advent of hyperpolarized MRS, described below.

Some of the key components of an MRI scanner are depicted in **FIGURE 4A**. In general, an MRI scanner is com-

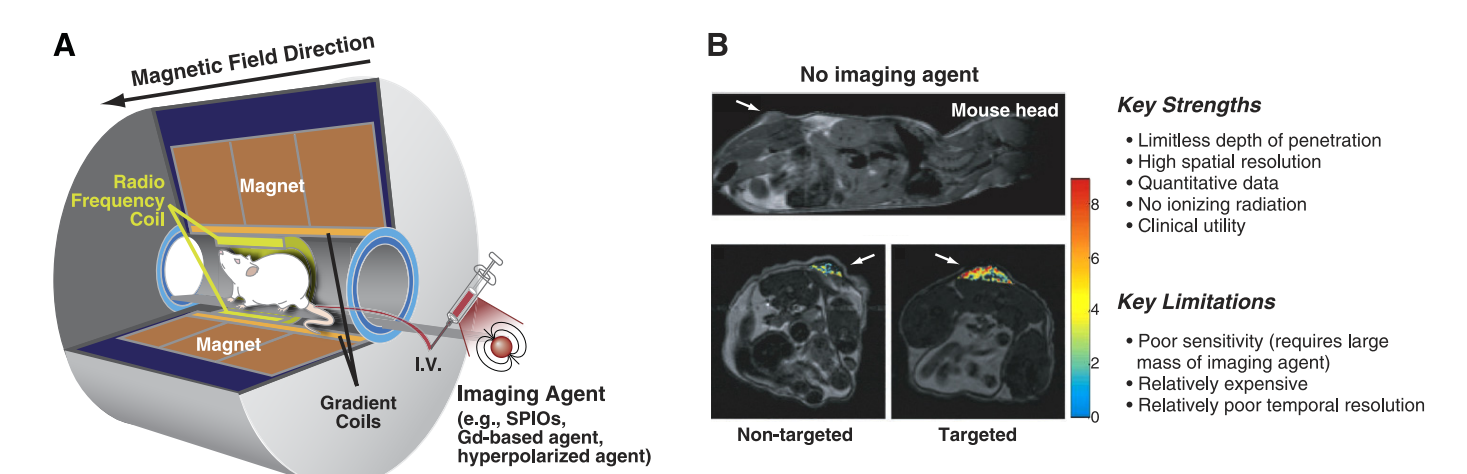


FIGURE 4. Small animal magnetic resonance imaging (MRI). A: schematic showing the basic principles of this technique. In general, an MRI scanner is comprised of a set of embedded coils: one coil that generates the main relatively homogenous magnetic field, "gradient coils" that produce variations in the magnetic field in the X, Y, and Z directions that are used to localize the source of the MR signal, and finally "RF coils" that generate an RF pulse responsible for altering the alignment of the magnetic dipoles. During an MRI scan, a living subject is placed inside a magnet (in this example the subject is a mouse). Unpaired nuclear spins within the body, known as magnetic dipoles, either align parallel or anti-parallel with the direction of the magnetic field. The MR signal is generated from the very small net difference in the number of parallel versus anti-parallel spins (slight majority of spins align parallel). B: MRI images from a study evaluating a novel MRI molecular imaging agent in a mouse model of glioma (402a). The top image is a sagittal cross-section MRI of the mouse, whereby the tumor is highlighted with an arrow. The bottom panel displays coronal MR images of the same mouse imaged 3 h postinjection of either nontargeting (left) or chlorotoxin-targeting (peptide found on surface of gliomas) superparamagnetic iron oxide (SPIO) nanoparticles. The MR contrast enhancement of the tumor is significantly greater for the mouse injected with targeted SPIO nanoparticles. These images demonstrate the advantage of using targeted MRI imaging agents for visualizing biochemical targets in living subjects. [From Sun et al. (402a), with permission form John Wiles and Sons.]

prised of a set of embedded coils: one coil that generates the main relatively homogenous magnetic field; "gradient coils" that produce variations in the magnetic field in the X, Y, and Z directions that are used to localize the source of the MR signal; and finally "RF coils" that generate an RF pulse responsible for altering the alignment of the magnetic dipoles (FIGURE 4A). After every RF pulse, the magnetic dipoles in the subject are "tipped" away from equilibrium and subsequently undergo two forms of relaxation back towards equilibrium known as spin-lattice (or longitudinal) relaxation and spin-spin (or transverse) relaxation. The contrast between different tissues in MR images is generated due to the different relaxation times of each tissue [longitudinal (T1) and transverse (T2) relaxation times]. For instance, proton nuclei in fat and hydrocarbon-rich environments have relatively short relaxation times compared with those in aqueous environments (276). These differences are exploited by modifying the timing parameters of a set of RF pulses (collectively known as a pulse sequence), thereby preferentially sensitizing image contrast to differences in either T1 or T2. For example, when an image is T1 weighted, a subacute hemorrhage will appear brighter than normal brain tissue, since hemorrhage has a shorter T1 than brain tissue. For an exhaustive description of the general theory of MRI, please refer to References 39, 75, 242.

B) DCE-MRI, DW-MRI, AND BOLD. Apart from providing detailed anatomical information, MRI is capable of providing physiological information via various specialized MRI techniques. Most MRI techniques rely on different pulse sequences to generate different information about the tissues being interrogated. A few examples of specialized MRI techniques include dynamic contrast-enhanced MRI (DCE-MRI), diffusion-weighted MRI (DW-MRI), and blood oxygen level dependent MRI (BOLD-MRI). These techniques are able to assess the physiological characteristics of the vasculature (DCE-MRI), the degree of tissue cellularity (DW-MRI), and the oxygen status of red blood cells in perfused regions of tissue (BOLD-MRI).

DCE-MRI involves the dynamic acquisition of T1-weighted MR images before, during, and after the administration of an appropriate contrast agent. MRI contrast agents produce their contrast by disturbing the local magnetic field in which they are placed. While low-molecular-weight paramagnetic gadolinium (Gd) complexes are the most common contrast agents for DCE-MRI, superparamagnetic iron oxide (SPIO) nanoparticles can also be used (321) (see sect. IIIE). Gd- and SPIO-based contrast agents shorten the T1 or T2 relaxation times, respectively, of neighboring protons, leading to measurable alterations in MR signal (positive contrast for Gd and negative contrast for SPIOs) (416). Some of the main applications of DCE-MRI include physiological imaging of tumor microvascularization (321), lymphatics (421), and inflammation (158).

Diffusion-weighted imaging (DWI) is a promising technique (73) that is capable of detecting the apparent diffusion coefficient of tissue water (ADC). Tissues with high cellularity display low ADC as the movement of water molecules in the interstitial space is restricted, whereas tissues with low cellularity, for example, necrotic tissue, have a high ADC. Since the diffusion of water molecules is affected in numerous pathological conditions, including tumor development and ischemic stroke, DWI can play a major role in diagnosis and clinical management of these conditions. For example, in the case of ischemic stroke, DWI can be used to identify regions containing salvageable tissue, and thus determine whether thrombolysis may be effective. In addition, DWI can provide accurate estimates of the time of stroke onset and can discriminate between old versus new strokes (366). DWI is also proving its use in other applications such as cancer imaging (54, 295, 408) in detecting response to therapy.

BOLD imaging is an extremely useful functional MRI (fMRI) technique, which is used extensively to study brain function in normal and disease states (108). Instead of using an exogenous contrast agent to image and gain insight about in vivo physiology, BOLD works by measuring regional alterations in endogenous deoxygenated hemoglobin. Since deoxyhemoglobin is paramagnetic and oxyhemoglobin is not, regions containing higher levels of oxygenated blood will appear more intense on T2 weighted MRI images. In the context of imaging brain function, it is believed that an increase in neuronal activity within a given brain region leads to a net increase in the amount of oxygenated blood flow in that region, and thus BOLD imaging can be used to identify activated regions and hence obtain information on brain function. BOLD has been used to study many aspects of brain function (and dysfunction), including memory (484), sensory perception (13), cognition (105), and depression (387). It should be noted that BOLD is not only used for imaging brain function but can also be used to measure differences in deoxyhemoglobin levels in other tissues (e.g., kidney), as well as to assess the oxygenation status of red blood cells in perfused regions of tumors (55).

While these specialized MRI techniques are able to provide important physiological information, they are limited by the fact they are relatively nonspecific and are unable to provide biochemical or receptor-related information. To address this issue, responsive Gd-based molecular imaging agents (79) were developed, and while they are capable of sensing metabolite levels and bulk tissue alterations in pH, redox, metal ions, and oxygenation, they too have their limitations. Such limitations are mainly concerned with quantitation and sensitivity, and only a handful of responsive MRI agents have shown promise in living subjects to date. More recently, chemical exchange saturation transfer (CEST) and paramagnetic-CEST (PARACEST) contrast agents have emerged as promising tools for probing specific

molecular and physiological events (mainly pH sensing) using MR imaging (79, 482) (see **TABLE 2** for examples). These agents are still in their early stages of development, and thus have their challenges (148), and most have not been evaluated in living subjects.

C) TARGETED CONTRAST AGENTS. Another important advance in MRI has been the development of "targeted" MRI contrast agents (targeted Gd-complexes or SPIOs) for visualizing molecular markers and their associated biochemical events. Some specific examples of targeted MRI agents and their molecular imaging applications include SPIO nanoparticles functionalized with specific peptides for detection of early atherosclerotic events (199), glioma imaging using SPIOs functionalized with peptides specific for matrix metalloproteinase-2 (402a) (FIGURE 4), and imaging  $\alpha v \beta 3$  integrins using Gd-containing liposomes (389). For further information on targeted SPIOs and Gd-based imaging agents for molecular MRI imaging, please see Reference 313.

D) KEY STRENGTHS AND LIMITATIONS. MRI has a number of important advantages compared with other imaging modalities including 1) no need for ionizing radiation; 2) unlimited depth of penetration; 3) high spatial resolution (clinical: ~1 mm compared with 5–7 mm for PET, preclinical: micrometers, as opposed to millimeter resolution achievable via optical and radionuclide imaging; **TABLE 1**); 4) unparalleled soft tissue contrast, superior to that attainable with CT; 5) concurrent collection of physiological or metabolic data (using, e.g., DCE-MRI and MRS, respectively) with high-resolution anatomical images, and even molecular information when used in conjunction with targeted MRI-compatible imaging agents; and 6) excellent clinical utility.

A major limitation of MRI is its extremely poor sensitivity compared with other molecular imaging modalities. This low sensitivity can lead to relatively long acquisition times, and in the case of physiological/molecular MRI, is the reason why large amounts of imaging agents are often required to obtain an adequate signal. These large amounts of imaging agents (i.e., many log orders higher compared with that needed for PET or SPECT) can be problematic due to the likelihood of altering the biological system of interest through pharmacological effects (generally proportional to the mass of agent administered). Toxicity issues associated with administrating large doses of MR imaging agents are also an important consideration. For this reason, MRI molecular imaging is sometimes thought to be more suited for targets within the vasculature, as then the imaging agent does not have to reach an extravascular target which would require a greater injected mass of imaging agent.

Overall, MRI is an extremely useful imaging modality. Although it does not have the most favorable sensitivity, and is relatively expensive, its ultra high spatial resolution has

revolutionized clinical medical diagnostics and has also proven useful in the basic research setting, enabling the interrogation of molecular processes in single cells, perfused organs, and intact living rodent models of disease (53).

E) MRS. Since initial observations in 1946 and the simultaneous discovery of nuclear induction (29), NMR spectroscopy has become an essential element of every chemist's tool belt (15). The fundamental principles of NMR spectroscopy involve applying electromagnetic pulses to a sample in an external magnetic field and using a probe to measure the resulting RF signals produced (132, 299). These measurements provide a spectrum of peaks, representing the chemical composition of the sample. NMR is routinely used as a nondestructive, analytical technique for probing and deciphering the molecular structure, purity, and chemical components present in biological samples, synthesized compounds, and/or natural products in a laboratory setting.

In the clinical setting, NMR is referred to as MRS due to the negative connotations surrounding the word "nuclear." The key difference between MRI and MRS is the inclusion of gradients to allow acquisition of position data during MRI (299). MRS, on the other hand, generates a spectrum of peaks with different "chemical shifts" indicative of molecular building blocks, mainly lipids and metabolites, in a particular voxel of interest.

Due to the sensitivity constraints described above, MRS measurements of metabolite protons suffer a reduction in signal of ~1,000-fold due to the lower concentration of these molecules relative to water. As a result, the spatial resolution of this information is killed; MRS is often performed with single voxels of 1–8 cm³, and MRSI with a resolution of around 1 cm³. However, MRS can easily be incorporated into existing MRI examinations, meaning the biochemical information obtained using MRS can be combined with the usual high-resolution anatomical images acquired with MRI. Furthermore, MRS of endogenous metabolites is often limited to applications in brain, breast, and prostate, where good magnetic field homogeneity and the use of local acquisition coils means high signal-to-noise ratio can be achieved.

Despite these limitations, MRS can be used to detect spectral properties of highly abundant endogenous molecules such as choline, creatine, lactate, glutamate (and glutamine), lipids, and alanine to identify regions of abnormality/disease. For example, choline (a marker of membrane phospholipid metabolism) and choline-containing metabolites are notably increased in nearly all types of cancer (132), and thus MRS of these molecules can be used as a detection method for in vivo (where subjects are placed in an MRI scanner equipped with MRS software) or ex vivo (where biopsies are taken) applications. Recently, it was shown that the levels of choline and choline-containing

		Table I. Feat	ures of available and e	Features of available and emerging imaging modalities	ies			
Modality	Temporal Resolution	Spatial Resolution	Depth of Penetration	Sensitivity	Multiplexing Capability	Cost	Safety Profile	Used Clinically
Computed tomography (CT)	Minutes	50–200 $\mu$ m (preclinical) 0.5–1 mm (clinical)	Limitless	QN	Could be possible	98	lonizing radiation	Yes
Magnetic resonance imaging (MRI)	Minutes-hours	25–100 $\mu$ m (preclinical) $\sim$ 1 mm (clinical)	Limitless	10 <sup>-3</sup> to 10 <sup>-5</sup> M	N N	∠ \$\$\$	ion	Yes
Positron emission tomography (PET)	Seconds-minutes	1–2 mm (preclinical) 5–7 mm (clinical)	Limitless	$10^{-11} \text{ to } 10^{-12} \text{ M}$	o N	988 1	\$\$\$ Ionizing radiation	Yes
Single photon emission tomography (SPECT)	Minutes	1–2 mm (preclinical) 8–10 mm (clinical)	Limitless	$10^{-10} \text{ to } 10^{-11} \text{ M}$	Yes	98	lonizing radiation	Yes
Ultrasound (US)	Seconds-minutes	0.01–0.1 mm for superficial mm-cm [few mm depth] applications 1–2 mm for deeper [few cm depth] applications		Excellent when microbubbles are used (~10-12 M)	Not yet	<del>0</del>	Good safety profile	Yes
Optical fluorescence imaging	Seconds-minutes	2-3 mm	^1 cm	~10 <sup>-9</sup> to 10 <sup>-12</sup> M	Yes	<del>0</del>	Good safety profile but Emerging clinical depends on utility (see fluorophore used text) and mass needed	Emerging clinical utility (see text)
Optical bioluminescence imaging	Seconds-minutes	3–5 mm	1–2 cm	~10 <sup>-15</sup> to 10 <sup>-17</sup> M	Yes	<del>0</del>	Good safety profile L	Low potential for clinical translation (see text)
Surface-enhanced raman Minutes-days scattering (SERS) imaging	Minutes-days	ш	~5 mm	10 <sup>-12</sup> to 10 <sup>-15</sup> M	Yes	2		Limited clinical applications (see text)
Photoacoustic imaging (PAI)	Seconds-minutes	$\sim$ 10 $\mu$ m to 1 mm	6 mm to 5 cm	ΩN	Yes	<del>0</del>	Good safety profile but Clinically depends on imaging Transl agent used and mass needed	Olinically Translatable
Intravital microscopy (IVM)	Seconds-days	1–10 μm	~700 µm	$\sim \! 10^{-15}  \mathrm{to}  10^{-17}  \mathrm{M}$	Yes	<del>\$</del>	ON.	<u>Q</u>

ND, Not determined.

compounds reflect tumor grade in gliomas with greater accuracy than regular contrast enhancement using MRI alone (376). Senaratne et al. (375) found that MRS of choline in living subjects might also be useful for studying and detecting central nervous system (CNS) conditions such as bipolar disorder. Their studies demonstrated that choline-containing compounds were dramatically elevated in the hippocampus and orbitofrontal cortex in bipolar patients compared with that of age- and sex-matched healthy control subjects (375).

Although both of these examples (and many of the applications of MRS) do not require the use of an exogenous imaging agent to visualize molecular processes in living subjects, one can implement the use of an external imaging agent with this technique. This is commonly employed for MRS of non-proton nuclei, which in addition to the low concentration of metabolites in the body, may also suffer from low natural abundance (e.g., 1% of carbon exists as <sup>13</sup>C) and low gyromagnetic ratio (e.g., <sup>13</sup>C has a ratio onefourth that of <sup>1</sup>H). A specific example is the administration of [1-<sup>13</sup>C]glucose, in which the carbon at the 1 position in glucose has been enriched to make 100% <sup>13</sup>C, to enable in vivo observation and evaluation of glycolysis (a pathway that is significantly altered in cancer and certain brain diseases) (116, 132, 298). Even with these infusions, long acquisition times and low spatial resolution mean that to date, MRS of non-proton MRI has found limited clinical application. Recently, a method to overcome these profound sensitivity limitations has emerged, namely, hyperpolarized MRS, which is now entering clinical trials and will be discussed below.

F) HYPERPOLARIZED MRS. Efforts aimed at improving the sensitivity of MRS with non-proton nuclei have recently given rise to a technique called hyperpolarized MRS, capable of enhancing the signal to noise of MRS by over 10,000-fold (11, 271). Hyperpolarization involves forcing nuclei into artificially produced nonequilibrium distributions in an external system to the MRI magnet (355), creating a much larger net difference in the population of spins in the parallel versus anti-parallel states. This dramatically increases the polarization of the spins relative to that in the thermal equilibrium state to over 100,000 parts per million, and enables rapid acquisition and dynamic mapping of biological processes in vivo. There are several ways in which hyperpolarization can be achieved, including 1) optical pumping, 2) dynamic nuclear polarization (DNP), and 3) parahydrogen-induced polarization (PHIP). DNP, however, is the only method that has been demonstrated in a practical situation for in vivo and clinical imaging applications. Once the sample has been produced in a DNP system, the "hyperpolarization" decays away due to longitudinal relaxation, and thus must be used within the timeframe of  $\sim 5T_1$ (5 times the longitudinal relaxation time T1; this is usually accepted as the point at which the SNR becomes too low to be usable). While this places a strict limitation on the useful imaging window, it creates a significant benefit for visualizing fast biological processes, such as glycolytic flux and redox state in tumors.

Thus far, hyperpolarized MRS has mostly been performed with endogenous compounds that have been labeled with <sup>13</sup>C, the most successful being [1-<sup>13</sup>C]pyruvate, a key intermediate in glycolysis. [1-<sup>13</sup>C]pyruvate satisfies the criteria for a successful hyperpolarized substrate due to its long T1 relaxation time (up to 60s) and rapid metabolism in vivo. [1-<sup>13</sup>C]pyruvate has been extensively tested in animal models and has been shown to: correlate with tumor grade in prostate cancer (5), detect early development of hepatocellular carcinoma before anatomical manifestation (172), as well as detect response to both cytotoxic (71) and vascular targeted (33) agents as early as 6 h after drug administration. Recently, the first clinical study of a hyperpolarized small molecule, [1-<sup>13</sup>C]pyruvate, was performed to detect prostate cancer (5).

A wide range of hyperpolarized <sup>13</sup>C MRS probes have now been demonstrated in preclinical models, including [1-<sup>13</sup>C]urea for perfusion imaging (11); [1,4-<sup>13</sup>C2]fumarate, as an early marker of cellular necrosis (120); [<sup>13</sup>C]bicarbonate, as a measure of extracellular pH (119); [1-<sup>13</sup>C]dehydroascorbic acid, to detect tumor redox status (32); and [2-<sup>13</sup>C]-fructose, sensitive to both glycolytic and pentose phosphate pathway flux (205). For further details on the range of imaging probes available and their current status, consult the aforementioned reviews, as well as References 118, 233.

G) KEY STRENGTHS AND LIMITATIONS OF MRS AND HYPERPOLARIZED MRS. MRS is a highly valuable technique as it enables molecular imaging of biochemical processes, either using proton MRS, which does not require an exogenous agent, or using hyperpolarization to achieve adequate signals with non-proton MRS. The advantages of not needing an external imaging agent are 1) there is no risk of perturbing the processes you want to study, and 2) time and resources do not need to be spent on designing, synthesizing, and evaluating an imaging agent. Most of the contrast agents for MRS and hyperpolarization are endogenous molecules whereby particular carbon positions have been enriched for the "magnetically active" <sup>13</sup>C isotope. This reduces the risk of toxic or immunogenic responses, but they are often introduced at supraphysiological concentrations so toxicity effects should still be evaluated. Another advantage of proton MRS is that it does not require any new instrumentation, but instead can be performed at the same time as a regular MRI study using a modern MRI scanner (after certain MRS software has been installed). Since MRI and MRS are complimentary techniques (the former provides anatomical and physiological data and the latter provides biochemical information), combining the two is extremely advantageous.

The limitations of proton MRS include the fact that any arbitrary process cannot be imaged. Endogenous molecules and/or administered exogenous agents need to be present in very high concentrations to be detectable using proton MRS. The poor sensitivity of MRS can be partly resolved by increasing the magnetic field strength and also through the use of hyperpolarization techniques to image non-proton nuclei. The advantages of hyperpolarized MRS include its enhanced sensitivity (although still not better than that attainable using PET or SPECT), and its lack of background signal, which enable dynamic imaging of metabolic processes. The use of hyperpolarized MRS, however, is limited by the need for additional hardware including an additional "hyperpolarizer" magnet and the strict criteria for selecting contrast agents that satisfy the demands of a successful hyperpolarized probe, including the need for rapid delivery and metabolism within the window of the relaxation time.

While still in its early stages of development, hyperpolarized MRS is showing great potential in the imaging arena and has recently been demonstrated in the clinic. With continued efforts geared toward generating a range of new hyper-

polarized imaging agents, and by addressing limitations of this technique (which is already in progress), hyperpolarized MRS is predicted to evolve as a field in and of itself, and will more than likely play an important role in molecular imaging in the near future.

#### 3. PET and SPECT

PET and SPECT are radionuclide molecular imaging techniques that enable evaluation of biochemical changes and levels of molecular targets within a living subject. Both techniques have limitless depth of penetration and enable whole body imaging of molecular targets/processes with high sensitivity (TABLE 1).

A) BASIC PRINCIPLES OF PET. To image a certain molecular target using PET, one needs to first identify and synthesize a radiolabeled imaging agent that is specific and selective for the target of interest. Following this, a nanomolar amount of the chosen radiolabeled agent is administered to the patient/subject, typically via an intravenous injection (see **FIGURE 5B**). The radioactivity is then traced through the body and its distribution determined from scans obtained with a PET camera.

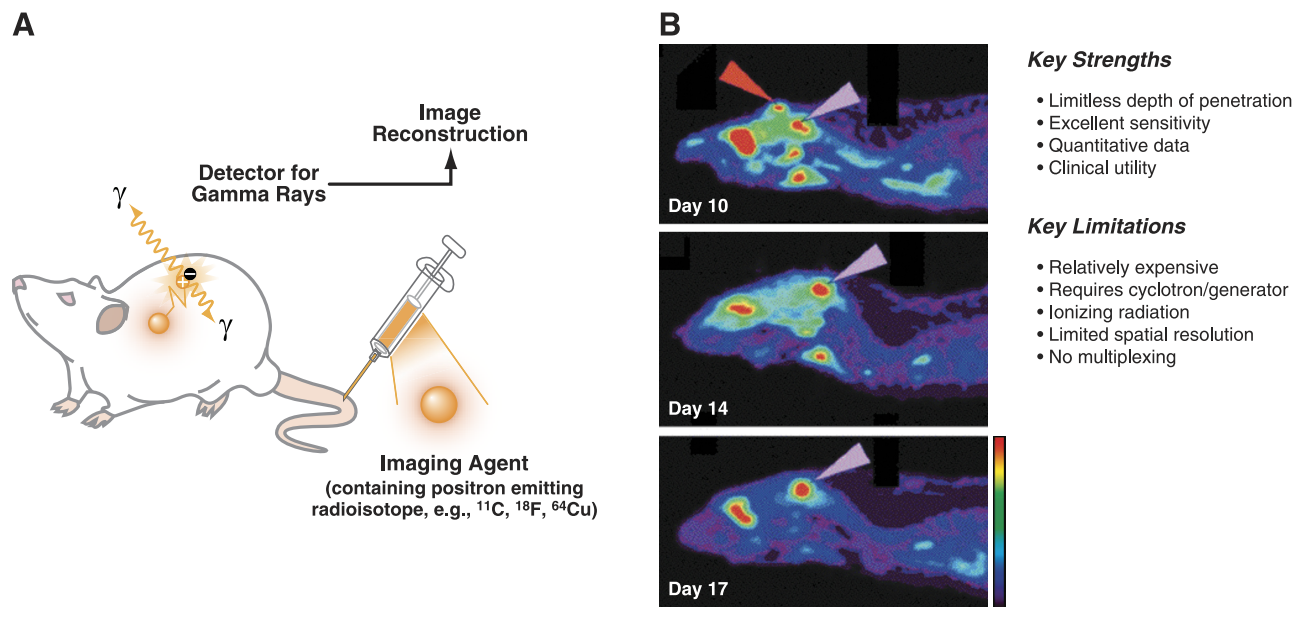


**FIGURE 5.** Small animal positron emission tomography (PET). *A*: schematic illustrating the basic principles of PET. First, a targeted imaging agent (e.g., small molecule, peptide, engineered protein, aptamer, nanoparticle) containing a positron emitting radioisotope is administered to the subject. Positrons are emitted from each imaging agent only once; these positrons travel short distances and collide with electrons in the surrounding tissues, an event known as annihilation, resulting in the production of two gamma rays, each with energy of 511 keV, traveling at opposite directions to one another (180° apart). Following the detection of gamma rays by the PET detector, the location of annihilation events are calculated by observing multiple events. The resulting electrical signals are converted into sinograms that are reconstructed into tomographic images. These images reflect the distribution of the imaging agent in the subject, and hence provide information on the biochemical event the agent was targeting. *B*: images demonstrating the noninvasive visualization of an orthotopic brain tumor (2.5 mm in diameter) in a rat via the use of [<sup>18</sup>F]-2-fluoro-2-deoxy-glucose ([<sup>18</sup>F]FDG), as early as 10 days (D10) after implantation. Pinks arrows show tumor, and red arrow shows wound due to intracerebral implantation of tumor cells (249). [From Lin et al. (249).]

PET requires the use of a cyclotron to generate short-lived radionuclides such as  $^{18}$ F ( $t_{1/2} = 109.8$  min),  $^{64}$ Cu ( $t_{1/2} = 12.7$  h), and  $^{76}$ Br ( $t_{1/2} = 16.2$  h), or ultra short-lived radionuclides such as  $^{11}$ C ( $t_{1/2} = 20.3$  min),  $^{13}$ N ( $t_{1/2} = 10$  min), and  $^{15}$ O ( $t_{1/2} = 2.04$  min) (143). PET takes advantage of the unique properties of radioactive isotopes (like those mentioned above) that decay via positron emission, otherwise known as beta-plus decay. Nuclei that decay in this manner have an excess of protons, making them unstable. This instability is rectified by transforming a proton into a neutron, a positron, and a neutrino. The newly formed short-lived positron is ejected from the nucleus, and due to inelastic interactions with electrons in surrounding tissue, rapidly loses kinetic energy causing it to slow down and collide with an electron, an event known as annihilation. Due to the conservation laws of energy and momentum, the combined mass of the positron and electron is converted into two photons, each with energy of 511 keV, traveling at opposite directions to one another, 180° apart (333) (FIGURE 5A). These high-energy photons lie within the gamma-ray region of the electromagnetic spectrum and thus display energy 10-fold higher than X-rays, increasing their chance of leaving the body to ensure external detection.

PET detectors take the form of a closed ring, or set of rings, surrounding the subject to be imaged. These rings are designed to detect annihilation events (gamma-rays) and convert the resulting electrical signals into sinograms that are ultimately reconstructed into tomographic images (FIGURE 5B), following dead time correction, detector normalization, subtraction of random coincidences, attenuation correction, and scatter correction (455).

In the clinic, PET is mainly used to image cancer through the use of the <sup>18</sup>F-labeled imaging agent [<sup>18</sup>F]-2-fluoro-2-de-oxy-glucose ([<sup>18</sup>F]FDG) (see sect. IVA). Whole body clinical PET [<sup>18</sup>F]FDG scans are routinely performed to locate, stage, and monitor cancer. [<sup>18</sup>F]FDG, first synthesized by Ido et al. in 1978 (176), is an analog of glucose whereby the 2-carbon hydroxyl group of glucose has been substituted for a radioactive fluorine atom (<sup>18</sup>F). The extent of [<sup>18</sup>F]FDG accumulation is thought to reflect glucose transporter activity, hexokinase II activity, and more generally, the metabolic requirements of cells (see **FIGURE 13** for mechanism of [<sup>18</sup>F]FDG). Since the metabolic demands of cancer cells are usually very different from most normal cells, and hence [<sup>18</sup>F]FDG accumulation in cancer cells is significantly higher than that observed in most normal cells, it can serve as an effective marker of cancer (**FIGURE 5**B).

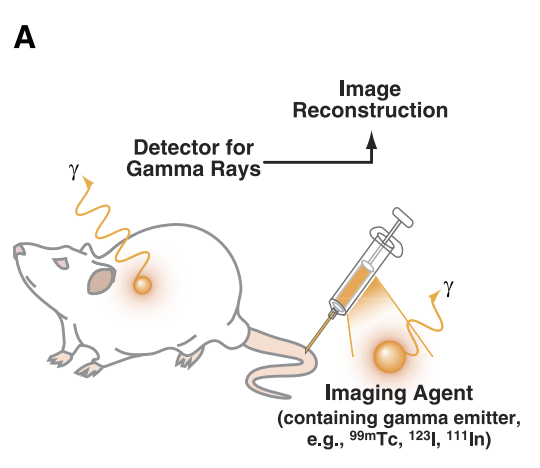
In addition to its clinical utility, PET has a wide range of applications in the basic research and preclinical arenas. For example, PET can be used to investigate basic physiological and molecular mechanisms of human disease through the use of appropriate radiolabeled imaging agents and rodent models (339, 358, 396). Furthermore, PET can be used to

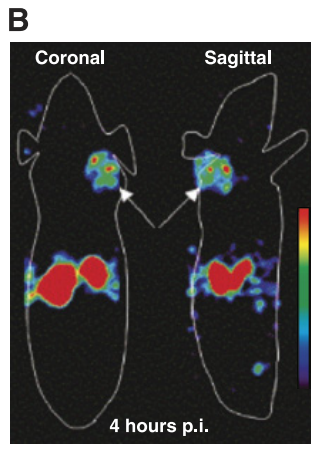
evaluate novel radiolabeled PET imaging agents, effectiveness of new therapies, and biodistribution of novel pharmaceuticals in suitable animal models. When imaging rodents, or other small animals with PET, a dedicated small animal PET scanner is required. These miniaturized PET scanners typically have spatial resolutions of  $\sim 1-2$  mm and sensitivities of  $\sim 10^{-11}$ - $10^{-12}$  M.

B) BASIC PRINCIPLES OF SPECT. SPECT uses nuclides such as  $^{99\text{m}}$ Tc ( $t_{1/2} = 6 \text{ h}$ ),  $^{123}$ I ( $t_{1/2} = 13.3 \text{ h}$ ), and  $^{111}$ In ( $t_{1/2} = 2.8 \text{ days}$ ), which decay via the emission of single gamma rays with differing energies (FIGURE 6). As the nuclides used in SPECT differ from those used in PET, a completely unique set-up is required to collect and reconstruct the data. SPECT employs the use of a gamma camera that rotates around the subject to capture data from numerous positions to obtain a tomographic reconstruction. Since position detection of photons in SPECT does not convey adequate information concerning the origin of the photon, it is not possible to define a "line of response," as done with PET. To address this issue, a lead or tungsten collimator is added to the modality so as to exclude any diagonally incident photons. The disadvantage of this is that the collimator rejects most of the photons that are not traveling at right angles to the crystal, so the sensitivity of SPECT is several orders of magnitude lower than PET. However, recent advances in micropinhole apertures have meant that high-resolution SPECT images are possible (19) with reasonable tradeoff between sensitivity, field of view (FOV), and spatial resolution.

Although the majority of clinically available SPECT compounds do not provide specific biochemical information, SPECT remains the most commonly used nuclear medicine modality in the clinic (236). Some examples of clinical SPECT imaging agents that target molecular processes include the radiolabeled small molecule [99mTc]TRODAT-1 for dopamine transporter (DAT) imaging (173), peptide [111In]-DPTA-octreotide for imaging the somatostatin receptor [intimately associated with small cell lung cancers (SCLC)] (423), and [99mTc]-Annexin V for imaging apoptosis (22). In the last few years, hand-held devices for both PET and SPECT have been developed and used for intraoperative applications (137, 433), and in both cases have proven successful in guiding excisions of various tumors. Van Haren and Fitzgerald (433) reported that [111In]-DPTA-octreotide in combination with an intraoperative hand-held gamma camera device helped identify a nonfunctional neuroendocrine tumor that other techniques, including a CT scan and intraoperative investigation, failed to locate.

Like PET, SPECT also has its own miniaturized instrumentation, known as small animal SPECT, specifically designed for imaging small animals (288) **(FIGURE 6A)**. Small animal SPECT has been used for many preclinical investigations (2) including visualizing dopamine transporters in the rat brain





#### Key Strengths

- Limitless depth of penetration
- Excellent sensitivity
- Multiplexing capabilities
- Clinical utility

## **Key Limitations**

- · Relatively expensive
- Ionizing radiation
- Limited spatial resolution
- Lack of attenuation correction (therefore only semi-quantitative)

**FIGURE 6.** Small animal single photon emission computed tomography (SPECT). A: diagram illustrating the principles of SPECT, i.e., a targeted SPECT imaging agent (containing a gamma emitting radioisotope) is administered to the subject and the gamma rays are detected via a gamma camera (rotated around the subject). The detected gamma rays are then reconstructed into tomographic images, providing information on the location of the imaging agent in the subject. B: SPECT images demonstrating the utility of visualizing gastrin-releasing peptide receptor (GRPR), a receptor often found in high levels in prostate cancer, via the administration of [99mTc]-HABN in mice bearing human prostate xenografts. Arrows point to tumor; clear visualization of tumor is possible at 4 h postinjection (p.i.). [From Ananias et al. (10a). Copyright 2011, American Chemical Society.]

with [123I]-FP-CIT (307), imaging mice bearing glioma (U87MG) xenografts with [125I]-c-Met binding peptide (211), assessing cell death in ischemic-reperfused rat hearts using 99mTc-C2A-glutathione-S-transferase (GST) (254), and imaging GRPR in mice bearing human prostate xenografts using [99mTc]-HABN (10a) (see **FIGURE 6B**), to name a few. In 2005, Beekman et al. (19) reported the development of a new rodent SPECT instrument, called the U-SPECT-I, enabling imaging at submillimeter spatial resolutions. Four years later, the same research group published work on a second generation U-SPECT, called the U-SPECT-II, allowing imaging at resolutions less than half a millimeter (431).

C) KEY STRENGTHS AND LIMITATIONS OF PET AND SPECT. Since biochemical changes generally occur before anatomical changes in disease, PET and SPECT have a clear diagnostic advantage over anatomical techniques such as classical CT and MRI. However, PET and SPECT have a key disadvantage, namely, the lack of an anatomical reference frame. This shortcoming has recently been addressed by combining these instruments with either CT or MRI, producing a single scanner capable of accurately identifying molecular events with precise correlation to anatomical findings (334). This type of approach is known as "multimodality imaging," whereby two or more modalities are used in combination to compensate for the weaknesses of each imaging system whilst exploiting their individual strengths.

Another limitation of radionuclide imaging techniques is their safety profile. Since PET and SPECT both require the use of ionizing radiation, there is a limit to how many scans a subject can have per year. For the general public, the maximum exposure is 5 mSv (millisieverts) per year,

whereas radiation workers can be exposed up to 50 mSv over the same period. This needs to be considered when planning clinical studies.

The key strengths of PET include its excellent sensitivity  $(10^{-11}\text{-}10^{-12} \text{ M})$ , limitless depth of penetration, and quantitation capabilities (TABLE 1). While it is a relatively costly technique and its spatial resolution is limited compared with MRI, it is extremely flexible in terms of the types of imaging agents that can be used to bind specific molecular targets. Imaging multiple different targets simultaneously ("multiplexing") is not yet possible with PET because isotopes that are positron emitters result in the production of two gamma rays with energies of 511 keV. On the other hand, SPECT has some multiplexing capabilities due to different nuclides giving rise to gamma rays with differing energies. This is advantageous when one wishes to image multiple biochemical targets simultaneously.

Other advantages of SPECT (like PET) are its high sensitivity ( $10^{-10}$ - $10^{-11}$  M) and limitless depth of penetration. While SPECT is less expensive and more widely available than PET, it is generally less sensitive and has a lower spatial resolution (8–10 mm, compared with 5–7 mm seen with clinical PET) (27). PET scans have a higher count rate and hence generate images containing less noise that are ultimately easier to interpret. In addition, PET provides the opportunity of attenuation correction, affording quantitative data, whereas this is not possible with SPECT (117, 429).

Unlike MRI and optical imaging techniques, both PET and SPECT only require small mass amounts of imaging agent (nanogram to milligram range), and for this reason radio-

nuclide-based imaging agents used in PET/SPECT studies are usually nontoxic and are unlikely to exert pharmacological effects.

Overall, PET and SPECT are extremely valuable imaging modalites for investigating molecular processes in living intact subjects/patients. Currently both PET and SPECT are being used clinically, and as a research tool, to image a vast range of biological processes and disease states (109, 333).

#### 4. US

Medical US is an imaging tool that exploits the properties and behavior of high-frequency sound waves as they travel through biological tissue. US is a unique modality in the sense that it can be used both for diagnostic imaging and as a therapeutic tool.

A) BASIC PRINCIPLES OF US. Clinical diagnostic US scanners typically use sound frequencies between 1 and 20 MHz (245). During an US study, a transducer (also called a probe) sends and receives sound waves (FIGURE 7A). In simple terms, the transducer converts electrical signals to US waves, the US waves enter the body, and some sound waves are reflected back to the transducer where they are detected and converted into electrical signals. These signals are then processed by a computer and displayed as an image.

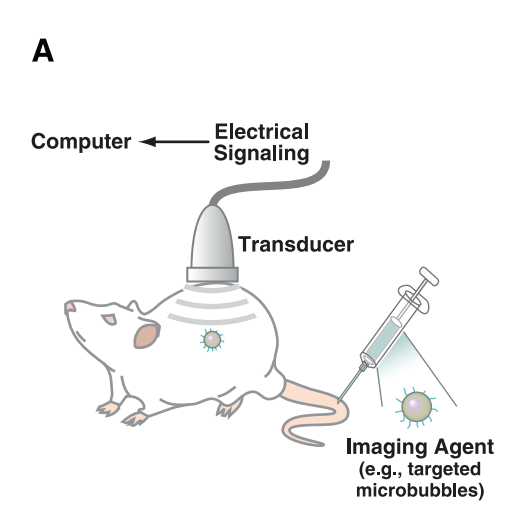
A basic overview of a typical US study is outlined below.

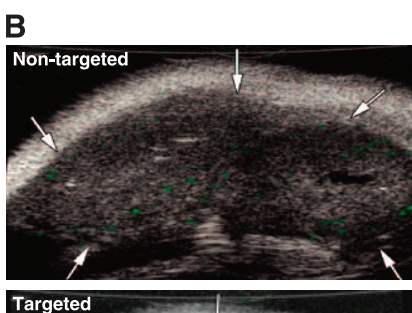
1) Short pulses of high-frequency sound are transmitted into the subject at recorded time intervals by a transducer.

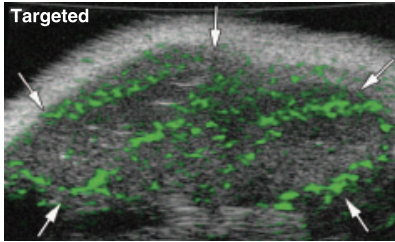
- 2) Sound waves travel through the body and reflect or produce echoes when faced with different tissue interfaces.
- 3) Reflected "sound signature" is analyzed. The distance and direction of any given reflection, with respect to the transducer, can be calculated by using the speed of sound in tissue (5,005 ft./s or 1,540 m/s), the time of arrival and the axis of the sound wave. Amplitude and frequency of the reflections also need to be recorded and assessed. This is important when constructing the two-dimensional image. All of these properties depict information on the internal structures being imaged.
- 4) Analyzed data (distances and intensities of reflections) are used to produce a two-dimensional image

Resolution of US improves significantly with higher frequencies, but at the cost of depth of penetration. This decrease in depth of penetration is due to the fact that highfrequency sound waves possess shorter wavelengths, meaning they are more likely to interact with matter and slow down, thus reducing their traveling distance. Depending on the subject and on the required data, the imager needs to consider resolution versus depth.

B) US USING TARGETED MICROBUBBLES. US, like MRI and CT, has historically been used as a morphological imaging modality. Contrast agents, in the form of gas-filled microbubbles typically coated with lipids or biopolymers, and a few micrometers in diameter, are available for enhancing the reflection signal-to-noise ratio for blood. These microbubbles







#### Key Strengths

- · Relatively inexpensive
- Quantitative data
- No ionizing radiation
- Good temporal resolution Excellent sensitivity with microbubbles
- Clinical utility

#### **Key Limitations**

- · Limited depth of penetration
- Primarily anatomical information
- No multiplexing
- · Limited molecular imaging applications
- · Limited to imaging soft-tissues only (no bone or air structures)
- Coupling of instrument to subject

FIGURE 7. Small animal ultrasound (US). A: schematic illustrating the general principles of molecular imaging using US. After administration of a targeted US imaging agent (e.g., targeted microbubbles), high-frequency sound waves are transmitted into the subject at recorded time intervals by a transducer. The sound wave reflections produced due to traveling through the subject are recorded, converted into electrical signals, analyzed, and constructed (using a computer) into an image representative of the subject's internal structures and the location of targeted imaging agents. The instrument needs to be coupled to the subject via an appropriate coupling medium. B: US images demonstrating the significant advantage of using microbubbles targeted to vascular endothelial growth factor receptor type 2 (VEGFR2) compared with nontargeted microbubbles for visualizing tumor angiogenesis in mice (437). [From Willmann et al. (461), Copyright Radiological Society of North America.]

are several orders of magnitude more reflective than normal blood, predominately due to their ability to resonate within the US field (246). Although these contrast agents have provided useful imaging data, they do not enable imaging of specific molecular events. However, by attaching certain peptides, antibodies, or other targeting moieties to the surface of microbubbles (effectively functionalizing them) these particles can be used to target specific biochemical processes, thus enabling US to be used for molecular imaging purposes (84, 85, 462).

The superior acoustic backscatter response of microbubbles can improve the sensitivity of US significantly, allowing detection of single micron-sized particles (218). Because of their size and inability to escape the vasculature, microbubbles developed for molecular imaging are predominately targeted towards intravascular markers such as antigens like endothelial cell receptors, blood cell markers, or the blood protein fibrin (21).

Targeted microbubbles are currently being used in preclinical investigations of both inflammation and angiogenesis. For example, endothelial cell adhesion molecules have been attached to microbubble shells for visualization of P-selectin, providing insight on molecular aspects of inflammation (250). In addition, moieties targeted toward specific angiogenic markers, including monoclonal antibodies against murine alpha V integrins, have been conjugated to microbubbles for observation of angiogenesis (239). Willmann et al. (461) attached anti-vascular endothelial growth factor receptor-2 (VEGFR2) antibodies to microbubbles, for targeting VEGFR2, an angiogenic marker upregulated on endothelial cells of tumor blood vessels. US imaging studies were conducted using either targeted microbubbles or control microbubbles in tumor-bearing nude mice. Imaging results demonstrated a significantly higher average intensity in images from studies using targeted microbubbles compared with studies using only control microbubbles (461) (see FIGURE 7B). Following these results, Willmann et al. (460) investigated the use of a dual-targeted microbubble for visualization of angiogenesis by conjugating two different antibodies known to bind different markers of angiogenesis, VEGFR2 and  $\alpha v \beta 3$  integrin, to the shell of perfluorocarbon-filled microbubbles. Results from these US imaging studies, using human ovarian cancer xenograft tumor model in mice, showed that dual-targeted microbubbles provided superior images compared with that of microbubbles targeted at one or the other angiogenic marker (either VEGFR2 and  $\alpha v \beta 3$  integrin) (460).

The specific in vivo binding of targeted microbubbles, and their whole body biodistribution can be evaluated by techniques like intravital microscopy (IVM) and PET, respectively (459). In the near future molecular imaging using US is expected to transition from a preclinical mo-

dality to a fully clinically useful technique through the use of different clinically translatable instrumentation, such as endoscopes (345, 459), and novel US-compatible imaging agents that are able to extravasate (e.g., silica nanoparticles) (190).

C) KEY STRENGTHS AND LIMITATIONS. The main strengths of US include its relative cost effectiveness, wide availability, portable nature, good temporal resolution, good safety profile (no ionizing radiation), and excellent sensitivity (picogram level) when microbubbles are used. On the other hand, US is limited by its difficulty in imaging structures that contain bone or air, due to the tendency of air and bone not to transmit sound waves and also by its limited depth of penetration (see TABLE 1). Other limitations of US include the fact that 1) the instrument needs to be coupled to the subject via a coupling gel, 2) it primarily affords anatomical information, and 3) multiplexing is not currently possible. Furthermore, microbubbles are very large and are limited to intravasculature molecular targets, and at high US frequencies (still within the allowable limits) numerous microbubbles are damaged, in effect destroying the tool required for visualizing molecular events of interest (246).

Of all the molecular imaging agent-based techniques, targeted US imaging is one of the more recent, and due to being in its infancy will most likely see an enormous expansion in the near future.

## 5. Optical fluorescence and bioluminescence imaging

The visualization of cells and tissues using light has long been one of the most informative and facile approaches in basic research and medical diagnostic imaging. Since the construction of the first microscope in 1674 by Anton van Leeuwenhoek, much progress has been made (370). Useful microscopy techniques have been developed, including bright field, dark field, and differential interference contrast, the latter of which provides notable depth of resolution and three-dimensional optical effects. Over the past two decades, the introduction of fluorescence microscopy has revolutionized the field of cellular biology. Fluorescence microscopy typically involves the use of genetically encoded fluorescent reporters, or fluorescent-tagged molecules, either of which can be used to facilitate the visualization of molecular events in living cells and other ex vivo tissue samples, in real time. Through the use of fluorescent microscopy, researchers have been able to observe intracellular protein-protein interactions and other micro-scale events (such as gene delivery and RNAi knockdown) in live intact cells. Please see the following references for detailed information on live cell fluorescence microscopy (65, 104, 301, 330, 399,

Alongside the developments in live cell fluorescent microscopy, a number of macroscopic optical imaging modalities have emerged. These macroscopic imaging techniques enable noninvasive, repetitive, whole body imaging of living small animals using sizable fields of view (ranging from several millimeters to several centimeters). Two examples of such macroscopic optical techniques are fluorescence and bioluminescence imaging.

The required infrastructure for optical fluorescence and bioluminescence imaging, namely, a charge-coupled device (CCD) camera and a source of filtered light, is relatively inexpensive and easy to setup. For increasing sensitivity, a cooled CCD camera is also often used. Imaging sensitivities achievable with these techniques are typically very good (as low as picomolar to femtomolar concentrations; TABLE 1), and since they involve the detection of low-energy photons, as opposed to high-energy gamma rays detected by PET and SPECT, they are considered relatively safe. However, the use of low-energy photons means that the depth of penetration is limited to only a few centimeters, which makes it virtually impossible to study deep tissues in large animals or human subjects, unless one uses endoscopes or their equivalent to get closer to the tissue(s) of interest. This limitation cannot be overcome by using a higher intensity laser due to the risk of overheating the tissue/system being studied (80). Depth of penetration is not so much of a problem in mice and small animals (no bigger than a rabbit) due to their size. In fact, many of the commonly used fluorescent and bioluminescent imaging agents can be visualized in internal organ structures of small animals (80), making these optical imaging techniques suitable for preclinical research.

The following definitions for absorption, attenuation, scatter, and transmission apply in this section, unless the context otherwise requires.

Absorption is the process by which energy of light is transferred to a medium through which it is moving.

Attenuation is the progressive loss of intensity (of a signal, electric current, or other oscillation) through a particular medium.

Scatter is the diversion of (light, sound, or other) particles from a straight path due to variabilities in the medium they are traveling in.

Transmission is the process by which particles (light, sound, or other) pass through a medium without being scattered or absorbed.

A) FLUORESCENCE IMAGING. One of the most exciting and important developments in the field of imaging over the past

decade has been the introduction and use of fluorescent proteins. Please refer to the following reference (65), published in 2010 in *Physiological Reviews*, for a detailed discussion regarding fluorescent proteins and their applications in imaging. In addition, please see our supplementary section for a brief summary of fluorescent proteins, their different spectral classes, ideal characteristics, and some key references concerning their use in molecular imaging. It is important to note that in addition to fluorescent proteins, fluorescent dyes, and other materials with fluorescent properties can also be used in fluorescent molecular imaging studies. We will now describe some of the key steps and considerations involved in conducting a fluorescence imaging experiment.

I) Fluorescence imaging experiment. When attempting to pass light through biological tissues there is one major challenge: overcoming attenuation and scattering of light. Absorption of light by hemoglobin and other molecules (such as water) may reduce fluorescent signals by a factor of  $\sim 10$ , per centimeter of tissue (67). Organs with high vascular content, such as the liver and spleen, have the lowest transmission, due to absorption of light by oxy- and deoxyhemoglobin. Skin and muscle, on the other hand, have high transmission of light. By taking advantage of the near-infrared (NIR) part of the electromagnetic spectrum, one can overcome the problem of scattering and attenuation to a certain extent. For example, by choosing fluorescent-based imaging agents with emission wavelengths between 650 and 900 nm, absorption of light by cytochromes, hemoglobin, and water within living organisms is lowest. Fluorescent imaging agents that emit light in this region can be imaged at greater depths and can increase the sensitivity of the technique by significantly decreasing the extent of tissue autofluorescence (fluorescent signal from tissues where no imaging agent is present) (80, 261).

A general molecular imaging study using fluorescence imaging in living intact subjects involves the following steps:

1) Selection of a fluorescent entity (e.g., a protein, chemical, dye, or other molecular entity possessing fluorescent properties) with suitable properties (e.g., emission wavelength, photostability) for the particular imaging study. In the case of using a fluorescent protein, such as GFP, one must either A) transfect the GFP reporter gene into a cell-line of interest, B) purchase a transgenic animal already expressing the reporter gene of interest, or C) fuse the cDNA of GFP to the gene for a target protein of interest. If, on the other hand, the fluorescent entity is a dye, it typically needs to be conjugated to a peptide/aptamer/antibody/nanoparticle designed to specifically target the protein or molecular pathway of interest prior to conducting the study. One also needs to decide whether an activatable imaging agent is better suited for the study (i.e., an imaging agent that only fluoresces or "switches on" after it interacts with its target)

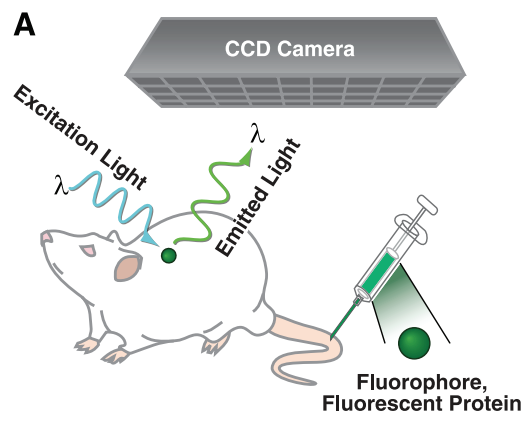
(see sect. III for more information on activatable/smart imaging agents).

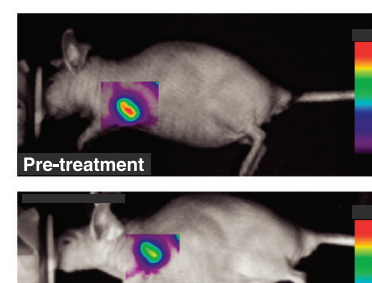
- 2) Identification of an external light of appropriate wavelength for excitation of the chosen fluorescent molecule/protein/entity.
- 3) Injection of subject with suitable amount of the fluorescent imaging agent. If, however, a genetically encoded reporter protein is used for fluorescence, there is no need to administer an exogenous fluorescent imaging agent.
- 4) Application of external light source. This will trigger an immediate emission of light that will be lower in energy and longer in wavelength than the excitation light from places that the fluorescent imaging agent has accumulated in the subject. The emitted light then travels back out of the subject and is detected by a CCD camera (276). Additionally, it is important to allow sufficient time for unbound imaging agent to clear from the tissues of interest prior to imaging, to improve the signal to background ratio (the timing of this will vary depending on the pharmacokinetics of the imaging agent used).
- 5) Conversion of recorded light photons into electrons, and subsequent formation of an electric charge pattern that parallels the intensity of emitted photons through the use of semi-conductors.
- 6) Collection of received data (charge pattern) from the CCD, which is then fed into an output register and amplifier, whereby it is collated and analyzed by a camera con-

troller that is connected to a computer system. A final image is usually formed showing number of photons from different regions of the subject.

As far as types of fluorescent entities go, there is a rapidly expanding list, that includes near IR Cy 5.5, the Alexa Dye Series, indocyanine green, quantum dots (QDots), and a variety of fluorescent proteins. Examples of fluorescent proteins include GFP, which emits light at 509 nm when excited by 395 nm, and red fluorescent protein (RFP), which emits light at 618 nm (see sect. VII for more information on fluorescent proteins). A recent addition to the list of fluorescent entities is the lanthanide-based imaging agents. These agents have a number of advantages over the aforementioned dyes and proteins, namely, their remarkably long luminescence lifetimes, and narrow, nonoverlapping emission bands, allowing quantitative, multiplexed measurements of the intracellular analyte concentrations (414) (see **FIGURE 8**).

Quantification of fluorescent optical imaging experiments is not entirely straightforward. Variations in the extent of light attenuation in different organs and tissues need to be accounted for (e.g., less light will be detected from the same number of Qdots/Cy 5.5 molecules/GFP in the liver compared with the lung) (263). Also, there are "surface weighting" problems, meaning that anything closer to the surface will appear brighter. These factors need to be taken into consideration when analyzing data and drawing conclusions from any given fluorescence study. A comparison of different optical instruments and their performance is detailed elsewhere (204, 297).





В

#### Key Strengths

- Relatively inexpensive
- User friendly
- Multiplexing capabilities

#### Key Limitations

- Limited depth of penetration
- · Poor spatial resolution at greater depths
- Surface weighted images
- Autofluorescence

**FIGURE 8.** Optical fluorescence molecular imaging. *A*: schematic showing the general principles of molecular imaging using optical fluorescence. Following the administration of a fluorescent imaging agent (fluorophore, fluorescent protein, GDot etc.), an excitation light of appropriate wavelength is used to illuminate the subject. In the case of using a protein such as GFP, one must first transfect the GFP reporter gene into the cell-line of interest or one can purchase a transgenic animal already expressing the reporter gene of interest, and then illuminate the subject. This leads to excitation of the fluorophore/fluorescent protein and the subsequent emission of light. The light is detected via a CCD camera, collated, analyzed, and converted into an image detailing the location of emitted light (due to imaging agents) from subject. *B*: fluorescence images demonstrating the feasibility of visualizing human epidermal growth factor receptor-2 (HER2) positive xenografts in mice using AlexaFluor68O-labeled-affibody as an imaging agent. Through this imaging strategy, Van de Ven and colleagues were able to monitor response of HER-2-positive tumors to treatment with heat shock protein 90 (HSP90) inhibitor (425). [From Van de Ven et al. (425), with permission from American Association for Cancer Research.]

Fluorescence optical imaging can be used for a variety of molecular imaging applications in living subjects. Some specific examples include the study of matrix metalloproteinases activities using activatable imaging agents (35, 447), detection of human epidermal growth factor receptor 2 (HER2/neu)-tumors in animal models using antibodies conjugated to rhodamine green (229), monitoring tumor growth and metastases using GFP-expressing tumors (161), and NIR activatable fluorescent imaging agents for imaging Alzheimer's disease that only "switch on" when bound to amyloid-beta (Abeta) protein (348).

The advent of fluorescence molecular tomography (FMT) has led to three-dimensional reconstruction of fluorescent imaging agent accumulation in living animals based on light recordings collected at the tissue boundary. FMT has been used to visualize and quantitate a variety of cellular and molecular events, and as opposed to planar fluorescence imaging, yields quantitative information and allows imaging at greater depths, up to several centimeters (309). An example of a study using FMT is that by Haller et al. (144) in 2008, whereby FMT was used to quantitate pulmonary response in a murine mouse model of LPS-induced airway inflammation. Time domain imaging has also been used to obtain depth information for optical fluorescence imaging, and reviewed elsewhere (203).

II) Key strengths and limitations. Fluorescence imaging has a number of limitations that need to be considered, including its limited depth of penetration (<1 cm) and the potential toxicity of some of the imaging agents it employs (e.g., QDots which are cadmium based) which may limit its use in humans. Also, the mass amount of fluorescent agent needed for imaging is considerably larger than for radionuclide imaging (see TABLE 1). Furthermore, fluorescence imaging suffers from issues associated with autofluorescence that ultimately decreases the sensitivity of the technique. There are a number of strategies and factors that can improve overall sensitivity of fluorescence imaging, including methods that correct for autofluorescence, the type of imaging agent selected, and the type of imaging instrumentation used.

Overall, fluorescence molecular imaging is a versatile technique with a number of key advantages including its relative low cost (especially when studying reporter gene systems in animals), and the fact it does not require the administration of a substrate like bioluminescence imaging does. Fluorescence optical imaging serves as a useful tool for preclinical evaluation of imaging agents prior to moving them into other more expensive modalities. One of the most important strengths of fluorescence imaging is that it enables multiplexed imaging. Furthermore, there is potential for clinical translation where depth of penetration is not an issue, for example, in the endoscopy setting as well as intraoperative techniques.

III) Clinical translatability. Potential clinical applications for optical fluorescence imaging include intraoperative devices, dedicated breast imaging, and endoscopy-related imaging instruments. Recent developments in instrumentation such as dual-axes endoscopes (253) and handheld probebased optical imagers (28, 128), coupled with the use of fluorescent molecular imaging agents targeted at disease, could be extremely useful in detecting and/or treating numerous pathologies early and accurately. A specific example of an optical molecular imaging technique that has undergone preliminary evaluation in a clinical setting is a colonoscopy-based technique involving the use of a fluorescein-labeled heptapeptide (identified via phage display screening of peptide libraries) and a standard colonoscope fitted with a fluorescence confocal microendoscope fed though the instrument channel, to detect dysplastic colonocytes (colorectal cancer). Initial results demonstrated that fluorescent-labeled heptapeptides bound more strongly to regions containing displastic colonocytes compared with adjacent normal tissue (170).

B) BIOLUMINESCENCE IMAGING. *I) Basic principles*. Bioluminescence relies on the production of light from the enzymatic oxidation reaction of luciferase with its substrate. Different luciferase enzymes can be introduced into a biological system as a molecular reporting device (see **FIGURE 9A**). These enzymes are usually introduced into cells via transfection with the gene that encodes them. Unlike fluorescence imaging, bioluminescence does not need an external light source. Due to this, and because tissues do not exhibit endogenous bioluminescence, greater sensitivities and higher signal to background ratios can be achieved compared with fluorescence techniques.

There are several types of luciferase enzymes that have been discovered in nature (some of which are listed below), each requiring different conditions for the enzymatic reaction to proceed.

- 1) FLuc (North American firefly luciferase, *Photinus pyralis*): molecular mass = 62 kDa. This luciferase is the most commonly used bioluminescent reporter. It requires benzothiazoyl-thiazole luciferin (D-luciferin), and oxygen, ATP, and magnesium as cofactors. FLuc is found in the cytoplasm, where it oxidizes its substrate D-luciferin, emitting light with a broad spectrum (530-640 nm) and a peak at  $\sim 560$  nm (374). Light from FLuc peaks at  $\sim 10-12$  min after injection of D-luciferin and then decreases slowly over 60 min. Because it emits at wavelengths above 600 nm, it is able to travel through several centimeters of tissue (353, 360). D-Luciferin distributes throughout the animal very rapidly and is able to cross the blood brain barrier.
- 2) RLuc (sea pansy luciferase, *Renilla reniformis*): molecular mass = 34 kDa. RLuc requires a different substrate compared with FLuc. Instead of D-luciferin, RLuc interacts

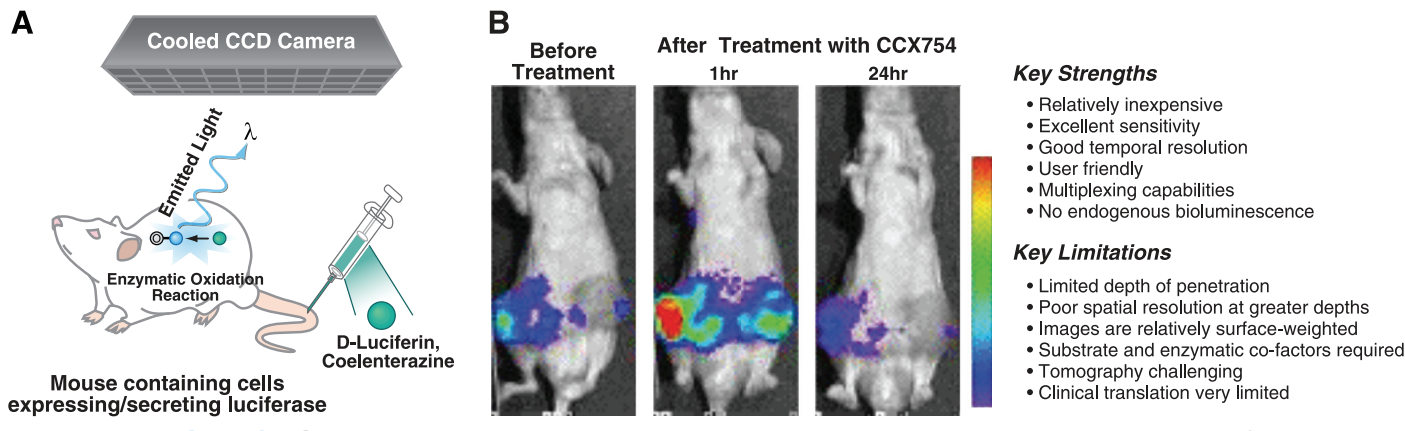


**FIGURE 9.** Optical bioluminescence molecular imaging. *A*: schematic illustrating the general principles of molecular imaging using optical bioluminescence, i.e., first a small animal model needs to be developed that is capable of expressing/secreting one of the luciferase enzymes (this could be a transgenic mouse or a rodent that has been injected with cells that can express/excrete luciferase). Second, an appropriate substrate needs to be administered to the animal; this will lead to production of light from the enzymatic oxidation reaction of luciferase with its substrate. The light is then detected via cooled CCD cameras and an image is produced. *B*: bioluminescence images demonstrating the feasibility of monitoring changes in chemokine receptor dimerization over time (before and) after treatment with pharmacological agent (CCX754). This study used a protein fragment complementation strategy based on firefly luciferase (FLuc) (262). [From Luker et al. (262).]

with coelenterazine (and its analogs) and requires oxygen as a cofactor but does not need ATP and Mg<sup>2+</sup>. This is a potential advantage as it is less likely to cause perturbation in the cells it is present in since it does not "steal" ATP from other processes or pathways. RLuc releases blue light across a broad range, peaking at 480 nm (280). This is not the most favorable emission wavelength as it is not red-shifted and so cannot penetrate tissues as easily as light with a red-shifted wavelength. RLuc is found inside cells and thus its substrate, coelenterazine, must pass through cell membranes to interact with it. RLuc is rather hydrophobic and tends to self-associate, forming inactive dimers and higher molecular weight species (280). RLuc also has a low quantum yield, 6% compared with >88% for FLuc (280, 409). However, it is important to note that several mutants of RLuc have been developed that allow for greater stability and/or red-shifted emission (255, 256). Furthermore, the RLuc protein can be used outside of the cell where ATP is scarce. Thus, instead of introducing a RLuc gene into cells, one can introduce the protein directly in vivo. This technique can be used, for example, to image a cell-surface receptor by fusing RLuc to an engineered antibody (436).

3) GLuc (marine cope pod luciferase, Gaussia princeps): GLuc is the smallest identified luciferase (molecular mass = 19.9 kDa). Similar to RLuc, GLuc is independent of ATP, but requires coelenterazine and oxygen. GLuc is secreted from the cells it is present in and reacts with its substrate in the extracellular space. GLuc emits light at a peak of 480 nm, but with 200-fold higher bioluminescence output compared with RLuc when present in mammalian cells under similar conditions in vivo. Moreover, GLuc displays a significantly more intense signal than RLuc and a comparable signal to FLuc in subcutaneous tumors in mice (409); however, its emission half-life is very short. Mutants of GLuc

have been developed to address this issue, and the resultant proteins display much longer luminescence half-lives (453). Further studies are needed to clarify some issues related to absolute signal differences between these luciferases, due to the intracellular signal verses signal from secreted protein.

The limited biodistribution, rapid clearance rates, and poorer signal-to-background of the coelenterazine substrates are unfavorable and directly related to sensitivity of detection and predictability of the models that use either RLuc or GLuc. These factors along with the blue emission wavelength of these enzymes have somewhat limited their use (261). However, the mutants of RLuc are helping to solve some of these limitations (255, 256).

Bioluminescence imaging has been used to investigate numerous enigmatic protein-protein interactions. One such study used a firefly luciferase-based protein fragment complementation assay to visualize and assess interactions between CXCR4 and β-arrestin molecules. CXCR4 is a chemokine receptor that modulates tumor growth and metastasis; its interaction with  $\beta$ -arrestin molecules is a process that occurs in the initial stages of chemokine receptor signaling (337). Other applications of bioluminescence imaging include drug screening (e.g., evaluating kinase inhibitors by measuring their phosphorylation efficiency via split firefly luciferase-assisted complementation system) (50), examining the roles of various cells though cell tracking (e.g., visualizing luciferase-expressing bone marrow cells in brain inflammation in living mice) (4), and visualizing receptor dimerization via a protein fragment complementation strategy based on FLuc (see FIGURE 9B).

II) Key strengths and limitations. One of the main advantages of bioluminescence imaging compared with fluores-

cence imaging is its higher sensitivity due to enzymatic amplification of signal and low background signal due to the lack of natural bioluminescence from tissues (however, it should be noted that substrates themselves also lead to background signals, especially in the liver in the case of coelenterazine). Although bioluminescence imaging has limited depth of penetration like fluorescence imaging, its primary limitation is getting light out of the subject, whereas fluorescence imaging is limited by both the ability to pass light into and out of a subject. Overall bioluminescence imaging is a relatively cost effective technique for investigating fundamental biochemical processes. Its multiplexing capabilities, by combining different luciferases/substrates, make it a flexible and highly useful modality. The substrate requirements of bioluminescence may limit its clinical translatability.

C) BIOLUMINESCENCE RESONANCE ENERGY TRANSFER. Fluorescence resonance energy transfer (FRET) and bioluminescence resonance energy transfer (BRET) technology involves the nonradiative transfer of energy between a donor and acceptor molecule by the FÖRSTER mechanism (9, 291). FRET has long been considered a powerful method in cell culture for studying complex interactions including the interaction of two proteins (154, 281). Since FRET depends on an excitation source, it is less suited for applications in living subjects. BRET does not require an excitation light source and instead uses a bioluminescent protein as a donor. This donor if in close proximity to an acceptor (e.g., fluorescent protein or QDot) will lead to a resonance energy transfer, and therefore detectable signal (393). BRET can be used to study the interaction of two proteins of interest in living subjects (72, 74, 329). An alternative to BRET for the study of protein-protein interactions is the use of split reporters. In this case, a biochemical event of interest brings together two split reporter proteins through complementation or reconstitution, and produces a signal in the presence of the bioluminescence substrate. Further details of split reporter strategies and BRET are covered extensively elsewhere (126, 277, 325-328, 440, 458).

D) CERENKOV LUMINESCENCE IMAGING. Recently, another technique for imaging photons known as Cerenkov luminescence imaging (CLI) was described (356). CLI exploits the fact that radionuclides can emit visible light consistent with Cerenkov radiation (CR), a form of electromagnetic radiation produced when a charged particle exceeds the speed of light while traveling in a dielectric medium. The resulting light produced by radionuclides is a continuous spectrum mainly in the ultraviolet blue bands of the electromagnetic spectrum. In 2009, Robertson et al. (356) demonstrated the imaging of mice injected with [<sup>18</sup>F]FDG using an optical imaging instrument fitted with highly sensitive CCD detectors. Similar studies were reported at around the same time by Lui et al. (252), whereby a range of radioisotopes (beta<sup>+</sup>,

beta and gamma-emitters) were evaluated for their use in optical imaging (252).

# **B.** Emerging Modalities and Techniques

## 1. Raman imaging

Raman spectroscopy (RS), also known as "spontaneous Raman spectroscopy," is a spectroscopic technique used to probe the internal structure of molecules. Traditionally, RS has been used as an analytical chemistry tool for studying alterations in chemical bonding (e.g., when a substrate interacts with its corresponding enzyme). More recently, RS has shown potential in a clinical setting as a diagnostic tool, providing a means for discriminating between disease and normal tissue, through detecting endogenous spectra. The diagnostic capabilities of RS were initially explored ex vivo using rat and pig organ samples and traditional RS instrumentation (258, 266). The success of these studies led to the development of a Raman-based clinical molecular imaging modality by adding a Raman component (fiber-optic bundle) to a standard white light endoscope (384). By using this Raman-modified endoscope, Shim et al. (383) demonstrated that Raman spectra of human gastrointestinal tissues could be obtained with acceptable signal-to-noise ratio and good temporal resolution. Moreover, through the use of diagnostic algorithms for classifying colon polyps based on their spectral characteristics, adenomatous polyps could be differentiated from hyperplastic polyps with great accuracy (296, 383).

A) BASIC PRINCIPLES OF RS. When a beam of monochromatic light is used to excite a molecule, most photons are scattered elastically (Rayleigh scattering). However, 1 in every 10 million incident photons are scattered inelastically (known as Raman scattering) and display a shift in frequency compared with the frequency of the excitation light. The size of this observed shift in frequency, called the "Raman shift," is independent of the excitation frequency and is thus an intrinsic characteristic of the matter being studied. Essentially, every molecule has its own unique vibrational signature or "spectral fingerprint," meaning that RS can be used to detect numerous different molecules within the same region of interest simultaneously, demonstrating its high multiplexing capabilities (456, 479). This is extremely important in the context of molecular imaging, as being able to visualize more than one biochemical target simultaneously will likely yield a more complete picture of biological systems.

There are two types of Raman scattering: stokes and antistokes. The former occurs when the molecule being studied absorbs energy from incident photons, thus resulting in a scattered photon with lower frequency compared with that of the laser source. Whereas, anti-stokes scattering is where the molecule loses energy, resulting in a scattered photon of higher frequency.

Although spontaneous RS is a technique with high molecular specificity, it suffers from extremely poor sensitivity due to the low numbers of inelastically scattered photons. Newer RS techniques have emerged that address this issue of sensitivity, namely, 1) stimulated Raman scattering (SRS) and 2) surface enhanced Raman scattering (SERS). We next discuss SERS and its molecular imaging applications. See also section VII for a brief discussion of SRS.

B) SERS. SERS is a surface-sensitive technique that was discovered over 30 years ago through studies that demonstrated a distinct enhancement of a pyridine molecule's vibrational spectra following its adsorption on an electrochemically roughened silver electrode (1). Since then, there has been much debate concerning the exact mechanism behind this observed phenomenon. The two main theories at present are as follows: 1) the electromagnetic theory (involving the excitation of localized surface plasmons), and 2) the chemical theory (relying on chargetransfer).

C) THE SERS EFFECT EXPLAINED. The SERS effect can simply be described as an enhancement of Raman scattering from a molecule. This effect is observed when a molecule is placed in close proximity to a metal substrate (456). The number of inelastically scattered photons can be increased by several orders of magnitude, and as a result, the vibrational signature of a given molecule becomes more intense, and in some instances, peaks that were previously undetectable using standard RS techniques become much easier to detect. The degree of SERS enhancement and the reproducibility of any given SERS spectral fingerprint greatly depends on the type, quality, size, and shape of the metal substrate used. This is mainly because these factors have a direct effect on the ratio of absorption and scattering events, and they also influence the localized surface plasmon resonance (LSPR) excitations excited at interstitials or sharp edges. These LSPR excitations are thought to be the key players behind the huge enhancements seen with SERS (169).

Due to the high sensitivity and multiplexing capabilities of SERS, there has been a growing amount of interest concerning the use of this technique for imaging molecular processes in biological systems (480). Much work has been centered around the investigation of "Raman-active" nanoparticles (see sect. IIIE for details on these types of imaging agents). In brief, Raman-active nanoparticles (or SERS nanoparticles) are known to significantly enhance the Raman scattering efficiency (221) and thus improve the detection limits (sensitivity) of the technique to around three orders of magnitude lower than that achievable via fluorescence imaging (101). By administering different SERS nanoparticles (**FIGURE 10A**), one can theoretically visualize several targets simultaneously. This is a major advantage, especially compared with modalities such as PET, where there are no easy possibilities for multiplexing. A recent study demonstrated the multiplexing capabilities of Raman active gold nanoparticles in living animals using normal mice (203) (see **FIGURE 10***B*).

An important aspect of SERS molecular imaging is the process of "targeting" these SERS particles to specific biomarkers of disease. This can be achieved by conjugating certain peptides, antibodies, or other molecular entities specific for particular receptors/enzymes/targets to the SERS particles, a process also known as "functionalization." Two separate studies have demonstrated the feasibility of imaging epidermal growth factor receptor (EGFR) positive tumors in mouse models using targeted SERS particles (192, 346). Other groups have conjugated different molecular entities

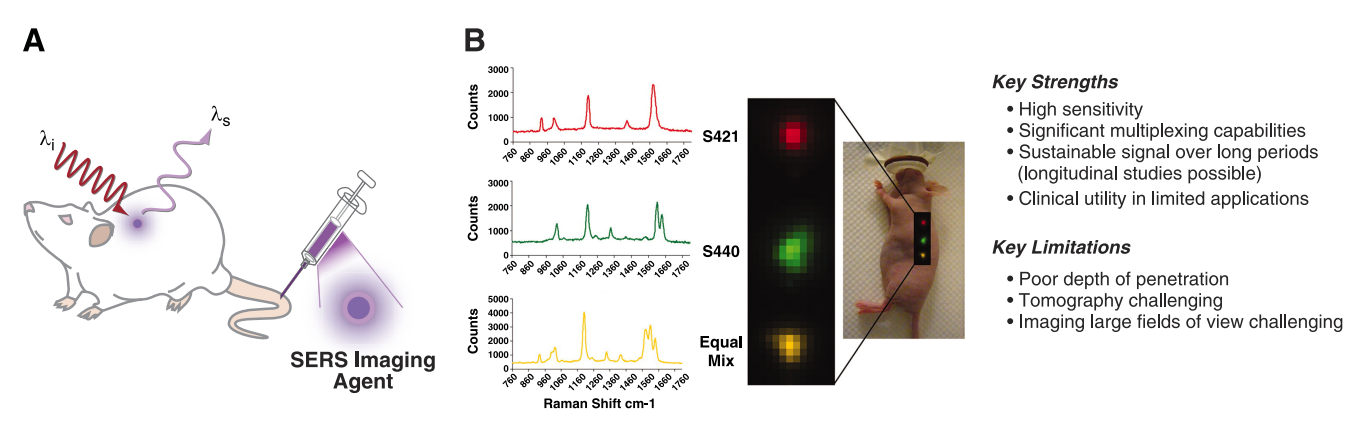


FIGURE 10. Surface enhanced Raman scattering (SERS) imaging. A: schematic illustrating the basic principles of SERS molecular imaging. The diagram shows the administration of SERS imaging agents (e.g., gold-based Raman-active nanoparticles) that can be functionalized with targeting ligands (e.g., peptides, aptamers, antibodies) specific for a particular disease process. An excitation laser (λi) is used to illuminate the subject, and the inelastically scattered light (λs) from the localized SERS imaging agents is collected and translated into a spectrum, mapping the accumulation of imaging agent within a certain region of the subject. B: illustrates the multiplexing capabilities of SERS imaging. Multiple batches of SERS nanoparticles (shown here as S421, S440 and equal mix), each with their own unique spectral fingerprint, can be administered simultaneously with the potential to look at multiple molecular processes (204). [From Keren et al. (204).]

to gold nanoparticles; however, many are yet to be evaluated in intact living animals. One such study showed the successful detection of HER2 cancer markers in MCF7 cells (containing high levels of the target) using antibody-conjugated hollow gold nanospheres (237). Further imaging studies, in living intact subjects, using different SERS imaging agents and various animal models of disease are required to determine the usefulness of SERS molecular imaging.

D) KEY STRENGTHS AND LIMITATIONS. Overall, Raman-based molecular imaging, and in particular SERS imaging, is a promising new area of research. The sensitivity of SERS and its multiplexing capabilities are major strengths of the technique (TABLE 1). Also, the fact that Raman signals are detectable over long periods of time (without issues of photobleaching) means that longitudinal studies are feasible. SERS imaging, however, is not without its shortcomings, including its extremely limited depth of penetration (~5 mm) and difficulties with imaging large fields of view. Ultimately these limitations, along with tomography challenges, mean that one cannot perform whole body deep tissue imaging with SERS-based techniques. Thus most future clinical applications of SERS imaging will be geared toward situations where depth of penetration is not an issue, such as endoscopy.

## 2. Photoacoustic imaging

First reported by Alexander Graham Bell in 1880 (24), the photoacoustic effect is an important phenomenon that can be exploited for imaging purposes. The effect itself can be described as the production of sound waves resulting from the absorption of light. As an emerging imaging modality, photoacoustic imaging (PAI) has the potential to facilitate the investigation of anatomical and/or biochemical features of both normal and disease states in living subjects in a noninvasive manner.

A) BASIC PRINCIPLES OF PAI. One can use what is known about the photoacoustic effect to probe the structure and organization of microvasculature in small animals without the need for an exogenous imaging agent. This is achieved by illuminating laser pulses, lasting several nanoseconds, at the tissue of interest. These IR light pulses lead to a slight localized heating of the tissue causing thermoelastic expansion and the subsequent production of ultrasound waves. The resulting acoustic waves can be detected on the skin surface, and by measuring the wave's amplitude and the time of arrival, the structure of blood vessels can be determined (388). It is important to note that the input source does not need to be IR light, but can also be other forms of energy, including radiofrequency.

B) THE DIAGNOSTIC POTENTIAL OF PAI. Most diseases, particularly in their early stages, do not exhibit an endogenous photoacoustic contrast, thereby limiting the sensitivity and

specificity of PAI as a stand-alone technique. The sensitivity issue can be addressed by introducing imaging agents that possess a superior ability to absorb light and hence produce strong photoacoustic signals. Examples of some PAI-compatible imaging agents include methylene blue, singlewalled carbon nanotubes (SWNTs), and gold nanoparticles. An example of a specific application of one of these agents is the use of nontargeted gold nanocages for PA imaging of a sentinel lymph node (394). To address the specificity issue and use PAI for investigating biochemical processes (thus transforming it into a molecular imaging modality), one must attach a targeting moiety (e.g., small molecule, peptide, aptamer, antibody) to a photoacousticcompatible imaging agent. For example, one could conjugate cyclic Arg-Gly-Asp (RGD) to SWNTs [RGD is a peptide known to bind alpha-v beta-3 ( $\alpha_v \beta_3$ ) integrins, which are dramatically upregulated in cancer] (112). Functionalizing SWNTs with targeted peptides like RGD enables them to specifically "home in" on cancer cells. A study performed by our laboratories investigating photoacoustic detection of SWNTs in xenograft tumor mouse models demonstrated that the photoacoustic signal in tumors was eightfold higher in the mice that were injected with targeted RGD-SWNTs compared with those injected with nontargeted nanotubes (78) (FIGURE 11B). These results were validated ex vivo using Raman microscopy by taking advantage of the strong Raman signal of SWNTs at 1,593 cm<sup>-1</sup> (204). This study and those similar (209, 268) demonstrate the utility of targeted nanoparticles and PAI for specific and sensitive detection of biochemical markers implicated in disease states of interest. Recently, the utility of a trimodality nanoparticle (capable of producing a MRI, photoacoustic, and Raman signal) was demonstrated for imaging and intraoperative margin determination in an orthotopic glioma rodent model (213) (see sect. IIIF for details).

C) KEY STRENGTHS AND LIMITATIONS. One of the main advantages of PAI is its depth of penetration ( $\sim$ 6 mm to 5 cm), which is superior to that of most optical techniques (388). Additionally, the spatial resolution of PAI is not adversely affected by increases in depth of penetration, as is typically the case with some other optical modalities and US. Furthermore, its ability to afford endogenous information without the need for an imaging agent, favorable temporal resolution (up to  $\sim$ 30 frames per second in some reported systems), and relatively modest cost, add to the attraction of PAI.

When compared with US, PAI has a couple of key advantages: 1) the amount of imaging agent used for PAI is picograms to micrograms, whereas US requires microgram to milligram amounts of imaging agent; and 2) US images contain speckles (noise) due to coherent addition of sound waves. In the case of "light in and sound out, PAI" there is very minimal interference for the sound waves on their way out; therefore, the images are speckle free.

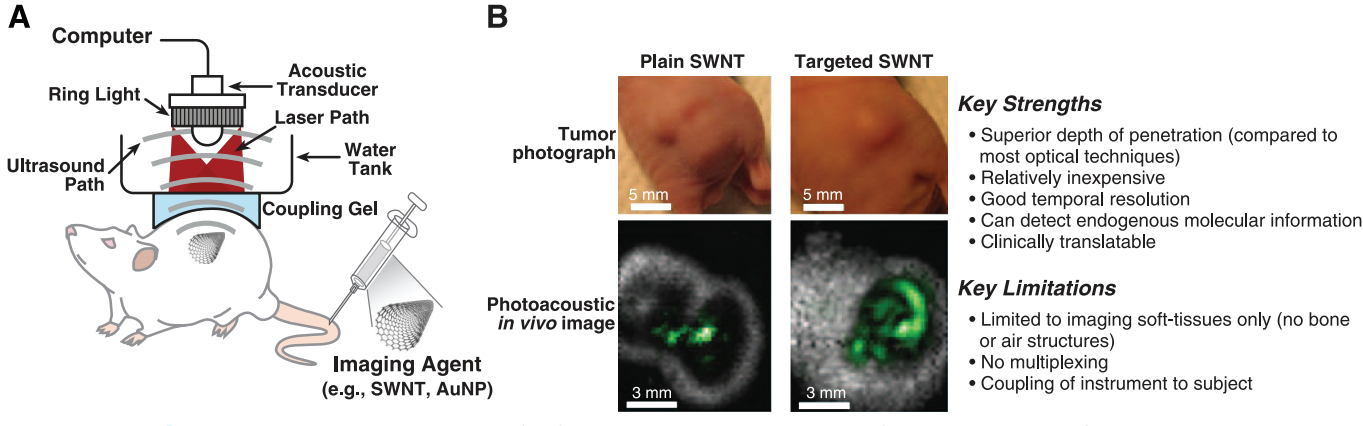


**FIGURE 11.** Photoacoustic imaging (PAI). A: schematic representation of the basic concept of PAI. Following the administration of an imaging agent with strong light-absorbing capabilities [e.g., single-walled carbon nanotubes (SWNTs) or gold nanoparticles (AuNPs)], light is illuminated on the subject. A photoacoustic signal is produced due to PAI-compatible molecules heating up upon light absorption, and the subsequent emission of sounds waves. These sound waves are detected in a similar fashion to that seen in US via an acoustic transducer. The instrument needs to be coupled to the subject via an appropriate coupling medium. B: photoacoustic images demonstrating the advantage of using RGD-functionalized SWNTs (targeted SWNT) compared with nontargeted SWNTs (plain SWNT) for imaging tumor neovasculature in mice. In this particular study, the photoacoustic signal in tumors was eight times higher in mice injected with targeted SWNTs compared with nontargeted nanotubes (78). [From De la Zerda et al. (78).]

Some disadvantages of PAI include its limited depth of penetration compared with the limitless depths achievable via CT, MRI, and radionuclide techniques, as well as its inability to image through bone or air-filled structures (e.g., bones or lungs). Furthermore, the instrument needs to be coupled to the subject via an appropriate coupling medium (see **FIGURE 11A**). No commercial clinical application has emerged from PAI as yet; however, there are a few companies currently working on the development of photoacoustic-based breast scanners in the hope of replacing mammography. These scanners will first need to show improved sensitivity-specificity compared with the current gold standard technique before being considered as a possible replacement diagnostic strategy.

Although a relatively new area of molecular imaging, PAI holds great promise in the field of medical diagnostics, especially when paired with compatible targeted imaging agents.

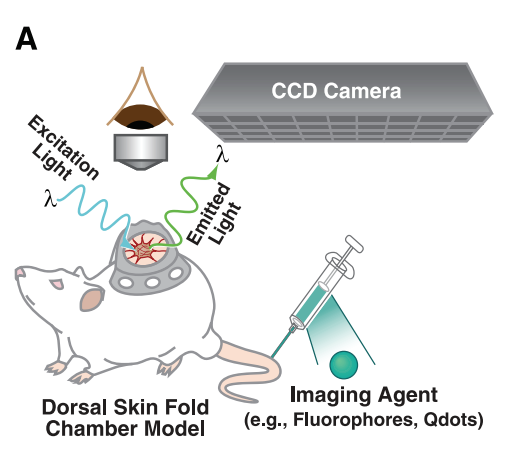
#### 3. IVM

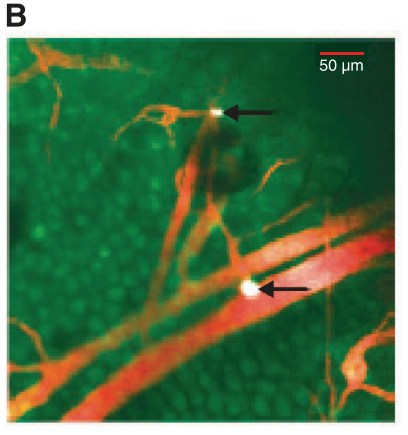
IVM is an optical imaging platform that enables visualization and real-time examination of a range of cellular and biochemical processes in a living animal. One can study events such as cell trafficking, vasculature formation, tumor development, and neuronal circuitry on a nanoscale (at a cellular-to-subcellular level) via the use of this microscopy technique. In addition to measuring biochemical and physiological parameters, IVM can be used to quantify delivery and response to therapeutic strategies (182).

A) BASIC PRINCIPLES OF IVM. The principles of IVM are essentially the same as traditional fluorescence microscopy; how-

ever, IVM uses modified instrumentation to allow anesthetized rodents to be placed on a microscope stage (183). In brief, IVM involves the use of a microscope with a digital camera detection setup and an image acquisition network. To sort and analyze the retrieved data, a computer equipped with relevant algorithms and mathematical models is needed.

Prior to studying rodents or other small mammals with IVM, subjects typically require some form of surgical preparation. Examples of such preparations include surgically implanted chronic-transparent window models (such as dorsal skin fold chambers (FIGURE 12) and cranial windows) (175, 225, 289, 363, 478), acute tissue preparations (where the animal is surgically prepared to reveal an internal organ such as the liver, mammary tissue, or lymph nodes) (361, 443), and in situ preparations (where, for example, tumor-lymphatic relationships can be studied at the molecular level in a rodent tail or ear) (167, 182, 240). There are definite advantages and disadvantages associated with each of these models. An important strength of implanting a chronic transparent window (consisting of a titanium frame and a removable cover glass for microscopic observation) is that it provides excellent motion stability and transparency, essentially allowing the exact same region to be viewed and monitored in a living animal longitudinally using time-lapse imaging. This level of stabilityinduced accuracy is extraordinarily difficult to achieve with in situ preparations. On the other hand, when using skin fold chambers for studying a tumor and its vasculature, the tumor being visualized is typically forced into an unnatural spatial orientation, thus affecting the microenvironment (and biology) of the process being investigated. Conversely, other types of chronic window models (such as cranial windows) leave the region of interest intact so that longitudinal





#### Key Strengths

- Excellent spatial resolution
- Multiplexing capabilities
- Dynamic information about microscopic cellular events (real-time imaging)
- Yields quantitative measures of cell size and motility

#### **Key Limitations**

- · Poor depth of penetration
- Small field of view
- · Can require multiple laser excitations
- · Longitudinal studies can be challenging
- Animal models are limited

**FIGURE 12.** Intravital microscopy (IVM) imaging. *A*: schematic of the general principles of IVM. The principles are essentially the same as traditional fluorescence microscopy; however, IVM uses modified instrumentation to allow anesthetized rodents to be placed on a microscope stage. In IVM, prior to studying rodents or other small mammals, subjects typically require some form of surgical preparation (e.g., dorsal skin fold chamber model shown in this diagram); this preparation essentially allows the same internal region of a living animal to be viewed and monitored longitudinally using time lapse imaging. *B*: IVM image illustrating the use of IVM for visualizing the binding of arginine-glycine-aspartic acid (RGD)-functionalized quantum dots (QDots) to tumor blood vessels in a living tumor-bearing mouse. The use of angiosense and tumor cells that express green fluorescent protein (GFP) is what makes the blood vessels and tumor cells appear red and green, respectively, in this image (392). Arrows point to QDots. [From Smith et al. (392). Copyright 2008 American Chemical Society.]

studies can take place in the native environment. Taking these points into consideration, and depending on which process one wants to study, it may be necessary to use an intelligent combination of models when employing IVM to gain a more accurate understanding of complicated pathologies (183).

As far as the hardware for IVM goes, there are several different systems to choose from, fitted with a varying number of lasers and output channels. Many IVM instruments are highly customized to suit the needs of a particular lab. Generally, a two-photon system comprises of tunable Ti: Sapphire lasers (typically tunable from  $\sim$ 650–1100 nm depending on the model), fluorophores that excite below  $\lambda/2$ nm, and appropriate filters, whereas a single-photon instrument typically employs a laser that corresponds to commonly used fluorescent agents (e.g., GFP, ~488 nm) and output channels/filters to match. The majority of recent IVM instruments will use at least one NIR laser to take advantage of increased tissue penetration at those wavelengths. One specific IVM setup is the Olympus IV100 system consisting of four lasers (488, 561, 633, and 748 nm) for fluorescence excitation, fiber optic cables (that produce a "confocal like" effect helping to reduce out-of-focus light), and a tiltable scan-head. This particular instrument enables imaging of the subject from different angles (ranging from  $-10-70^{\circ}$  from the normal) so that one does not always need to be normal to the surface. Both confocal and multi-photon laser scanning microscopes enable enhanced depth of imaging, the latter of these possessing clear advantages over the former, including less phototoxicity, greater depth of penetration of up to 700  $\mu$ m, and better sensitivity (signal to noise) (320, 344).

Subject to the specific biological question being asked and what one wants to investigate (e.g., anatomical features, physiology, cellular events, and/or biochemical processes), a suitable fluorescent imaging agent is selected alongside a pertinent animal model and microscopy technique. In terms of using IVM for cell tracking, one can either use a genetic fluorescent label or an extrinsic fluorescent label to "tag" the cell population of interest. For example, IVM has been used to monitor different stages in cancer metastasis in mice through the visualization of cells stably expressing GFP following transfection with a vector containing highly fluorescent variant gene of wild-type GFP (303). Many studies of this nature have been performed to gain insight on a variety of cellular processes, including angiogenesis (182) and immune cell motility/cell-cell interactions (67, 182, 217, 402).

A specific example of using an extrinsic fluorescent label and IVM for cell tracking is a study performed by Miller et al. (290) whereby individual migratory paths of T cells labeled with the fluorescent molecule carboxyfluorescein diacetate succinimidyl ester (CFSE) were observed using two-photon IVM. The study involved injection of CFSE-labeled CD4 $^+$  cells, followed by surgically exposing the inguinal lymph node on a dorsal skin flap. The anesthetized mice were injected with tetramethyl-rhodamine dextran (to highlight blood vessel architecture) and then imaged using IVM  $\sim$ 18 h following administration of cells. The rapid rate of acquisition (30 frames/s) meant that dynamic information

concerning the behavior of these cells could be obtained as they sped through the microcirculation. Contrary to in vitro findings, the results revealed that T cell trafficking through the secondary lymphoid organs was not necessarily orchestrated or influenced by chemokine gradients, but instead, appeared to be a more stochastic operation (290).

IVM can also be used to image certain biochemical events of interest by employing targeted QDots. For example, Cai et al. (45) imaged tumor vasculature in athymic nude mice bearing subcutaneous U87MG human glioblastoma tumors using RGD peptide-labeled QDots. Due to their excellent intrinsic fluorescent properties, QDots have been used as optical reporters in cell biology and animal models of disease (26) (please refer to sect. IIIE for more information on QDots).

In addition to investigating cellular and biochemical events, IVM can also be used to provide insight on how nanoparticles behave in a living subject. Nanoscale observations are crucial to understanding what nanoparticles are doing, where they go, and what they do once they reach their destination. This is of great importance, especially given the explosion of interest in nanotechnology and the potential of nanoparticles in the diagnosis and treatment of various diseases, such as cancer. When using IVM to evaluate a particular type of nanoparticle and their ability to target cancer cells, the researcher is typically interested in 1) whether the given type of nanoparticle is able to extravasate, i.e., escape the blood vessels (this will depend on the permeability of the vasculature surrounding the tumor, and the size and surface chemistry of the nanoparticle), and 2) whether the nanoparticle is capable of specific binding to the tumor. Studies of this type conducted in our laboratory have shown that RGD-functionalized-QDots arrive at and bind to tumor vessels but do not extravasate (392) (see FIGURE 12B for image).

B) KEY STRENGTHS AND LIMITATIONS. The dynamic, real-time, viewing facilitated via IVM means that one can obtain video image sequences of dynamic processes, and thus extract information regarding the kinetics of a particular event. Although in vitro assays are useful for understanding biology on the nano-level, they are devoid of dynamic information concerning the multifaceted cascades, pathways, and mechanisms behind biochemical events. Consequently, static data from in vitro experiments make it difficult to understand positive- and negative-feedback loops, whereas IVM helps provide a more accurate and complete picture of biological systems.

Other advantages of IVM include its excellent lateral spatial resolution ( $\sim$ 0.5  $\mu$ m), and, like most optical techniques, its multiplexing capabilities, meaning multiple biological targets can be imaged simultaneously. Moreover, IVM can afford quantitative measures of cell motility (velocity, dis-

placement, and chemotactic and motility indices) in the native microenvironment of a living animal. Other modalities, such as PET and SPECT, cannot afford this kind of microscopic data on individual cells.

Compared with other modalities, IVM has a large range of temporal resolution capabilities, meaning it is highly flexible in terms of the cellular and/or biochemical events it can visualize. IVM can be used to investigate fast processes (capturing 30 frames/s) and can also image events that have slow kinetics (e.g., over days, although the issue of photobleaching needs to be considered). Fluorescence and bioluminescence imaging typically only enable observations over seconds to minutes, and modalities like MRI, PET, and SPECT usually allow imaging over minutes to hours.

One of the main disadvantages of IVM is its extremely limited depth of penetration, which depends directly on the type of instrument, animal model, and imaging agent(s) that are used. A multi-photon setup is generally considered to be capable of achieving a depth of up to 800  $\mu$ m (452), whereas a one-photon setup is typically capable of achieving  $\sim 100-200 \mu m$ . In addition, the volume of tissue (field of view) that can be analyzed using IVM over a given period of time is exceptionally small (e.g., one can only look at a minute fraction of cells that make up an entire tumor). CT, MRI, PET, and SPECT, on the other hand, are ideal for whole body imaging at limitless depths within a reasonable time-frame (minutes-hours); however, they do not have sufficient spatial resolution to look at tiny groups of cells like IVM does. IVM is also limited by the types of available animal models that are suitable for use with this technique. Lastly, longitudinal studies using IVM can be challenging due to many factors, including the accumulation of imaging agents over time. This ultimately restricts the frequency of imaging dynamic processes in longitudinal studies.

#### 4. Optical frequency domain imaging

Recently, Vakoc and colleagues (412) reported the development of a new technique called optical frequency domain imaging (OFDI) that circumvents some limitations of IVM, most importantly, the need for an exogenous imaging agent. By exploiting intrinsic features that provide contrast, using novel techniques, and newly developed algorithms, OFDI is able to provide rapid, wide-field, high-resolution imaging at substantial depths (412). The authors demonstrated the use of OFDI in the investigation of angiogenesis, lymphangiogenesis, tissue viability, and treatment effectiveness. OFDI exploits the fact that tissue scattering is contingent on cellular structure and thus can provide detailed three-dimensional images of microstructures and enable the discrimination of necrotic tissue from viable tissue.

Vakoc and colleagues (412) demonstrated rapid visualization of microanatomy and cellular processes within the tumor local environment repeatedly over time without the

need for exogenous imaging agents over a much larger volume of the area of interest, compared with traditional IVM techniques. This study also illustrated the use of OFDI in assessing cancer cell therapies by examining the effects of diphtheria toxin on window dorsal skin fold chamber mice bearing a colorectal adenocarcinoma xenograft. The results depicted large necrotic regions within the treated tumor 24 h post-treatment (412). Overall, OFDI is a promising technique, however, it requires further exploration to determine its advantages over other imaging techniques.

## III. MOLECULAR IMAGING AGENTS

A molecular imaging agent is typically comprised of a targeting component and a signaling component. The main purpose of a molecular imaging agent is to interrogate and report back about a specific target (or targets) of interest during the course of a molecular imaging study. It is important to note that there are some molecular imaging techniques such as MRS (299), RS (445), and coherent antistokes Raman scattering microscopy (59) that do not necessitate the introduction of an exogenous agent for visualizing certain biochemical targets and pathologies. In most other cases, a molecular imaging agent designed to specifically interact with one or more molecular targets needs to be first introduced to study biochemical processes. For the most part, the development of such an agent is not straightforward and is therefore a key rate-limiting step in molecular imaging. Imaging agents have a long list of alternative names including probes, imaging probes, agents, molecular beacons, molecular spies, molecular detectives, radiopharmaceuticals, tracers, radioligands, and radiolabeled probes. The last four terms are used to describe agents that have been tagged/labeled with a radioisotope. The term *contrast* agent is also sometimes used as an alternative name for molecular imaging agent; however, this name can be misleading as it usually refers to an agent that does not specifically target a biochemical process of interest (e.g., classical iodine contrast agents in CT imaging).

Ideally, a molecular imaging agent should have the following characteristics: good ratio of specific to non-specific binding, high selectivity for biochemical target/process of interest, suitable pharmacokinetics, excellent in vivo stability (metabolism should not negatively affect functional binding), good safety profile (lack of toxicity to subject), potential for clinical translation, time and cost effective synthesis, signal amplification, and multiplexing capabilities.

For an effective imaging agent, the ratio of specific to non-specific binding needs to be high to ensure a signal that is truly reflective of the biochemical target/process of interest. In the case of imaging low-density receptors, this ratio needs to be >3 (335). High selectivity is also an important factor, whereby the imaging agent should possess the greatest affinity for, or functional interaction with, the intended bind-

ing site/process, and only negligible interaction with other sites/processes (143).

Nonspecific binding occurs due to the adhesion of an imaging agent to proteins and lipids. Although it is not easy to predict the extent of in vivo nonspecific binding, it is generally believed that the lipophilicity of an imaging agent is somewhat proportional to the degree of nonspecific binding (335). Therefore, lipophilicity is an important aspect to consider whilst designing an imaging agent.

A molecular imaging agent should display suitable pharmacokinetics for visualizing the biochemical target/process of interest. One must consider the rate of absorption and delivery of the imaging agent to the target site, its metabolism, excretion, and whether it will be reabsorbed in the enterohepatic circulation. Ideally, one would prefer an imaging agent that has rapid binding to or interaction with its target, fast blood clearance, urinary excretion, and persistent, high accumulation at the target site. Although the factors that influence pharmacokinetics of an imaging agent are poorly understood, it is generally accepted that size plays an important role and that charge, and lipophilicity, can also have a significant impact, depending on the type of imaging agent (257, 311, 369, 418). Generally, one aims to match the half-life of an imaging agent's signaling component, to its pharmacokinetics, and the pharmacokinetics of the process of interest.

To ensure accurate visualization of a target site (e.g., receptor, ion channel), an imaging agent must have good metabolic stability in vivo. It is important that the targeting part of the imaging agent remains intact and that the signaling component stays attached. Metabolic stability should be assessed to make sure unwanted signaling metabolites, resulting from the body's ability to break down imaging agents via intrinsic metabolic pathways, do not contribute to specific binding. If unwanted signaling metabolites redistribute to the target region, this can cause noise in the signal of interest. There are, however, numerous cases where metabolism of the imaging agent is required for visualization of the biochemical process of interest. For example, the phosphorylation of [18F]FDG leads to trapping and accumulation of imaging signal, indicative of glucose transport and hexokinase II activity (see FIGURE 13). Additionally, many smart/activatable imaging agents only emit a signal once they have been enzymatically cleaved/modified by a specific enzyme of interest. In any case, one should ensure that metabolism does not negatively affect functional binding/interaction of an imaging agent.

Ideally, the addition of a signaling component should not affect the functional binding/interaction of the imaging agent, and the imaging agent should not perturb the environment one wishes to visualize. Moreover, it is important that the imaging agent is nontoxic, especially in cases where

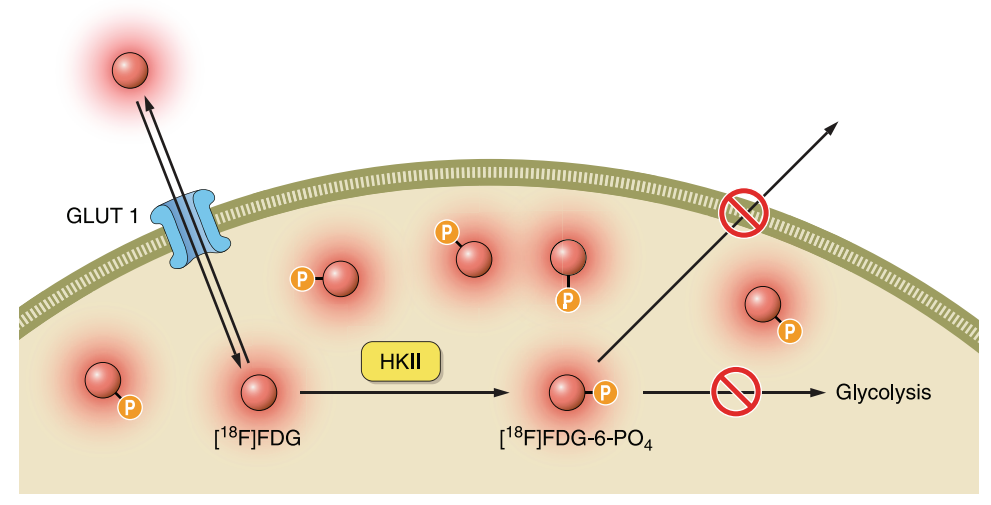


**FIGURE 13.** Mechanism of [<sup>18</sup>F]FDG signal amplification. The small molecule imaging agent [<sup>18</sup>F]FDG is an analog of glucose, whereby the 2-carbon hydroxyl group of glucose is substituted with a fluorine atom. Like glucose, [<sup>18</sup>F]FDG is taken up by cells via the glucose transporter (GLUT1) and phosphorylated by hexokinase II (HKII) to form [<sup>18</sup>F]FDG-6-PO<sub>4</sub>; however, (unlike glucose), further metabolism is prevented due to the absence of the required 2-carbon hydroxyl, and hence [<sup>18</sup>F]FDG remains trapped within the cell. [<sup>18</sup>F]FDG-6-PO<sub>4</sub> accumulates in cells over time, leading to signal amplification and making this imaging agent a suitable indicator of hexokinase II activity as well as a cell's need for glucose.

large amounts are required to achieve a measurable signal, e.g., CT and MRI imaging agents. A good safety profile, along with a relatively simple and cost effective synthetic route, that is easy to scale-up, automate, and mass-produce is important if the ultimate goal is clinical translation.

Amplification of imaging signal is another characteristic of an ideal imaging agent, as it serves to increase the overall sensitivity of target detection. One way of achieving this is to trap the imaging agent inside a cell without consuming the target molecule in the process. Enzyme substrate imaging agents are perfect for this as they often undergo a chemical modification (e.g., phosphorylation) that prevents them from being able to leave the cell. A classic example of this is the phosphorylation of the glucose analog [18F]FDG by hexokinase II (see FIGURE 13 for mechanism). This is similarly seen with the [18F]FHBG-HSV1-tk reporter probe/reporter gene system (see below paragraph on indirect imaging agents and sect. IVD for applications of this system). Another way of amplifying signal is to use an imaging agent that can carry multiple signaling components (e.g., certain radiolabeled or fluorescent-labeled nanoparticles have the potential to carry many signaling components per particle).

Since numerous genes play a role in any average, complex disease, it can be advantageous to devise ways of imaging more than one target simultaneously. This can be accomplished via the use of multiplexing strategies. For example, some imaging agents are available in different "flavors" (e.g., fluorophores, fluorescent proteins, luciferases, SERS nanoparticles), meaning they can be targeted towards different processes and imaged simultaneously, producing a single picture of multiple biochemical targets. It is believed

that, visualizing multiple targets, as opposed to taking a reductionist approach, will ultimately lead to a more complete picture of biological processes.

# A. Types of Currently Available Molecular Imaging Agents

There are numerous categories of molecular imaging agents including small molecules, peptides, aptamers, high-molecular-weight antibodies, engineered protein fragments, and various nanoparticles (FIGURE 14). Each type of agent falls within a different size range and thus possesses different pharmacokinetic and binding properties.

Within each individual class of agents there are agents that can be used for "direct imaging" and others for "indirect imaging" purposes. Direct imaging involves the use of an agent that is targeted to a specific molecular target such as a receptor, transporter, or enzyme [e.g., [11C]WAY-100635 binds directly to the serotonin-2A receptor (5HT-2A) that is used to image this site]. Indirect imaging is a more generalizable system that may be used to image many different biological processes with the same basic technique. Reporter gene imaging falls under this category (see sect. IVD) and involves imaging a reporter gene protein product resulting from reporter gene expression as an indirect measure of the location and levels of expression of another gene of interest. For example, the small molecule imaging agent [18F]FHBG can act as a reporter probe of herpes simplex type 1 thymidine kinase (HSV1-TK) reporter gene expression (471) as it is only phosphorylated and subsequently trapped inside cells containing the expressed reporter gene.

Туре	Small molecule	Peptide	Affibody	Aptamer	Antibody	Nanoparticle
Size	<1 nm <0.5 kDa	~1–4 nm ~0.5–2 kDa	~5–10 kDa	~5–15 kDa	~150 kDa	~10–200 nm (no larger than 1,000 nm)
Example	ОН НО НО ОН [ <sup>18</sup> F]	D-Tyr  Lys  HO  NH  Asp  Gly				
	[ <sup>18</sup> F]FDG	RGD-Cy5.5	[ <sup>68</sup> Ga]-DOTA- MUT-DS	Molecular Beacon	ICG- Trastuzumab	RGD-SWNT
		Quencher Donor	Signalin	ng componen	ıt	

**FIGURE 14.** Key types of molecular imaging agents, their approximate size range, and an example from each class. Fluorine-18 radiolabeled fluorodeoxyglucose ([ $^{18}$ F]FDG) is a small molecule positron emission tomography (PET) imaging agent for visualizing activity and levels of hexokinase type II and glucose transporter I. Arg-Gly-Asp (RGD) peptide labeled with cyanine 5.5 (RGD-Cy5.5) is a fluorescent peptide imaging agent for imaging alpha-v beta-3 ( $\alpha$ v $\beta$ 3) integrins. Affibody PET agent Gallium-68 labeled DOTA-MUT-DS ([ $^{68}$ Ga]DOTA-MUT-DS) and fluorescent antibody agent indocyanine green (ICG) labeled Trastuzumab are both used to image human epidermal growth factor receptor type 2 (HER2). A general representation of an apatamer molecular beacon (also known as smart/activatable probe) is shown as an example of an aptamer imaging agent. Lastly, RGD conjugated single-walled carbon nanotube (RGD-SWNT) is depicted as an example of a nanoparticle imaging agent.

Generally speaking, direct imaging is more accurate than indirect imaging as the molecular target of interest is being studied directly. Indirect approaches are typically based on multiple assumptions concerning the relationships between the target(s) being imaged and the target(s) of interest. These assumptions may not always be reliable and therefore can compromise the integrity of the data obtained. The advantage of indirect imaging is that the same imaging agent can be used to interrogate multiple different biochemical events without the need to develop a novel imaging agent for each independent event. Direct imaging, on the other hand, requires a new imaging agent to be developed for every new target. This can be extremely time consuming and costly.

Molecular imaging agents can also be classified as either "activatable" or "continually signaling" agents. Activatable imaging agents (also known as "smart probes") only release signal when bound to, or interacting with, their target. An example of an activatable probe is a quenched optical agent that emits fluorescent signal only following enzymatic cleavage by the cystein protease cathepsin B (267). Bioluminescence imaging using luciferase is another example of a smart/activatable imaging system as signal is only emitted (after it encounters its substrate) from locations where a luciferase enzyme gene is expressed, and hence, there is little or no background signal. On the other hand, continually emitting agents constantly produce a signal (e.g., all radionuclide-based agents). They are always

switched on, so you cannot distinguish between bound and unbound imaging agent, and therefore the background signal can be a significant issue.

The main classes of molecular imaging agents will now be briefly discussed.

## **B. Small Molecules**

Small molecules play an enormous role in molecular imaging. The small size of these chemical entities (usually <500 Da) means they can access and image a large range of molecular targets (including intracellular and CNS targets). In addition, they are generally less likely to suffer from unfavorable biodistribution-related issues that large-molecular-weight entities often do. Typically, small molecules can escape the vasculature with relative ease, passively or actively cross biological barriers (depending on charge and lipophilicity), bind to or interact with their target, and clear from the biological system, all in a relatively short period of time (418).

There are two main types of small molecule imaging agents: 1) molecules that bind specific receptors, transporters, or ion channels, e.g., [11C]PK11195 is a PET radioligand that binds to the peripheral benzodiazepine receptor (PBR) and is used to visualize microglia and neuroinflammation in a variety of brain diseases (437, 439); and 2) molecules that

enable imaging of metabolism/enzymatic activity/transport, e.g., 3'-deoxy-3'-[<sup>18</sup>F]fluorothymidine ([<sup>18</sup>F]FLT), a specific PET radioligand used to visualize thymidine kinase 1 activity as a measure of cellular proliferation (135).

The main drawback of small molecule agents is the time it takes to discover, synthesize, and evaluate them. It is often a long, expensive, and arduous process that does not typically afford many successful imaging agents. Also, due to their small size, there are limitations concerning the type of signaling component that can be attached (and hence modality that can be used). For example, one cannot usually conjugate a large fluorophore to a small molecule without altering the pharmacokinetics and targeting properties of the molecule. PET isotopes such as <sup>11</sup>C and <sup>18</sup>F are considered to be some of the most suitable candidates for labeling small molecules due to their small size (one atom). Also, in the instances where carbon and/or fluorine already exist in the parent molecule, an imaging agent can be generated that is chemically indistinguishable from its parent. Hyperpolarized MRS small molecules also involve the replacement of a single atom (e.g., replacement of <sup>12</sup>C with <sup>13</sup>C). SPECTlabeled small molecules are generally cheaper and faster to synthesize compared with PET-labeled compounds due to their so-called "shake and bake" kits. However, because most SPECT isotopes (and some PET isotopes, e.g., <sup>64</sup>Cu) are not found naturally in molecules of interest, and often require a chelating moiety for labeling, they can be more difficult to work with, especially in cases where the structure of the parent molecule needs to be maintained. There are, however, imaging agents (typically larger molecules such as peptides, aptamers, and nanoparticles) in which SPECT radioisotopes are more suitable than PET isotopes due to the wide range of available longer-lived isotopes suitable for labeling imaging agents with relatively slow kinetics.

See **TABLE 2** for some key examples of small molecule molecular imaging agents used to image glucose metabolism, hypoxia, fatty acid synthase, reporter genes, and biochemical targets involved in brain disease. At present the main clinically used agents from this list are PET and SPECT radioligands; however, there are a number of MRI (hyperpolarized, CEST, and PARACEST) agents and optical agents showing promise in preclinical and clinical studies. Please refer to the following literature for examples of small molecule imaging agents for PET (142, 143, 166, 350), SPECT (164, 232), MRI (5, 148, 227, 381), and optical (61, 382) imaging studies.

#### C. Peptides

Peptides have emerged as a very important class of molecular imaging agents (238). The use of solid-phase peptide synthesis and phage display libraries have led to rapid high-throughput synthesis and screening of peptide-based molec-

ular imaging agents. Peptides are easily modified, are fairly small in size (up to 15 amino acids), and are rapidly cleared. They have a number of advantages over small molecules, including their superior selectivity and specificity, and also their flexibility in terms of the chemical modifications they can tolerate without altering binding properties or kinetics (149, 371). Although peptides generally display a lower affinity compared with antibodies, they have a much higher stability at room temperature and a greater ability to penetrate tissues/tumors due to their small size (365). Additionally, peptides are less likely to cause immunogenic effects (441) compared with antibodies and are more cost effective to produce (depending on the size of the peptide), as peptide synthesis is much cheaper than recombinant production techniques.

Peptide imaging agents can be used to visualize a range of targets, including integrins (20, 57, 294), matrix metalloproteinases (36, 187), caspases (91, 95), somatostatin receptors (82, 136, 331), neuropeptide Y receptor (253, 485), and gastrin releasing peptide receptor (372, 427, 428). See **TABLE 2** for some specific examples of peptide molecular imaging agents that can be used for optical, PET, and SPECT imaging.

The main disadvantage of using peptides as imaging agents is that they are prone to rapid proteolytic degradation in vivo and have a short plasma half-life. In addition, peptides used for PET and SPECT imaging mostly require prosthetic groups (265, 273) to label them with radioisotopes. Prosthetic groups add to the complexity and time of synthesis, and also alter the structure and can therefore change the binding of the peptide. Building the prosthetic group into the library to begin with can rectify some of these issues, however, not all. One can get around many of the stability related issues of peptides by utilizing several techniques, for example: 1) introducing appropriate D-amino acids, 2) using unusual amino acids, 3) substituting peptide bonds, and 4) cyclizing the NH<sub>2</sub> and COOH terminus (177, 314, 454).

## D. Aptamers

Aptamers may be defined as single-stranded DNA or RNA oligonucleotides that bind their target site with a high degree of specificity and selectivity (34). In the in vitro setting, aptamers have been successfully used for some time (410) and are fast replacing antibodies in many of the traditional in vitro diagnostic assays (186). In the therapeutic arena, aptamers are beginning to make a name for themselves, with the first aptamer (Pegaptanib) approved by the United States Food and Drug Administration (FDA) in 2004 for treatment of macular degeneration (88). There are also a number of other promising therapeutic aptamers currently undergoing clinical trials, including REG1 (reversible anticoagulant, to be given during percutaneous coronary intervention) (51) and NU172 (thrombin inhibitor, to be given during cardiopulmonary bypass) (198, 415).

	Type of Molecular Imaging Agent	Imaging Agent	Biological Application(s) and/or Clinically References	Biological Target(s)	Application(s)	Used Preclinically and/or Clinically?	References
PET Amynidia knase 1 Caroar/cellular Chrical and activities the coxygen of deficient cells (intronmictazoles, FANSO) and FAZA, arrespecial to these reduced and trapped in these cells at races (intronmictazoles, proportional to introncellular oxygen levels) and FAZA, arrespecial to introncellular oxygen levels, proportional to introduced and deficient cells (APVI-4K reporter Per Reporter gene imaging Clinical and deficient cells (APVI-4K reporter Per Clinical and deficient cells (APVI-4K reporter Per Clinical and Coppanine receptor (APVI-4K reporter Per Clinical and Coppanine receptor (APVI-4K reporter) (APVI-4K reporter	Small molecule	[ <sup>18</sup> FJFDG	PET	Glucose metabolism (glucose transporter I and hexikinase II	Cancer	Clinical and preclinical	ldo et al., 1978; Silverman et al., 2001
PET   Appendix California and Clinical and deficient cells		[ <sup>18</sup> F]FLT	PET	Thymidine kinase-1 activity	Cancer/cellular proliferation	Clinical and preclinical	Grierson et al., 2000
Hypoxia Clinical and deficient cells  PET HOV14K reporber Reporter gene imaging Clinical and and cell		[ <sup>18</sup> F]FMISO	PET	Viable oxygendeficient cells (nitroimidazoles, such as FMISO and FAZA, are reduced and trapped in these cells at rates inversely proportional to intracellular oxygen levels)	Hypoxia	Clinical and preclinical	Chang et al., 2007
PET HSV1-tk reporter Reporter gene imaging Clinical and and cell a		[ <sup>18</sup> F]FAZA	PET	Viable oxygen- deficient cells	Hypoxia	Clinical and preclinical	Postema et al., 2009
PET Presynaptic dopamineration metabolism  PET Fatty acid synthesis Cancer (prostate, bladder, Clinical and renal), Myocaerdial preclinical infraction, ischemia protein plaques protein plaques Dopamine receptor Pet S-/3 (D2/D3) schizophrenia, preclinical and schizophrenia, and protein plaques plaques protein plaques protein plaques protein plaques protein plaques plaques protein plaques protein plaques protein plaques plaques plaques plaques protein plaques plaques plaques plaques plaques plaques plaques protein plaques		[ <sup>18</sup> F]FHBG	PET	HSV1-tk reporter gene expression and cell proliferation	Reporter gene imaging	Clinical and preclinical	Yaghoubi et al., 2001
PET       Fatty acid synthesis       Cancer (prostate, bladder, clinical and infanction, ischemia       Clinical and protein plaques         PET       Amyloid-beta (Aβ)       Atzheimer's disease       Clinical and protein plaques         PET       Dopamine receptor parkinson's disease, clinical and activated microglia       Clinical and schizon addiction         PET       Activated microglia       Atzheimer's disease, clinical and multiple sclerosis, addiction         PET       Activated microglia       Atzheimer's disease, clinical and herpes encephalitis, receptor (PBR)       Preclinical and clinical and clisease, anxiety preclinical and nicotinic         PET       Alpha(4)beta2- disease, anxiety preclinical and nicotinic       Alzheimer's disease       Clinical and clinical and clinical and deficient cells		[ <sup>18</sup> FJFDOPA	PET	Presynaptic dopaminergic metabolism	Parkinson's disease	Clinical and preclinical	Luxen et al., 1992; Rakshi et al., 2002
PET Amyloid-beta (Aβ) Alzheimer's disease Clinical and protein plaques  Pet Barkinson's disease, Clinical and 2/3 (D2/D3) schizophrenia, preclinical and depression, addiction  PET Activated microglia Alzheimer's disease, clinical and imaging/peripheral multiple sclerosis, preclinical benzodiazepine herpes encephalitis, receptor (PBR) Huntington's disease  PET Alpha(4)beta2- Alzheimer's disease Clinical and disease, anxiety preclinical and disease, anxiety preclinical and nicotinic acetylcholine receptors  [α4β2-nAChR]  PET Alpha(4)beta2- Alzheimer's disease Clinical and deficient cells Clinical and preclinical and deficient cells Clinical and deficient cells Clinical and deficient cells		[ <sup>11</sup> C]acetate	PET	Fatty acid synthesis	Cancer (prostate, bladder, renal), Myocardial infarction, ischemia	Clinical and preclinical	Sandblom et al., 2006; Walsh et al., 1989; Oyama et al., 2003
PET Dopamine receptor Parkinson's disease, Clinical and 2/3 (D2/D3) schizophrenia, preclinical and depression, addiction  PET Activated microglia Alzheimer's disease, imaging/peripheral multiple sclerosis, preclinical and imaging/peripheral multiple sclerosis, preclinical and clisease pet GABA <sub>A</sub> receptor (PBR) Huntington's disease preclinical and disease, anxiety preclinical and nicotinic acetylohine receptors  [A4B2-nAChR]  PET Alzheimer's disease Clinical and deficient cells  [A4B2-nAChR]  PET Alzheimer's disease Clinical and deficient cells  [A4B2-nAChR]  PET Clinical and deficient cells  [A4B2-nAChR]  [A4B2-nAChR]  [A4B2-nAChR]  [A4B2-nAChR]  [A4B2-nAChR]  [A4B2-nAChR]  [A4B2-nAChR]		[ <sup>11</sup> C]PIB	PET	Amyloid-beta (A $eta$ ) protein plaques	Alzheimer's disease	Clinical and preclinical	Mathis et al., 2003
PET Activated microglia Alzheimer's disease, Clinical and imaging/peripheral multiple sclerosis, preclinical benzodiazepine herpes encephalitis, receptor (PBR) Huntington's disease PET GABA <sub>A</sub> receptors Epilepsy, cerebrovascular preclinical and disease, anxiety preclinical and nicotinic acetylcholine receptors  [a4β2-nAChR] PET Alzheimer's disease Clinical and nicotinic acetylcholine receptors  [a4β2-nAChR] PET Alzheimer's disease Clinical and preclinical and deficient cells  [Colinical and Clinical and deficient cells		[ <sup>11</sup> C]raclopride	PET	Dopamine receptor 2/3 (D2/D3)	Parkinson's disease, schizophrenia, depression, addiction	Clinical and preclinical	Farde et al., 1989
PET GABA <sub>A</sub> receptors Epilepsy, cerebrovascular Clinical and disease, anxiety preclinical and nicotinic acetylcholine receptors  [α4β2-ηΔChR]  PET (α4β2-ηΔChR)  PET (γible αχgen- Hypoxia Clinical and deficient cells preclinical and deficient cells preclinical and deficient cells		[ <sup>11</sup> C]PK11195	PET	Activated microglia imaging/peripheral benzodiazepine receptor (PBR)	Alzheimer's disease, multiple sclerosis, herpes encephalitis, Huntington's disease	Clinical and preclinical	Camsonne et al., 1984; Shah et al., 1994
PET Alpha(4)beta2- Alzheimer's disease Clinical and nicotinic and nicotinic and nicotinic and nicotinic and acetylcholine receptors (α4β2-nAChR)  PET Viable αχιση- Ηγραχία Clinical and deficient cells preclinical		[ <sup>11</sup> C]flumazenil	PET	$GABA_A$ receptors	Epilepsy, cerebrovascular disease, anxiety	Clinical and preclinical	Savic, 2000
PET Viable oxygen- Hypoxia Clinical and deficient cells preclinical		[ <sup>11</sup> C]nicotine	ЬЕЦ	Alpha(4)beta2- nicotinic acetylcholine receptors (α4β2-nAChR)	Alzheimer's disease	Clinical and preclinical	Wu, J et al., 2010
		[ <sup>64</sup> Cu]ATSM	PET	Viable oxygen- deficient cells	Hypoxia	Clinical and preclinical	Lewis, JS et al., 1999

		Table 2	Table 2.—Continued			
Type of Molecular Imaging Agent	Imaging Agent	Imaging Modalities	Biological Target(s)	Application(s)	Used Preclinically and/or Clinically?	References
	[ <sup>123</sup> ]JFP-CIT	SPECT	Dopamine transporter (DAT), serotonin transporter (SERT)	Parkinson's disease	Clinical and preclinical	Booij et al., 1997
	[ <sup>123</sup> ]JCLINDE	SPECT	Activated microglia imaging/PBR	Alzheimer's disease, multiple sclerosis, herpes encephalitis, Huntington's disease	Clinical and preclinical	Arlicot et al., 2008
	[ <sup>123</sup> ]-5-A-85380	SPECT	lpha 4 eta 2-nAChR	Alzheimer's disease	Clinical and preclinical	Mitsis et al., 2009 Wu et al., 2010
	[ <sup>123</sup> ]JMIBG	SPECT	Norepinephrine transporter (NET)	Heart failure, cardiac sympathetic dysfunction	Clinical and preclinical	Agostini et al., 2008
	[ <sup>123</sup> ]JMIP-1072 and [ <sup>123</sup> JJMIP-1095	SPECT	Prostate specific membrane antigen (PSMA)	Prostate cancer	Olinical and preclinical	Maresca et al., 2009
	l <sup>99m</sup> Tc∏BDD∆T	SPECT	DAT	Parkinson's disease	Clinical and	Hillier et al., 2009 King et al., 1997
		5	Ī,	Depression	preclinical	
						Wu et al., 2011
	5-Hydroxy-tryptophan	MRI (CEST)	pH sensor	Cancer	Preclinical	Ward et al., 2000
	EUDO I A-[giy]4	Mai (PARACESI)	Townsond	Callcer's hading	Precinical	Suesbe et al., 2011
	Im-DOIINIA 71 1301 - Tionia	MAPI (PARACEST)	lemperature/pH sensor	Cancer (e.g., brain)	Preclinical	Coman et al., 2010
	[1~C]Pyruvate	MKI (nyperpolarized MKS)	Glycolysis	Cancer (e.g., prostate)	Cilnical and preclinical	Albers et al., 2008
	[1,4- <sup>13</sup> C2]Fumarate	MRI (hyperpolarized MRS)	Cell death	Tumor cell death, ischemia	Preclinical	Gallagher et al., 2009
	[2- <sup>13</sup> C]Fructose	MRI (hyperpolarized MRS)	Glycolytic and pentose phosphate pathway	Cancer	Preclinical	Keshari et al., 2009
Peptide	[ <sup>18</sup> F]Galacto-RGD	PET	lpha eta eta3 Integrin	Cancer	Clinical and preclinical	Haubner et al., 2001; Beer et al., 2008
	(18FJFPPRGD2	PET	lphaV $eta$ 3 Integrin	Cancer	Clinical and preclinical	Liu et al., 2009; Mittra et al., 2010
	Lys[111]DOTA-4,Phe7,Pro34-NPY	SPECT	Neuropeptide Y receptor	Cancer	Preclinical	Zwanziger et al., 2008
	(99mTcJEDDA/HY NIC-TOC	SPECT	Somatostatin receptor	Cancer	Clinical and preclinical	Pavlovik et al., 2010
	[ <sup>99m</sup> ToJRP527	SPECT	Bombesin receptor 2/gastrin releasing peptide receptor (BB2/GRP)	Cancer	Clinical and preclinical	Van de Wiele et al., 2000; Van de Wiele et al., 2008
	c(RGDyK)-Cy 5.5	Fluorescence	ανβ3 Integrin	Cancer	Preclinical	Cheng et al., 2005

Type of Molecular Imaging Agent	Imaging Agent	Imaging Modalities	Biological Target(s)	Application(s)	Used Preclinically and/or Clinically?	References
	MMP-2 peptide substrate with quenched near-infrared fluonochromes	Fluorescence	MMP-2	Cancer	Preclinical	Bremer et al., 2001
	Activatable cell-penetrating peptides (ACCPs)-Smart Probe	Fluorescence	MMP-2 and -9	Cancer	Preclinical	Jiang et al., 2004
	AB50-Cy5.5	Fluorescence	Caspase 3 and 7	Apoptosis/cancer	Preclinical	Edginton et al., 2009
Aptamer	[ <sup>99m</sup> TcJNX21909	SPECT	Human neutrophil elastase	Inflammation	Preclnical	Charlton et al., 1997
	[ <sup>99m</sup> Tc}TTA-1	SPECT	Extracellular matrix protein tenascin-C	Cancer	Clinical and preclinical	Hicke et al., 2006
	Rhodamine Red-X-TTA-1	Fluorescence				
Engineered Protein	[ <sup>124</sup> ]JG250-mAb	PET	Carbonic anhydrase4X	Cancer	Clinical and Preclinical	Divgi et al., 2007
<pre>(antibody, affibody, etc.)</pre>	[ <sup>124</sup> l]CA19-9-mAb	PET	Carbohydrate tumor antigen CA19-9	Pancreatic cancer	Preclinical	Girgis et al., 2011
	[ <sup>18</sup> F]FB-T84.66-diabody	PET	CEA	Cancer	Preclinical	Cai et al., 2007
	[ <sup>124</sup> ]]T84.66-minibody	PET	CEA	Cancer	Preclinical	Sundaresan et al., 2003
	( <sup>18</sup> FJFBOZHER2: 477-affibody	PET	Human epidermal growth factor receptor 2 (HER2)	Cancer	Preclinical	Cheng et al., 2008
	[ <sup>64</sup> Cu]DOTA-Cys-diabody	PET	Activated leukocyte cell adhesion molecule (ALCAM)	Cancer	Preclinical	McCabe et al., 2011
	[ <sup>99m</sup> Tc]Anti-TNF-α mAb-infliximab Remicade	SPECT	Tumor necrosis factor-alpha (TNF- $lpha$ )	Inflammation	Clinical and preclinical	Conti et al., 2005
	[99mTc]IMMU-4 CEA-Scan	SPECT	Carcinoembryonic antigen (CEA)	Cancer	Clinical and preclinical	Moffat et al., 1996
	[ <sup>99m</sup> Tc]Annexin V	SPECT	Phosphatidylserine	Apoptosis, cancer, transplant rejection, cardiovascular risk	Clinical and preclinical	Belhocine et al., 2002
	[ <sup>99m</sup> Tc]Rituximab	SPECT	CDSO	Cancer	Clinical and preclinical	Wang et al., 2006
	[111In]DOTAZ(HER2:342-pep2)-affibody		HER2	Cancer	Clinical and preclinical	Orlova et al., 2007
	[ <sup>111</sup> ln]panitumumab-affibody	SPECT	HER1/EGFR	Cancer	Preclinical	Ogawa et al., 2009
	Cy7-6649	Fluorescence	Tumor-associated glycoprotein (TAG)-72	Cancer	Preclinical	Zou et al., 2009
	ICG-Trastuzumab, (also known as ICG-Herceptin)	Fluorescence	HER2	Cancer	Preclinical	Ogawa et al., 2009
	Herceptin-RhodG	Fluorescence	HER2	Cancer (intraoperative visualization of metastases)	Clinical and preclinical	Koyama et al., 2007
	Anti-CEA-Diabody-RLuc8	Bioluminescence	CEA	Cancer	Preclinical	Venisnik et al., 2006
Nanoparticle	[ <sup>64</sup> Cu]DOTARGD-(PASP-10)	PET/MRI	$lpha \kappa eta eta$ Integrins	Cancer	Preclinical	Lee et al., 2008
	[64Cu]cRGD-SPIO	PET/MRI	$\alpha \nu \beta \beta$ Integrins	Cancer	Preclinical	Yang et al., 2011
	[125]]CBGD-PFG-anid nanoparticles		was Integrine	Cancer	Precinical	Delvardo et al., 2003

		C TITE				
		l able 4.—	able 2.—Continued			
Type of Molecular Imaging Agent	Imaging Agent	Imaging Modalities	Biological Target(s)	Application(s)	Used Preclinically and/or Clinically?	References
	lodinated nanoparticles	Ь	Macrophages	Atherosclerotic plagues	Preclinical	Hvafil et al., 2007
	PSMA-gold nanoparticles	CT	PSMA	Cancer	Preclinical	Kim et al., 2010
	Fibrin-targeted PARACEST perfluorocarbon nanoparticles	MRI	Fibrin	Cardiovascular plaques	Preclinical	Winter et al., 2006
	CR2-conjugated SPIO nanoparticles	MRI	Tissue-bound C3 activation fragments (C3 inflammation)	Inflammatory, Autoimmune diseases	Preclinical	Serkova et al., 2010
	EGFRvIII antibody-iron oxide-nanoparticles	MRI	EGFR deletion mutant (EGFRvIII)	Human glioblastoma multiforme (GBM)	Preclinical	Hadjipanayis et al., 2010
	HER2-Affibody-SPIO-nanoparticles	MRI	HER2	Cancer	Preclinical	Kinoshita et al., 2010
	Cy5.5-SPIO-chlorotoxin nanoparticles	MRI/fluorescence	Matrix metalloprotein	Cancer	Preclinical	Veiseh et al., 2005
			a se-2 (MMP-2)			
	Annexin A5-micellar nanoparticle, carving multiple Gd-labeled and fluorescent lipids	MRI/fluorescence	Phosphatidylserine	Apoptosis, cancer, transplant rejection, cardiovascular risk	Preclinical	van Tilborg et al., 2010
	HER2-QDots	Fluorescence/IVM	HER2	Cancer	Preclinical	Tada et al., 2007
	RGD-QDots	Fluorescence/IVM	αvβ3 Integrins	Cancer	Preclinical	Cai et al., 2006
	Folate-NIR-polyacrylic acid (PAA)-coated ion oxide nanoparticles, loaded with cancer therapeutic	Fluorescence/MRI/theranostic	Folate receptors	Cancer	Preclinical	Santra et al., 2009
	HER2-gold nanorods	Raman/IVM/PAI	HER2	Cancer	Preclinical	Ding et al., 2008
	EGFR-SERS	Raman	EGFR	Cancer	Preclinical	Qian et al., 2008
	EGFR affibody-gold-silica nanoparticles	Raman	EGFR	Cancer	Preclinical	Jokerst et al., 2011
	RGD-SWNTs	Raman/PAI	lpha eta eta Integrins	Cancer	Preclinical	De la Zerda et al., 2008
	HER2 IgY-SWNTs	Raman/PAI	HER2	Cancer	Preclinical	Xiao et al., 2009
	$\alpha \gamma \beta 3$ -Antibody-SWNTs	PAI	$\alpha \vee \beta \beta$ Integrins	Cancer	Preclinical	Xiang et al., 2009
	EGFR Antibody-gold nanoparticles	PAI	EGFR	Cancer	Preclinical	Mallidi et al., 2009
	$[{\sf Nle}^4, {\sf d-Phe}^7]$ - $\alpha$ -melanocyte-stimulating	PAI	Melanocyte-	Melanoma	Preclinical	Kim et al., 2010
	hormone-gold nanocages		stimulating			
			normone			

See text for definitions and references.

The superior targeting capabilities of aptamers, comparable to that of antibodies, along with their relative ease of synthesis (113, 241, 415), high diversity, and relatively inexpensive production, have made these 5- to 15-kDa chemical entities an attractive candidate for molecular imaging agents.

Even though the concept of using aptamers for in vivo diagnostic imaging emerged a little over 30 years ago (23), the field of aptamer imaging remains in its infancy, with only a few reported studies involving the use of targeted aptamers for molecular imaging purposes. One of these studies employed a  $^{99\rm m}$ Tc-labeled aptamer specific for human neutrophil elastase for imaging inflammation in a passive Arthus reaction model in rats using SPECT (52). Results from this study demonstrated a marked improvement in target to background ratio compared with that observed with the clinically used IgG antibody for inflammation imaging (4.3  $\pm$  0.6 at 2 h for the aptamer, compared with 3.1  $\pm$  0.1 at 3 h for the antibody). Although these results were encouraging, there was a large amount of nonspecific binding observed with the scrambled version of the aptamer.

A separate study reported the use of a RNA aptamer specific for extracellular matrix protein tenascin-C (155), TTA-1, a protein found in high quantities in many solid tumors. The 13-kDa high-affinity aptamer TTA-1 (dissociation constant,  $5 \times 10^{-9}$  M) was labeled with the SPECT radioisotope 99mTc via MAG2 chelator and evaluated in mice bearing glioblastoma (U251) or breast cancer (MDA-MB-435) tumor xenografts in separate studies using planar scintigraphy (FIGURE 15). The results showed rapid tumor uptake and fast blood clearance, affording a tumor-to-blood ratio of 50 within 3 h for radiolabeled-TTA1. Scintigraphic images obtained at 18 h depict the tumor as the brightest structure and demonstrate the almost complete clearance of radioactivity from the body (FIGURE 15). Radiolabeled-TTA1 could also be used to clearly visualize breast tumor xenografts (MDA-MB-435) at 20 h, illustrating the use of this aptamer for detecting different tumor types (155). TTA-1 is presently in clinical trials, and preliminary results show clear images of lung and breast tumors, including metastases, with good tumor-to-background ratios (220).

Apart from these studies there are several published articles describing the labeling of aptamers with either fluorophores for optical imaging, or radioisotopes for PET/SPECT imaging (411, 477); however, these have not yet been evaluated in living subjects. There also exist a range of smart/activatable aptamer imaging agents that are being used for in vitro studies, including the anti-thrombin aptamer. This aptamer forms a stable, quenched "stem loop" structure in the absence of thrombin, and an unquenched, G-quartet conformation when thrombin is added (145). The binding of thrombin results in fluorescence emission due to the conformational change, no longer allowing quenching of fluoro-

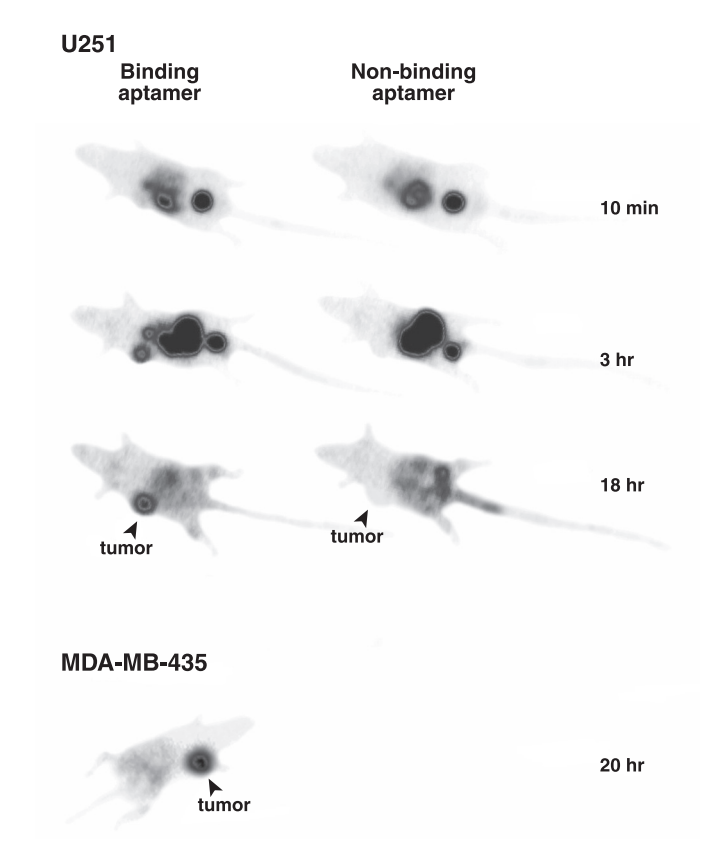


FIGURE 15. Evaluation of a radiolabeled binding aptamer [[99mTc]-TTA1] specific for extracellular matrix protein tenascin-C, verses a radiolabeled nonbinding aptamer, in mice either bearing glioblastoma (U251) or breast cancer (MDA-MB-435) tumor xenografts using planar scintigraphy. The results show rapid tumor uptake and fast blood clearance of the binding aptamer [99mTc]-TTA1, affording a tumor-to-blood ratio of 50 within 3 h. Scintigraphic images obtained at 18 h depict the tumor as the brightest structure and demonstrate the almost complete clearance of [99mTc]-TTA1 from the body, whereas the tumor cannot be visualized using the radiolabeled nonbinding aptamer. [99mTc]-TTA1 could also be used to detect breast tumor xenografts (MDA-MB-435) at 20 h, illustrating the use of this aptamer for detecting different tumor types (155). [From Hicke et al. (155), with permission of the Society of Nuclear Medicine.]

phore on the 5' end by the quencher on the 3' end. These types of smart aptamers have great potential, although since the utility of aptamers as molecular imaging agents has not yet been fully explored in living subjects, it could be some time before these agents are routinely used.

Currently, there are a few key limitations associated with using aptamers as molecular imaging agents, including 1) low in vivo stability due to serum degradation, 2) poor membrane passage due to their size and charge (i.e., pharmacokinetics are rather variable and difficult to predict), and 3) small size, leading to an increased chance of renal filtration and short half-life. To overcome these issues, the following areas are being explored: 1) modification of aptamers to increase stability [i.e., via internucleotide phosphodiester linkages, known as "locked nucleic acids" (LNAs)]; 2) the use of systematic evolution of ligands by

exponential enrichment (SELEX) in physiological environments, to improve pharmacokinetics; and 3) addition of PEG to aptamers, to improve their circulation half-life (198).

In addition to their extremely high affinity and specificity, another benefit of working with aptamers is that their chemical synthesis enables site-specific labeling with a signaling moiety and facile scaling up to large quantities. Synthesis of antibodies, on the other hand, is challenging to scale-up, and there are additional time-consuming steps to incorporate signaling components. Furthermore, aptamers do not have issues with immunogenicity (198).

Overall, aptamers are an attractive class of molecular imaging agents. Since they have the unique capability of discriminating between remarkably similar molecules, they have the potential to provide a highly specific means of diagnosing and differentiating a large variety of diseases at early stages.

## E. Antibodies and Engineered Proteins

Monoclonal antibodies (mAbs), also known as immunoglobulins, are highly specialized, ~150 kDa, Y-shaped proteins. Unlike small molecules and peptides, mAbs are not restricted to interacting with binding pockets or active sites, but instead can bind adhesion molecules, activation markers, antigens, and receptors (270). Their relatively facile synthesis and unparalleled ability to recognize and bind their target site with ultra high affinity and specificity have made mAbs (and their engineered fragments) important players in the therapeutic and diagnostic arenas (448).

Presently, there are over 20 FDA-approved mAb therapeutic agents and greater than 8 radiolabeled-mAbs approved for SPECT molecular imaging (317, 432). The first approved mAb molecular imaging agent was [1111]n]satumomab pendetide (OncoScint) in 1992 (31). In 1996 both [99mTc]arcitumomab (CEA Scan) (296) and [1111]n]capromab pendetide (Prostascint) (272) were approved, followed by [1111]n]ibritumomab tiuxetan (Zevalin) in 2002, and [1311]tositumomab (Bexxar) in 2003 (317).

While these early mAb molecular imaging agents have been instrumental in understanding the pharmacokinetics and dynamics of antibodies in living subjects in real time, they have not had a dramatic impact on clinical outcomes. This is likely due to the following:

- 1) Immunogenicity issues associated with murine antibodies. Since antibodies of mouse origin are recognized by the human immune system as foreign, their use can initiate a cascade of unwanted side effects.
- 2) Suboptimal targets. Early mAb imaging agents were either aimed at non-disease specific targets or targets found in

both normal and diseased tissues. This gave rise to uncertain diagnoses and poor signal-to-background ratios. The target for Prostascint (PSMA) is fairly cancer specific (mainly human prostate adenocarcinoma), however, because it binds to the intracellular part of PSMA, and MAbs for the most part cannot naturally cross cell membranes. It mainly localizes in necrotic regions of tumors, where cell membranes have been disrupted, instead of identifying viable cells (419).

- 3) Limitations of SPECT. Since all approved mAb imaging agents are SPECT agents, the resulting images are not quantitative and suffer from poor spatial resolution.
- 4) General limitations of mAbs. Since intact mAbs reside in the blood for extended periods of time (from days to weeks), their use in imaging studies can result in low signal-to-background ratios and poor image quality (466).

Current efforts in the field of mAb molecular imaging agents are focused towards developing chimeric, humanized, or fully human mAb imaging agents (to eradicate immunogenicity issues) specific for a wide range of promising targets, both from a diagnostic and therapeutic standpoint. These efforts include devising efficient strategies for conjugating these mAb-imaging agents with PET isotopes (87, 130), fluorescent dyes (229, 311), Qdots (133, 405), or iron-oxide nanoparticles (83, 140) in a rapid, stable, and cost-effective manner, so as to exploit the advantages of a variety of imaging modalities.

PET isotopes currently being explored for mAb labeling are gallium-68 ( $^{68}$ Ga;  $t_{1/2}$ , 1.13 h), fluorine-18 ( $^{18}$ F;  $t_{1/2}$ , 1.83 h), copper-64 ( $^{64}$ Cu;  $t_{1/2}$ , 12.7 h), yttrium-86 ( $^{86}$ Y;  $t_{1/2}$ , 14.7 h), bromine-76 ( $^{76}$ Br;  $t_{1/2}$ , 16.2 h), zirconium-89 ( $^{89}$ Zr;  $t_{1/2}$ , 78.4 h), and iodine-124 ( $^{124}$ I;  $t_{1/2}$ , 100.3 h) (432). These isotopes have the requisite half-lives for imaging (i.e., they allow time for mAbs to reach an appropriate target-to-background ratio) and enable relatively simple and stable coupling. PET-labeled mAbs should afford more useful images and information compared with early SPECT-labeled mAbs in terms of image quality, spatial resolution, and quantification.

An important clinical example of a chimeric PET-mAb molecular imaging agent is <sup>124</sup>I-G250. <sup>124</sup>I-G250 specifically binds carbonic anhydrase-IX and is showing promise as a means of identifying patients with the most common type of kidney cancer, known as clear cell renal carcinoma (CCRC), to help with treatment planning. Divgi and colleagues showed, in a study involving 25 renal cancer patients (16 with CCRC, and 9 with the non-aggressive form), <sup>124</sup>I-G250 accurately identified 15 of 16 of the subjects with CCRC, and did not accumulate in any of the 9 patients with non-clear cell renal masses (87, 432). This example demonstrates the benefit of mAb molecular imaging when identi-

fying appropriate treatment strategies for individual patients (i.e., personalized medicine).

Selection of suitable patients for mAb therapy has long been a difficult and somewhat unreliable process. Traditionally, biopsies from patients are taken and analyzed to confirm target overexpression or gene amplification using immunohistochemistry (IHC) or fluorescence in situ hybridization. However, a single biopsy does not provide a complete picture of target expression levels in all regions of disease over time (432). Since it is not feasible and far too invasive to collect multiple biopsies from different areas of the same patient over time, noninvasive imaging using mAb molecular imaging agents represents a more accurate and rapid means for determining target expression levels in a patient. These real-time read outs of target expression levels help with predicting responders versus nonresponders when selecting patients for mAb therapies. Seeing that mAb therapy is expensive and only benefits a handful of patients, predicting responders/nonresponders prior to treatment is of great value.

Although there are many promising mAb-type molecular imaging agents emerging for a range of different imaging platforms, their overall versatility and usefulness has remained fairly limited due to their inescapably long residence in blood and their restricted ability to transverse biological barriers (e.g., the blood-brain barrier and cell membranes). The emergence of smart antibody imaging agents (e.g., target-cell-specific activatable fluorescence imaging probes; Ref. 222) have addressed some of the aforementioned issues and have demonstrated the feasibility of using antibodies as magic-bullet-type imaging agents. In addition, efforts to improve the pharmacokinetics of mAbs without compromising affinity and specificity have been made through protein engineering. Initially, small fragments with one antigen binding site, namely, single chain variable fragments (scFv, 25 kDa), were developed and evaluated. However, these fragments cleared too rapidly and did not adequately accumulate at their target site (317). Further efforts led to the production of diabodies and minibodies, both of which are showing enormous promise on the preclinical research front.

### 1. Diabodies and minibodies

Diabodies are ~55-kDa dimeric antibody-based molecules comprised of two noncovalently associated single-chain variable fragments (scFv) that interact with and bind to their corresponding antigen in a divalent manner. Minibodies, also known as fusion proteins, are scFvs fused to single Fc domains, and are roughly 80 kDa in size. Both diabodies and minibodies display more favorable blood clearance kinetics, superior tumor penetration, and higher tumor-to-blood ratios compared with intact mAbs, generating high-contrast images at earlier times postinjection (432, 483).

Both SPECT and PET-labeled anti-CEA T84.66 diabodies have been synthesized and evaluated in tumor-bearing mice (165, 404). Of these, the <sup>124</sup>I- and <sup>18</sup>F-labeled versions gave the best images, the latter of which afforded high-contrast images as early as 1 h postinjection, with only background levels of activity detected in CEA-negative C6 tumors (44). Similarly, anti-CEA minibodies have been made and labeled with radioisotopes for imaging tumor-bearing mice. The slightly larger size of minibodies compared with diabodies led to less accumulation in the kidneys, whilst maintaining similar tumor-to-background ratios (10.93 for <sup>124</sup>I-diabody compared with 11.03 for <sup>124</sup>I-minibody) (404).

There have been a number of other diabodies and minibodies developed for different targets that have been modified for use in bioluminescence (436) and fluorescence (390) imaging studies (see Refs. 113, 317 and **TABLE 2** for some examples).

#### 2. Affibodies

Another promising type of engineered protein is an affibody. Affibodies are small in size (~58 amino acids, ~7 kDa), display high affinity, and possess good in vivo stability. Their fast clearance from blood, rapid accumulation at their target site, and relatively short in vivo biologic half-life mean these proteins can potentially be radiolabeled with PET/SPECT isotopes of shorter half-lives (<sup>18</sup>F and <sup>99m</sup>Tc) (349).

In 2008, Cheng et al. (60) synthesized a monomeric and dimeric version of a <sup>18</sup>F-labeled HER-2 affibody molecule. Both affibodies were evaluated using the same SKOV3 tumor-bearing mouse model and imaged using small animal PET. The monomeric version outperformed the dimeric form with its high and rapid uptake into HER-2 containing tumors, whereas the dimeric affibody showed low tumor accumulation and poor tumor-to-normal tissue ratios. The monomeric <sup>18</sup>F-labeled HER-2 affibody shows significant potential for clinical translation (60).

Affibodies for HER2 have also been labeled with <sup>125</sup>I, <sup>111</sup>In, and <sup>99m</sup>Tc, and all have resulted in high-contrast images of tumors at early times post postinjection (317). Recently, a HER2 affibody was conjugated to AlexaFluor680 and used to image HER2-positive xenografts in mice to monitor their response to treatment with heat shock protein 90 (HSP90) inhibitor (425) (see **FIGURE 8***B* for images). Affibodies have also been labeled with SPIOs for in vivo MRI imaging of HER2-positive tumors (212).

With the recent explosion in antibody-based molecular imaging agents and the plethora of encouraging preclinical data, it is likely that antibodies and their engineered fragments will play a important role in diagnosing diseases, planning treatment strategies, and monitoring response to therapies (317).

## F. Nanoparticles

Over the past decade, the attributes of nanotechnology in biomedical applications have sparked enormous interest in the scientific community, generating an increase in funding mechanisms through both government and industry, with the aim of translating these nanomaterials and technologies into the clinic (469).

In terms of imaging agents, nanoparticles are emerging as an exciting new set of diagnostic tools, capable of both passive and active targeting. Since there exist a range of different shaped nanoparticles of varying size, that can be composed of different materials, with unique surface properties and reactivities, it is not surprising that nanoparticles are among the most flexible imaging agents with respect to the types of imaging modalities they are compatible with. Although there is no fixed size constraint for what constitutes a nanoparticle, people typically consider them to be on the order of  $\sim$ 10–100 nm, and no larger than 1000 nm. Generally speaking, nanoparticles are larger than many proteins and small molecules (FIGURE 14), yet they are smaller than cells. Their relative large size (compared with small molecules and many proteins) means they are often taken up by the reticuloendothelial system (RES). Polymercoated "stealth" nanoparticles, on the other hand, can partially avoid entrapment by the RES (for hours to days) (191). Due to their high surface area-to-volume ratio, many nanoparticles are able to carry substantial payloads of 1) targeting and/or signaling moiety and 2) therapeutic drug. The former means that for each nanoparticle bound to a target there can be a large increase in signal generated compared with, for example, the one signal generated for each small molecule imaging agent bound to a target. This multivalent mode of attachment is known as avidity and is particularly important in cases where sensitivity of the imaging modality is an issue (e.g., MRI). Also, due to the large number of targeting moieties attached to the surface of nanoparticles, they typically have a greater chance of binding to their target. Being able to transport a therapeutic payload means that nanoparticles have the potential to reduce unwanted side effects of many therapies (e.g., chemotherapeutics), as drug molecules can be delivered to diseased areas in a site-specific manner. Note, however, that the advantages of nanoparticles come at the expense of generally fewer particles being delivered to a particular target site of interest, compared with the delivery of small molecules. This is typically due to nanoparticles rapidly accumulating in the RES, specifically the liver, spleen, and bone marow following their administration, and thus less of the dose is "available" for targeting/delivery.

The therapeutic and diagnostic capabilities of nanoparticles highlight their great "theranostic potential" (see sect. IVF), as they can effectively deliver a signaling and therapeutic payload to the pathological site of interest simultaneously.

Overall, due to their unique properties, nanoparticle-based imaging agents are predicted to form the basis of a new paradigm for detecting, monitoring, and treating pathologies. Some key types of nanoparticles currently impacting the field of molecular imaging are outlined below (see **TABLE 2** for some specific examples).

### 1. Single-walled carbon nanotubes

Single-walled carbon nanotubes (SWNTs) are composed of a tubular graphene sheet (230). The dimensions of these cylindrical carbon particles vary and are easily controlled, but for biomedical applications are generally on the order of a few nanometers in diameter and several hundred nanometers in length. Due to their carbon composition, high aspect ratio, intrinsic NIR fluorescence, and relative ease of conjugating different targeting and signaling moieties to their surface, SWNTs are ideal for use with a variety of different imaging modalities (245). For example, SWNTs have been used in Raman (479), PET (283), and photoacoustic (78) imaging studies. To detect SWNTs using PET, molecules containing a positron emitting radionuclide need to be attached to their surface, whereas Raman imaging can detect SWNTs without any surface modification due to their sizable intrinsic Raman peak at 1,593 cm<sup>-1</sup>. Similarly, due to their highly absorbing nature, SWNTs make good PAI agents without the need to attach additional signaling components (78). That said, our laboratory reported an enormous increase in photoacoustic signal after modifying SWNTs with certain dye molecules (77). To use SWNTs for imaging molecular phenomena, targeting moieties (e.g., small molecules, peptides, aptamers, or engineered proteins), specific for the biochemical process of interest, need to be conjugated to their surface, transforming them into targeted SWNTs.

An example of targeted SWNTs used in PAI and Raman molecular imaging studies are RGD-conjugated SWNTs for investigating angiogenic vessels in living xenograft tumorbearing mice (78, 479) (refer to sect. IIB2 for details of studies). SWNTs have also been functionalized with anti-HER2 chicken IgY antibody (HER2 IgY) for breast cancer imaging (470).

Overall, SWNTs are attractive molecular imaging agent candidates due to their flexibility and promiscuity in terms of imaging modalities they are compatible with. Moreover, their favorable shape enables them to move into and out of the vasculature and accumulate in tumor tissue via the enhanced permeability and retention (EPR) effect.\* However, their biodegradability and toxicity, once administered in the body, are the topic of much debate and may be the major limiting factor concerning their approval for human use. Our laboratory has conducted pilot toxicity studies in mice using intravenously administered SWNTs to show their potential safety; however, further tests need to be performed prior to clinical translation (368).

\*The EPR effect is based on the principle that macromolecules, including drugs and nanoparticles, can passively accumulate in tumor tissue to a greater extent than normal tissue due to the increased vascular permeability or "leakiness" associated with several tumor tissue types. This phenomenon is attributed to the abnormal architecture of the angiogenic vessels within the tumor tissue, often consisting of poorly aligned endothelial cells with wide fenestrations that can allow macromolecules to passively enter the tumor tissue site.

#### 2. QDots

QDots are small nanoparticles,  $\sim 10$  nm in size, typically comprised of the semiconductor materials cadmium and selenium. Their conducting properties are a direct result of a quantum effect intimately associated with the size and shape of individual crystals (80). Because of this, one can tune the emission wavelength of any given QDot by slightly altering its size. This high level of control is a key advantage of QDots as they can be optimized to meet the needs of a specific study and/or can be used in multiplexing experiments (i.e., a range of QDots can be synthesized, each with unique emission wavelengths and concurrent excitation so that one can image several targets simultaneously) (450). It is important to note that the size of QDots increases to  $\sim 20-30$  nm with addition of polymer coat and/or functionalization.

Compared with traditional fluorophores, QDots are much brighter due to their high quantum yield, and are more photostable (i.e., they undergo significantly less photobleaching). In fact, these semiconductor nanocrystals are believed to be  $\sim\!20$  times brighter and 100 times more photostable than standard fluorescent reporters (446), meaning images can be acquired over longer periods of time in a more sensitive manner.

QDots are commercially available in a wide range of emission wavelengths, and in terms of cancer molecular imaging, QDots have been functionalized with different tumor targeting agents for use in a variety of animal models (127, 468). A couple of specific examples include RGD peptidelabeled QDots for imaging integrins and tumor vasculature in mice (45) and QDots functionalized with monoclonal anti-HER2 antibody for visualizing HER2-overexpressing breast cancer in mice (405). While QDots appear to be suitable markers for various pathological targets, they have also proven extremely useful as a "model nanoparticle," helping imagers to understand the in vivo behavior of nanoparticles of similar size and shape (392).

The main disadvantage of QDots is their toxic core (made of cadmium), which has made clinical translation difficult, especially in the case of drug delivery, although adding a silica coating to cadmium QDots (58) or the development of new generation cadmium-free QDots (449) could help ad-

dress toxicity concerns. Other limitations of QDots include the fact that they are prone to aggregation due to their surface chemistry, and the available methods of attaching targeting moieties can be challenging and time consuming. Furthermore, there seems to be a limit as to how many QDots of different emission wavelengths can be used per study. It seems that one can only multiplex by using up to about three or four different Qdots before it becomes difficult to truly separate the signal from each QDot due to their relatively broad emission peaks. For detailed information on Qdots, please refer to the following reviews (26, 110, 449).

#### 3. Gold nanoparticles

Since colloidal gold is relatively inert and has been approved by the FDA for the treatment of arthritis (1), it is believed that nanoparticles made from gold could be a safer alternative to SWNTs and QDots. The FDA has approved several therapy-based gold nanoparticles (AuNPs) for human administration (284), such as Aurimune for the treatment of solid tumors.

Two common types of AuNPs used as imaging agents are spherical AuNPs and gold nanorods. Depending on their size, composition, and preparation, AuNPs can be used with a range of imaging modalities, including MRI, CT, radionuclide, and optical techniques. When using AuNPs for Raman imaging studies, one must first coat the outside of the particles with Raman-active molecules, a process known to enhance the Raman signal obtained from AuNPs by several orders of magnitude, allowing ultra-sensitive detection. This phenomenon is known as the SERS effect (see sect. IIB1 for description) and is due to a plasmonic resonance that occurs on the AuNP's surface when excited with a laser. There are a variety of Raman-active molecules that can be adsorbed onto the surface of AuNPs, e.g., 3,3-diethylthiatricarbocyanine, bis-pyridyl-ethylene, rhodamine 6G, and pyridine derivatives. Since these molecules each give rise to different Raman spectra, it is possible to produce multiple unique "flavors" of Raman-compatible AuNPs (known as SERS AuNPs), each with their own spectral fingerprint. By using different batches of SERS AuNPs (individually conjugated with different targeting ligands and administered together), one can theoretically image several targets, and hence biochemical processes, simultaneously. Our laboratory demonstrated the multiplexing capabilities of Raman by proving it is possible to detect up to 10 different types of spherical SERS AuNPs, each possessing its own unique Raman spectra, in living mice (204) (FIGURE 10B). To date, only a couple of targeted-SERS AuNPs for in vivo imaging have been reported, including affibody-conjugated (192) and single-chain variable fragment-conjugated (346) SERS AuNPs for detection of EGFR overexpressing tumors in living rodents.

Gold nanorods are well suited for both optical and photoacoustic imaging, due to their strong plasmon resonant absorption and emission in the visible to NIR region. The surface-plasmon peak positions of AuNRs depend on their aspect ratio, and hence can be tuned depending on the desired application (306, 417). Gold nanorods can convert optical energy into heat giving rise to intense local photothermal effects. For this reason, gold nanorods not only serve as a diagnostic (molecular imaging) tool, but also can be of therapeutic use. Recent studies using PEG-protected gold nanorods displaying excellent photothermal properties and long circulation half-life of ~17 h enabled destruction of all laser-irradiated human xenograft tumors in mice (444). An example of functionalized gold nanorods for preclinical molecular imaging studies is HER2 conjugated gold nanorods. Ding et al. (86) reported the synthesis and use of these nanorods for photothermal treatment assessment in tumor-bearing SCID mice. The results of these studies demonstrated a marked increase in local tumor temperature (and therefore effective treatment) in the mice treated with HER2-nanorods compared with the group that received nontargeted gold nanorods (86).

One of the main advantages of working with AuNPs is their flexibility in terms of the number of different imaging modalities that can detect them, thus creating the opportunity for multi-modality imaging (e.g., optical/CT/PAI). In addition, AuNPs are relatively easy to functionalize (306) with targeting moieties. The nonbiodegradable nature of AuNPs is an important consideration in terms of repeat imaging studies and toxicity. Although gold is relatively inert, and has been approved by the FDA as a therapeutic, the toxicity of different AuNPs needs to be thoroughly investigated to better understand their potential acute versus chronic toxicity, and how their nonbiodegradable nature may affect the number of allowed repeat studies. This is especially important when using imaging modalities with low sensitivities, such as CT or MRI, whereby a large dose of AuNPs would need to be administered to obtain a measurable signal.

The main limitation of working with large (>100 nm) spherical (gold-based and other) nanoparticles is their round shape, which makes it challenging for them to extravasate and reach their target site (unless their target site is within the blood vessel itself). However, it has been shown that some cancers display a leaky vasculature, and nanoparticles of this size/shape can selectively accumulate due to the EPR effect. Nanorods, on the other hand, are likely to escape the vasculature with relative ease due to their favorable shape.

#### 4. Superparamagnetic iron oxide nanoparticles

Superparamagnetic iron oxide nanoparticles (SPIOs) are specifically designed for imaging studies using MRI (see sect. IIA2). They are typically comprised of an iron oxide (magnetite) core coated with a hydrophilic matrix material.

They produce their contrast by disturbing the local magnetic field in which they are placed. This disturbance results in ultrafast dephasing of neighboring protons (shortened T2), leading to a measurable alteration in MR signal (signal loss in MR images) (416; see sect. IIA2 for details on MR signal).

The size of SPIOs varies considerably, from 2–3 nm up to micrometers (416). The types of SPIOs used for molecular imaging purposes are typically in the tens of nanometers size range, contain a dextran coat for stabilization, and can either be directly targeted to membrane receptors (via conjugating specific peptides or engineered proteins to SPIOs) or preloaded into cells of interest so they can be tracked over time (see sect. IVE for details on cell tracking).

Some examples of receptor imaging using SPIO molecular imaging probes include SPIO-chlorotoxin peptide conjugates (Cy5.5-SPIO-chlorotoxin) specific for imaging matrix metalloproteinase-2 (434) **(FIGURE 4B)**, anti-HER2 affibody-conjugated-SPIOs for detecting HER-2 expressing cancer cells (212), and complement receptor type 2 (CR2)-targeted SPIOs for localizing renal inflammation (378). Please refer to the following review (416) for a summary of synthetic strategies (including coprecipitation and microemulsion) for SPIOs.

SPIOs are generating much interest, not only due to their biodegradability (97), targeting (and cell-loading/tracking) abilities, and low toxicity, but also due to the fact that nontargeted SPIOs have been used in the clinic for some time now (making clinical translation of targeted-SPIOs easier). However, there are also a number of limitations associated with SPIOs, mainly due to the high amounts needed to obtain a detectable MR signal, and their often large size, which mostly limits them to targeting intravasculature sites, or to uptake by cells through phagocytic pathways.

## 5. Nanoparticle molecular imaging agents: concluding remarks

As exciting as nanoparticle-based imaging agents are, their limitations should be kept in mind. Their size can sometimes be a key factor concerning their effective utilization in living subjects. Delivery to target sites at a sufficient concentration remains a significant challenge, primarily due to competition for uptake via the RES. Other issues are related to slow clearance times, thereby making it potentially difficult to distinguish targeted nanoparticle bound to the target(s) of interest from nonbound nanoparticle. Also, due to their heterogeneity, one is not dealing with the exact same entity, as is the case for small molecules. This makes their characterization, toxicity, and potential translation more challenging. However, the growing number of approved therapeutic nanoparticles (100, 362) (such as Doxil, a liposome drug delivery system used to treat AIDS-associated

Kaposi's sarcoma and ovarian cancer) is currently serving as a template for the clinical translation of functionalized nanoparticles for molecular imaging purposes, thus accelerating progress in this area.

## **G.** Multimodality Probes

Multimodality probes are imaging agents capable of being detected via two or more different imaging modalities simultaneously. Since these types of probes have the potential to generate multiple readouts concerning the same biological phenomenon, they could be of great value for numerous clinical and basic research applications.

Multimodality probes are predominately nanoparticle based (e.g., SPIOs, gold nanospheres/nanorods, SWNTs, QDots); however, there are also examples of engineered proteins (312), peptides (96), and small molecule-type multimodality probes (293). Typical examples of the types of multimodality imaging these probes enable include MRI/ optical, MRI/PET, MRI/SPECT, PET/optical, SPECT/optical, PAI/Raman, and PAI/Raman/IVM imaging (see TABLE 2 for examples of multimodality probes).

A specific example of a multimodality probe that has been used for molecular imaging of angiogenesis is  $^{99m}\text{Tc-labeled}$  gadolinium-containing  $\alpha v\beta 3$ -targeted nanoparticles. SPECT and MRI imaging of these nanoparticles in tumor-bearing rabbits (248) demonstrated specific accumulation in tumor neovasculature. MRI molecular imaging along with 3D mapping of angiogenesis in the tumor showed that the neovasculature was asymmetrically located along the periphery of the tumor, whereas CT scanning could not delineate between tumor and lymph node, showing the benefit of a SPECT/MRI multimodality probe compared with imaging with a SPECT probe and SPECT/CT.

An example of a multimodality probe that is detectable via three different imaging modalities (MRI, PAI, and Raman imaging) is the MPR nanoparticle (213). This triple-modality probe was shown to accurately identify tumor margins in mice bearing orthotopic human glioblastoma tumors in the intact skull and also intraoperatively, highlighting its potential for helping solve the important clinical problem of glioma management. Current methods for delineating brain tumor margins, before and during surgery, are often fraught with difficulty due to inadequate sensitivity, specificity, and spatial resolution. With the use of the strengths of MRI, PAI, and Raman imaging, the MPR nanoparticle is able to sensitively and accurately detect tumor margins at high spatial resolution and is thus a promising new approach that warrants further investigation.

Some advantages of implementing a multimodality probe over single-function probes include 1) less time is required to obtain more information, 2) only one injection is needed, 3) favorable characteristics from complementary modalities can be ex-

ploited whilst overcoming limitations of individual modalities (e.g., one can potentially obtain high-resolution, high-sensitivity scans with PET/MRI multi-modality probes), and 4) a combined probe means that pharmacokinetics will be kept constant (259), whereas two separate probes will have different pharmacokinetics which can be problematic.

The main challenge involved in developing and using multimodality imaging probes is that some modalities (such as PET and MRI) differ in their sensitivities by more than three orders of magnitude (259). Hence, it is not ideal to simply add probes together, as a much higher mass of MRI probe is needed compared with a PET probe for detection, and if we simply combine the two in a 1:1 ratio, the high sensitivity of PET will be wasted. For this reason, a combined probe can lead to a compromise compared with using each component separately (30). An example of this was demonstrated by a multimodality probe consisting of iron oxide nanoparticles coated with <sup>64</sup>Cu-RGD whereby the <sup>64</sup>Cu-RGD peptide was shown to be a more favorable imaging agent compared with the multimodality probe combination (30). This was due to high nonspecific binding and high liver uptake of the multimodality probe (both 10-fold higher) due to increased circulation half-life and affinity of nanoparticles for the RES, respectively. For a thorough review of multimodality imaging probes, please see Ref. 259.

## IV. APPLICATIONS OF MOLECULAR IMAGING

## A. Oncology

Cancer is a devastating global health issue affecting every socioeconomic class, from the poverty stricken to the very affluent. Despite the considerable resources dedicated to fighting cancer, it remains the leading cause of death worldwide, accounting for a total of 7.9 million deaths (~13% of all deaths) in 2008, as reported by the World Health Organization (WHO). This number is expected to increase dramatically over the coming years and is projected to triple by the year 2030.

There have been numerous developments in cancer research over the past two decades, including the discovery of novel diagnostic strategies and therapeutics, identification of key causal factors, and the mapping of the entire genome sequences of two separate cancers (379). However, the above statistics speak for themselves and serve as a reminder that we still have a long way to go to impact this devastating disease.

Traditionally, cancers have been diagnosed and staged via biopsies, exploratory surgery, or anatomical imaging techniques such as CT or MRI. However, since biopsies are invasive and biochemical changes occur much earlier than morphological ones, these techniques have their limitations. On the other hand, molecular imaging can act as an enhanced, noninvasive means of detecting, staging, and monitoring cancer progression. Molecular imaging can also be used to expedite cancer drug discovery (373), predict responders versus nonresponders to certain treatments (398), and help determine the overall effectiveness of therapies longitudinally (260). Importantly, on a basic research level, molecular imaging can help to unravel the underlying mechanisms of cancer.

Generally speaking, cancer involves the alteration of numerous surface cell receptors (e.g., various growth factor receptors), sustained angiogenesis, alterations in signaling pathways, changes in cellular metabolism (e.g., as a direct result of increased requirements for amino acids, lipids, and/or glucose), and the modification of genes that regulate proliferation, vascular recruitment, hypoxia, apoptosis, evasion of the immune system, and metastasis (147, 282). When developing molecular imaging agents for cancer-related applications, a researcher can target any one of the aforementioned processes (e.g., angiogenesis) or a combination of a few simultaneously (via multiplexing approaches) (223). Currently, there are multitudes of imaging agents available for imaging various cancer-related targets at a basic research level (as well as some for clinical applications). Examples include agents for angiogenesis (25, 43, 68), hypoxia (230, 286), proliferation (201, 308), tumor metabolism (338), apoptosis (139, 141), and metastasis (131, 300, 322). The scope of this review does not allow for a detailed description of how molecular imaging agents can be used to visualize each of these processes; however, please refer to the reviews referenced above along with the following reviews (6, 121, 430) for further details. Provided next are a few examples of molecular imaging agents for clinical and preclinical oncology studies.

The metabolic imaging agent [18F]FDG (see sect. IIA3 and FIGURE 13) is commonly used in the clinic for detecting and staging different cancers (17, 98, 150, 178). More recently, [18F]FDG has shown promise for its ability to monitor and predict response to chemotherapy and radiation therapy (8). Choi et al. (63) demonstrated that [18F]FDG has the potential to predict response to therapy and patient survival in pancreatic cancer patients. In this particular study, 20 patients with locally advanced pancreatic cancer were scanned via [18F]FDG-PET following neoadjuvant induction chemotherapy, and then again after chemoradiotherapy. Mean survival for patients classified as responders via [18F]FDG-PET scans was 23.2, and 11.3 mo for those classified as nonresponders via [18F]FDG-PET. A separate study involving patients with locally advanced breast cancer demonstrated the possible role of [18F]FDG in differentiating responders from nonresponders following neoadjuvant chemotherapy (231). In this study, it was found that the sensitivity, specificity, and accuracy of [18F]FDG-PET/CT in identifying responders and nonresponders were 93, 75, and 87%, respectively. Other similar studies have also been performed; however, some found that [<sup>18</sup>F]FDG-PET uptake failed to correlate with long-term patient outcome (40). Further studies are required to determine the potential role of [<sup>18</sup>F]FDG-PET in therapy monitoring and predicting clinical outcome.

In terms of cancer molecular imaging in a preclinical setting, there are a number of different types of research initiatives being conducted, including (but not limited to) 1) the design, development, and validation of new cancer-detecting imaging agents/imaging techniques; 2) the creation of imaging agents specifically for monitoring response to therapy, or to serve as prognostic indicators; and 3) molecular imaging studies using techniques such as cell tracking (see sect. IVE) or reporter gene imaging (see sect. IVD) to study the underlying mechanisms and signaling pathways of cancer.

An example of a study involving the synthesis and assessment of a novel imaging agent for cancer detection is one reported by Yang et al. (474). In this study, the authors describe the use of optical/MRI dual-modality magnetic iron oxide (IO) particles targeted at the serine protease urokinase plasminogen activator receptor (uPAR) for detecting pancreatic cancer and its metastases in an orthotopic human pancreatic cancer mouse model (474). High levels of uPAR are often found in pancreatic cancer, and its presence is closely associated with tumor progression, metastasis, and shortened survival in patients (351). NIR dye-labeled amino-terminal fragment (ATF) peptides were conjugated to IO particles and injected in living mice for both MRI and optical fluorescence imaging studies. Results from this study demonstrated the ability of these targeted-IO particles to selectively bind to, and accumulate in, small pancreatic tumors (0.5–1 mm<sup>3</sup>) in living mice. Interestingly, there was a clear advantage of using Cy5.5-ATF-IO nanoparticles in tumor targeting compared with using Cy5.5-ATF peptides alone (FIGURE 16). Since these particles can be detected by both MRI and optical imaging platforms, there is significant potential for clinical translation, for both diagnostic applications (detection of pancreatic cancer lesions by MRI) and intraoperative applications for delineation of tumor margins (via optical fluorescence imaging), thus making this strategy a promising new way to image cancer.

Another preclinical example of cancer molecular imaging was reported by our laboratories, whereby a novel peptide-based imaging agent was compared head-to-head with [ $^{18}$ F]FDG. The study involved the comparison of both radioligands in a spontaneous lung tumor mouse model (304). The PET imaging studies demonstrated that the novel  $^{64}$ Cu-labeled knottin peptide (targeted to integrins upregulated during angiogenesis) displayed a higher tumor to background (normal lung) ratio compared with [ $^{18}$ F]FDG (6.01  $\pm$  0.61 vs. 4.36  $\pm$  0.68; P < 0.05), thought to be due to its high uptake, retention, and low background accumulation in the thorax region.  $^{64}$ Cu-labeled knottin

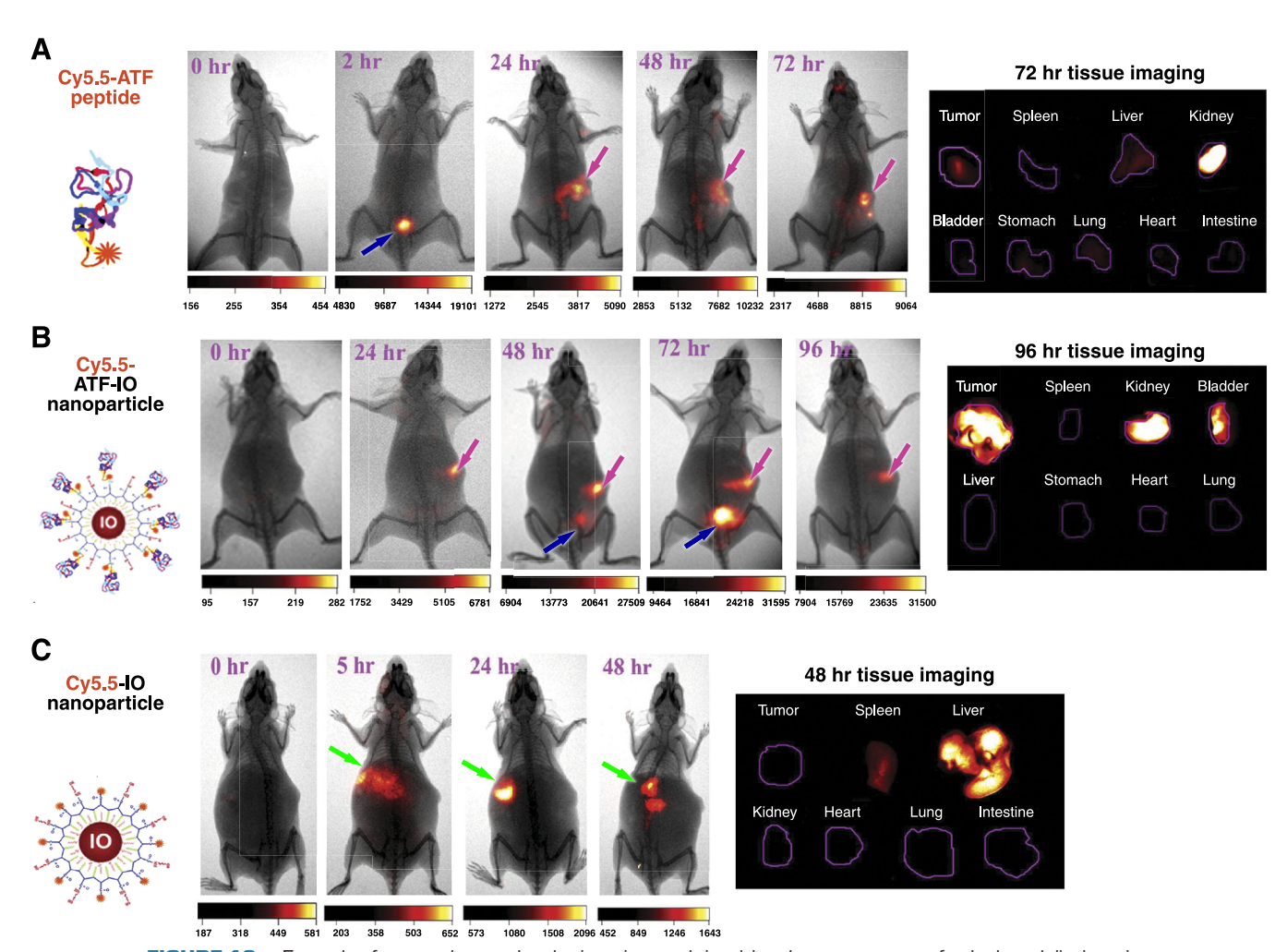


**FIGURE 16.** Example of an oncology molecular imaging study involving the assessment of a dual-modality imaging agent for detecting pancreatic cancer. Iron oxide (IO) particles functionalized with amino-terminal fragment (ATF) peptides labeled with near infrared (NIR) dye (Cy5.5) were administered to mouse models of human pancreatic cancer. Mice were imaged via optical fluorescence imaging to assess in vivo targeting abilities of the imaging agent (452). Blue arrow, bladder; pink arrow, tumor; green arrow, liver. On the *left* of the figure, chemical compostions of the imaging agents are represented. In the *middle* and *right* of the figure, in vivo fluorescence images at different time points, and fluorescent imaging of tissues are shown. A: free Cy5.5-ATF peptides. B: "targeted" Cy5.5-ATF-IO nanoparticles. C: nontargeted Cy5.5-IO nanoparticles. The imaging results demonstrated the ability of the targeted Cy5.5-ATF-IO particles to selectively bind to and accumulate in small pancreatic tumors (0.5–1 mm<sup>3</sup>) in living mice. Interestingly, there was a clear advantage of using Cy5.5-ATF-IO nanoparticles in tumor targeting compared with using free Cy5.5-ATF peptides, displaying a three- to fourfold greater accumulation in tumor regions. See Ref. 474 for quantitative analysis of images. Particles were able to be detected by both optical and MR imaging. [From Yang et al. (474), with permission from Elsevier.]

peptide could be a promising new agent for detecting and characterizing lung cancer.

Molecular imaging, in combination with traditional techniques, is essential to understanding the molecular targets and processes involved in cancer. The use of molecular imaging for cancer-related applications will hopefully lead to earlier diagnosis and better management of cancer patients, thus improving patient survival rates.

#### **B.** Neuroscience

The brain is a highly complex entity, and although there has been much progress in neurological research over the last few decades, many of the basic functions and pathologies of the brain remain enigmatic. Neurons account for 10% of the total brain cell population (~100 billion cells), while the other 90% are glial cells. Mechanisms of individual brain cells, their synapses, and how they operate are fairly well established; however, the way in which these cells interact with one another, form intricate networks, and participate in cross-talk is poorly understood. Furthermore, how and why particular neuropathologies arise within the brain is yet to be fully determined.

Our limited knowledge of the brain and the initial molecular processes involved in neurological disease has made early diagnosis of brain diseases a near-impossible task.

Traditionally, the presence of a particular CNS disease is confirmed in late stages of the condition (when clinical signs are obvious, and in many cases, extensive neuronal death has occurred) or via postmortem analysis. However, over the past few decades, this has been gradually changing, mostly due to the advent of noninvasive imaging techniques. Neuroimaging, using techniques such as MRI, PET, and SPECT, has enabled clinicians and scientists alike to understand some of the basic operations of the brain more clearly in a noninvasive manner. Researchers have been able to identify key hallmarks of many neurological diseases, whilst observing how they develop and progress over time. Molecular imaging has been used to interrogate and provide insight on multiple areas of neuroscience including neurodegenerative diseases (92, 103), neuroinflammatory conditions (401, 438), stroke (151), brain tumors (422), neuropyschiatric conditions (424), and changes in brain metabolism. The scope of this review does not allow for a detailed description of molecular imaging applications in each of these areas of neuroscience (for a thorough account, please see above references and Ref. 146 for a review of molecular neuroimaging). Some specific examples of different molecular imaging agents, and how they have been used to assist researchers and clinicians in understanding and diagnosing neuroinflammatory/neurodegenerative conditions will be described, from both a preclinical and clinical perspective.

Neurodegeneration is a process in which the cells in the brain and/or spinal cord gradually deteriorate and are lost over time. There are numerous theories regarding the etiology of this process, including those involving infection (193), free radical production (341), excitotoxic cell death (324), loss of neurotrophic factors (153), ingestion of a neurotoxin (319), mitochondrial dysfunction (18), and induction of apoptosis (315); however, a single causal factor is yet to be identified. The process of neurodegeneration is common to many disorders including Alzheimer's disease (AD), Parkinson's disease (PD), multiple sclerosis (MS), Huntington's disease (HD), human immunodeficiency virus (HIV) associated dementia, and Creutzberg-Jakob disease. The neurodegenerative process and resulting cell death for each of these diseases occurs in different brain regions and thus leads to different clinical hallmarks and symptoms, most of which have extremely debilitating consequences for the affected individual.

In the case of AD, there is an abnormal protein aggregation in and around neurons within the limbic, paralimbic, and neocortical structures of the brain, the regions controlling memory, thus causing a progressive loss of memory, cognitive decline, disorientation (regarding time and space), and impaired judgment. PD, on the other hand, is typified by the loss of dopamine (DA)-producing neurons in the basal ganglia, the brain region governing body movement, resulting

in pronounced motor-related clinical signs including bradykinesia (slowness in movement), rigidity, and tremor.

Due to the diversity and complexity of each type of neurodegenerative disease, it is important to investigate different biochemical aspects of neurodegeneration within each of these states. This will ultimately lead to a more complete understanding of these conditions and aid in devising better diagnostic and treatment strategies. There are a number of available molecular imaging agents for diagnosis and/or assessment of treatment efficacy in the clinical setting, all of which are either PET or SPECT based. In terms of AD, [18F]FDDNP has proven useful in detecting both plaques and tangles (202), and Pittsburg compound B ([11C]PIB) has gained attention as a suitable radioligand for quantitative imaging of amyloid plaques (219). Radioligands such as [11C]WIN 35,428, specific for the dopamine transporter (DAT), have been used as early indicators of PD since DAT levels are known to decrease in parallel with the loss of dopamine neurons in the initial stages of PD, before any clinical signs manifest (274). In terms of monitoring PD progression and treatment effectiveness, [18F]fluorodopa, a specific radioligand for measuring presynaptic dopaminergic metabolism (Table 5), has been used in a number of clinical trials (275). One such trial involving 186 PD patients demonstrated, via [18F]fluorodopa PET imaging, that patients receiving the DA agonist ropinirole displayed a significantly reduced loss of striatal uptake at 2 years compared with patients given levodopa (13 vs. 20%) (66).

On the preclinical research front, various molecular imaging agents have been developed to investigate more fundamental molecular events relating to neurodegeneration, in particular, the presence of neuroinflammation and its apparent involvement in the initial onset of degenerative conditions. One such target is the peripheral benzodiazepine receptor (PBR), also called the translocator protein (18 kDa) (TSPO) (323), known to be present at high levels in microglial cells upon their activation (an event intimately associated with neuroinflammation). In 2009, Venneti et al. (437) demonstrated that the retention of [11C]PK11195, a selective PET radioligand for the PBR, in transgenic AD mice correlated with the amount of microglial activation determined by histology, effectively proving the value of the PBR as an in vivo marker of microglial activation in neuroinflammatory and neurodegenerative conditions.

Since these results, and other similar results, it has become clear that imaging agents targeting the PBR may act as useful markers of neuroinflammation. Over the past two decades [\frac{11}{2}C]PK11195 has been used in numerous preclinical and clinical studies of neuroinflammation and has highlighted that microglial activation occurs in very early stages of AD and precedes brain atrophy (41). Currently, [\frac{11}{2}C]PK11195 is the most widely used pharmacological imaging agent for the study of the PBR in living subjects; it has

been used to visualize increased levels of PBR expression (and thus microglial expression) in patients with MS (16, 81), AD (41, 439), herpes encephalitis (42), and numerous other neurological disorders. **FIGURE 17** displays the results from a human PET study involving volunteers (both healthy and those with mild AD) and [11C]PK11195 as the imaging agent. The study found that the extent of [11C]PK11195 binding represented the severity of microglial activation/ neuroinflammation and could be used as a marker of early disease in the living brain (41). Since these early studies with [11C]PK11195, a number of newer PET and SPECT radioligands specific for the PBR have been synthesized with the aim of improving on the low brain permeability and high protein plasma binding observed with [11C]PK11195. The newer PBR specific radioligands, namely, [123I]CLINDE (12), [18F]FEDAA1106 (115), and [11C]DPA-713 (99, 184), are all currently undergoing human clinical trials to determine which is most useful as a PBR imaging agent. The development of such radioligands is important and may represent useful indicators of inflammatory-associated neurodegeneration, thus enabling earlier detection in conditions like AD. Moreover, these imaging agents, and others targeting markers of neuroinflammation, may assist in deciphering the role of microglia/inflammation in different pathological states.

Apart from radionuclide-based strategies, there have been a number of optical and MRI-based techniques developed for visualizing neuroinflammation, including the use of P-selectin targeted iron oxide nanoparticles for MRI imaging of early endothelial activation in poststroke inflammation (188), and the tracking of luciferase-expressing bone marrow cells via bioluminescence (4). The latter of these techniques involved the intravenous administration of luciferase-expressing bone marrow cells, known to differentiate into bone marrow-derived microglia after crossing the blood-brain barrier, induction of neuroinflammation via a stereotactic injection of lipopolysaccharide (LPS), and

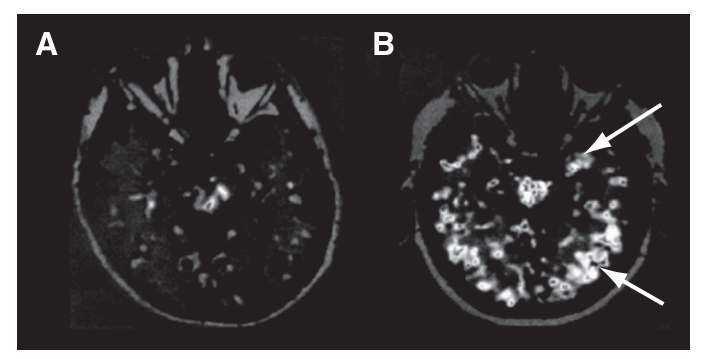


**FIGURE 17.** Example of a clinical molecular imaging study of neuroinflammation in patients with mild Alzheimer's disease (AD) using [<sup>11</sup>C]PK11195, positron emission tomography (PET), and magnetic resonance imaging (MRI). This figure shows brain PET images coregistered with MRI images for a normal elderly subject (A) and a patient with mild AD (B). Arrows represent regions of increased [<sup>11</sup>C]PK11195 binding found in mild AD patient and not in elderly control. [From Cagnin et al. (41a), with permission from Elsevier.]

tracking of the luciferase-expressing bone marrow-derived microglia through a cranial window in a mouse head using bioluminescence. These studies demonstrated that bioluminescence can be used to quantitatively and continuously visualize bone marrow-derived cells in a living subject (with a cranial window), as confirmed by immunohistochemistry.

Techniques such as these, whereby cells and molecular processes can be visualized in their natural environments, are beginning to shed considerable light on the biochemistry of brain inflammation and are thus serving as a means of unraveling this perplexing cellular pathway. Overall, noninvasive imaging of the brain is an important application of molecular imaging and has led to numerous developments and discoveries, and has great potential in the fields of psychiatry (47), neurology (180), neuroscience (179), and neuropharmacology.

### C. Cardiovascular

Cardiovascular (CV) disease, although preventable in many cases, is the number one cause of mortality in the United States and most European countries, ahead of cancer. Like cancer and neurological pathologies, CV diseases are complex, difficult to detect early, and vary from patient to patient. Some of the key types of CV diseases include atherosclerosis, heart failure, myocardial ischemia, and myocardial viability (467).

Traditional methods for detecting and studying these diseases have involved invasive angiography, stress echocardiography, anatomical imaging techniques (CT angiography, intravascular US), and a range of functional imaging strategies employing MRI, PET, and SPECT. Although these methods provide useful information, they are limited to detecting anatomical and physiological changes (such as contractile function or blood flow), which are not always accurate indicators of disease. For example, in atherosclerosis, a decrease in the size of the vessel lumen (detected via angiography) is typically used as a sign of plaque formation; however, some people show no physical, morphological, or physiological indications of disease via angiography prior to having a cardiac event. Others experience rupturing of plaques in areas containing small to modest luminal narrowing (467). Serum markers are also used for atherosclerosis patients, but mainly to predict future cardiovascular events (226); however, these markers can only provide information on the entire "cardiovascular burden" of a patient and cannot provide insight on the location and vulnerability of individual plaques (194).

Molecular imaging, involving the use of targeted imaging agents specific for various biochemical indicators of CV disease, could potentially enable earlier detection and more accurate monitoring of these conditions. Additionally, molecular imaging may help validate and assess the efficacy of

treatments such as statins, stem cell transplantation, and gene therapy. Please refer to the following reviews for detailed descriptions on the current status of CV molecular imaging (56, 364, 467). A few key examples of how molecular imaging is being used in atherosclerosis and heart failure (HF) will now be described.

#### 1. Atherosclerosis

Molecular imaging of atherosclerosis is an expanding area of CV research in which many approaches have been developed (279, 448). Most myocardial infarctions (heart attacks) and sudden cardiac related deaths occur due to thrombosis and subsequent rupture of plaques seen in atherosclerosis. Therefore, it would be of great value to be able to identify and stage asymptomatic vulnerable plaques at high risk of acute complications noninvasively and repeatedly over time, so as to implement appropriate treatments (89, 364).

Atherosclerosis is no longer viewed as a disease solely involving accumulation of pathological low-density lipoproteins (LDLs); it is now recognized as a chronic condition comprised of many intricate stages whereby the immune component is crucial to its initiation and progression (i.e., formation of plaques, their destabilization, and rupturing) (264, 400). The general process of plaque development and progression within atherosclerosis, and the molecular mechanisms underlying this condition, can be broken down into the following stages (62).

- 1) Endothelial activation: accumulation of LDLs (plasma proteins that carry cholesterol and triglycerides) and their subsequent oxidation, triggers the expression of adhesion molecules, such as ICAM, VCAM, and PECAM, on endothelial cells.
- 2) Recruitment of leukocytes: the expression of adhesion molecules leads to recruitment and firm attachment of T cells and monocytes. After monocytes differentiate into macrophages, they activate T cells, resulting in production of proinflammatory cytokines (e.g., IFN- $\gamma$  and TNF- $\alpha$ ). This perpetuates the cycle by activating macrophages, triggering the release of other inflammatory mediators.
- 3) Formation of foam cells and necrotic core: when macrophages endocytose LDLs they are termed "foam cells" (264). Formation and aggregation of foam cells results in "fatty streaks" and production of a necrotic core. The center of the core contains an abundance of apoptotic and necrotic cells (62).
- 4) Fibrous plaques: fibrous plaques are considered to be mature atherosclerotic plaques and are characterized by a necrotic core, consisting of lipids, cell debris, and a fibrous cap.

5) Advanced lesions and thrombosis: when macrophages secrete proteases and collagenases they can degrade the smooth muscle cell (SMC)-derived extracellular matrix (ECM) of the fibrous cap and cause the plaque to rupture. Calcification and angiogenesis are also common characteristics of advanced lesions and thrombosis (62).

Molecular imaging using specific and selective imaging agents can be used to interrogate each of the above outlined stages of plaque development (i.e., macrophage recruitment, adhesion molecules, apoptosis, angiogenesis, ECM degradation). Examples of such molecular imaging strategies include antibodies coupled to immunomicelles (for optical and MRI imaging of macrophage scavenger receptor CD204) (10), targeted microbubbles for US identification of VCAM-1 (196), 99mTc-labeled annexin A5 for SPECT imaging of apoptosis in fibrous caps (208), <sup>18</sup>F-galacto-RGD for PET imaging of vascular inflammation and angiogenesis (via detection of alpha-V beta-3) (234), and MRI probes for imaging MMPs involved in ECM degradation (235). All of these imaging strategies show promise, however, none is able to image processes that are entirely specific to atherosclerosis (e.g., apoptosis and angiogenesis are also hallmarks of other diseases such as cancer). This is an issue with many molecular imaging strategies in general, not just those for cardiac imaging.

Since the first study in 1987 proving [<sup>18</sup>F]FDG could detect inflammation in blood vessels (413), the metabolic molecular imaging agent has been used in numerous clinical studies to evaluate plaque progression (310, 359) and has demonstrated its use as a viable means of detecting and quantifying inflammation in atherosclerosis-related plaques (when coupled to CT or MRI) (38, 194). Although [<sup>18</sup>F]FDG has shown potential in imaging the inflammatory component of atherosclerotic plaques, and seems to correlate well with the number of macrophages present (310), it still remains unclear whether [<sup>18</sup>F]FDG uptake is a reliable indicator of plaque vulnerability, and whether it can accurately predict future CV events. Large-scale prospective studies need to be performed to begin answering these questions.

#### 2. Heart failure

Heart failure (HF), also called congestive heart failure (CHF), is a progressive disorder characterized by dyspnea, fatigue, generalized weakness, and edema. Traditionally, the basic assessment of HF patients has been performed by echocardiographic evaluation of left ventricular function. However, noninvasive imaging strategies are emerging for visualizing molecular processes involved in HF, including cellular injury, neurohormonal receptor function, and metabolism (107).

An example of a preclinical molecular imaging technique for visualizing HF is the imaging of cardiomyocyte apoptosis in a transgenic mouse model of HF using annexin-labeled fluorescent IO-nanoparticles (AnxCLIO-Cy5.5) and a 9.4-T MRI (395). Results of this study demonstrated that sparse amounts of apoptotic cardiomyocytes could be imaged using this approach with high spatial resolution and that this imaging strategy could be useful in the validation of new anti-apoptotic therapeutics for HF.

Clinical examples of molecular imaging strategies for HF include the use of [123 I]metaiodobenzylguanidine ([123 I]mIBG) as a prognostic indicator in HF patients (3, 181). Since [123 I]mIBG is simply a radiolabeled analog of the antihypertensive drug guanethidine, it is thus taken up by norepinephrine transporter system and accumulates in adrenergic nerve terminals (3). A reduced amount of [123 I]mIBG uptake is related to many CV diseases including HF. For more examples of how molecular imaging has been applied in managing and studying heart failure, please see Reference 386.

## D. Reporter Gene Imaging and Gene Therapy

Reporter gene imaging is an indirect imaging technique whereby the location, persistence, and expression levels of a reporter gene can be monitored repetitively over time, in a noninvasive manner. Over the past decade, reporter gene imaging has become increasingly important in terms of monitoring and optimizing gene therapy, investigating protein-protein interactions, imaging transgenic animals, cell tracking, and drug development.

In general, a reporter gene strategy consists of 1) a reporter gene and 2) a corresponding reporter probe. The reporter gene typically encodes a well-known protein (receptor, enzyme, or transporter) and the reporter probe is used to detect this protein via an imaging modality such as bioluminescence, PET, SPECT, or MRI. There are also reporter gene strategies for optical fluorescence imaging; however, they do not require a reporter probe per se, as the optical reporter genes (e.g., GFP, RFP) lead to the expression of a protein capable of producing detectable light (following excitation light reaching the reporter protein). In any case, the imaging signal detected in reporter gene strategies reflects the levels of reporter gene expression. The reporter gene is driven by a promoter of choice. This promoter can be a constitutive type that is always on (e.g., CMV promoter), or be activated based on some intracellular event. In this way the reporter gene expression is regulated by the choice of promoter.

## 1. What does molecular imaging offer that traditional reporter strategies do not?

Traditional reporter gene strategies either involve analyzing postmortem samples or taking tissue samples from living subjects, thus making it difficult to perform repeat measure-

ments. Also, the information yielded from these studies can be limited. For example, the gene expression in one tissue sample is not necessarily indicative of the expression levels in other regions of the body. In contrast, molecular imaging of reporter genes/products has the benefit of enabling non-invasive tracking of gene expression levels, their persistence, and location over time, in living intact subjects (123, 125).

## 2. Characteristics of an ideal reporter gene imaging strategy

- Reporter gene should be already present in mammalian cells, to circumvent an immune response, but not expressed.
- Apart from transgenic applications, the size of the reporter gene and its driving promoter should be small enough to fit into a delivery vector (e.g., plasmid, virus).
- The image signal should correlate with the levels of reporter gene mRNA and protein in vivo.
- The protein product of the reporter gene should not cause an immune response.
- The signal should only be detected in regions where the reporter gene is expressed.
- The strategy should not lead to alterations in the biological system of interest [e.g., in the D2R reporter gene system, it was found that DA was interacting with the reporter gene products, namely, the D2R, and causing G protein-mediated inhibition of cAMP production. After discovering this, Liang et al. (247) developed a mutant D2R reporter gene system whereby DA binding is uncoupled from signal transduction].

In systems where a reporter probe is required, the probe should ideally 1) only accumulate in regions where the reporter gene is expressed (the reporter probe should not engage in nonspecific binding or accumulate in tissues where the reporter gene is not expressed); 2) display excellent in vivo stability i.e., should not be the subject of metabolism prior to reaching its target; 3) be nontoxic (including its metabolites); 4) clear from the blood, and any other nonspecific tissues, rapidly so as to not interfere with the detection of the specific signal. However, if the reporter probe does not produce any signal until it interacts with reporter protein (e.g., D-luciferin and firefly luciferase), then rapid blood clearance is not necessary.

As mentioned above, the applications of reporter gene imaging are many; this section of the review will only discuss applications pertaining to gene therapy/targeted gene expression. Please refer to the following reviews (124, 195, 292, 377) and recent textbook (125) for a detailed account of the clinical and basic research applications of reporter gene imaging. Also, see section IVE for examples of how reporter gene imaging (as well as direct imaging approaches) can be used for cell tracking.

Gene therapy has great potential for treating many diseases (e.g., sickle cell anemia, Huntington's disease, cancer, blood disorders, etc.); however, the therapeutic benefit of these treatments is currently not convincing. Since reporter gene imaging can be used as a generic means of monitoring expression of therapeutic genes, it has the potential to help unravel the underlying problems of current gene therapy techniques and expedite their optimization and subsequent clinical translation.

Over the past decade, a number of reporter gene strategies have been developed that are capable of indirectly measuring levels of a given therapeutic gene (156, 347). This is typically achieved by coupling a therapeutic gene to a known reporter gene so that they can both be delivered and expressed simultaneously.

A recent preclinical example of this is the use of the MRIbased transferrin receptor (TfR) reporter gene system to monitor the expression levels of endostatin gene (449). The endostatin gene encodes the endostatin protein, which is known to be a potent inhibitor of angiogenesis. This specific example involved intratumoral injection of a specially designed retroviral plasmid containing both the TfR gene and endostatin gene, connected by an internal ribosomal entry site (IRES), in mice bearing breast tumors. Following this, the mice were injected with the reporter probe (transferrinconjugated ultrasmall SPIOs) and imaged using MRI. The results of the study showed that it was possible to visualize therapeutic gene expression in breast tumors in mice, and although the results were encouraging, there were a number of important limitations of the study. Some of these limitations included the poor sensitivity of MRI, the use of a retroviral vector for gene transfer (which has a number of associated risks that limit its clinical translation including possible immunogenic affects), and the intratumoral delivery route, which is not ideal as most gene therapies will be targeted towards diseases in which the exact location may not be known (e.g., cancer metastases). Further work is needed to fully explore and optimize this approach.

Another preclinical example of assessing a reporter gene imaging strategy for noninvasive monitoring of gene therapy is the use of the PET-based HSV1-tk reporter gene system and [18F]FHBG as a reporter probe for monitoring cardiac therapeutic gene delivery and expression in pigs (357) **(FIGURE 18).** PET/CT imaging revealed that there was [18F]FHBG accumulation in regions that received the gene therapy. Through these studies, it was found that the optimal time (with highest signal to background) to assess [18F]FHBG accumulation in the myocardium was 3 h after reporter probe administration.

This same reporter gene strategy has been evaluated in a clinical situation, whereby the expression of HSV1-tk in seven hepatocellular carcinoma (HCC) patients was monitored via [18F]FHBG PET imaging (332). Two days following intratu-

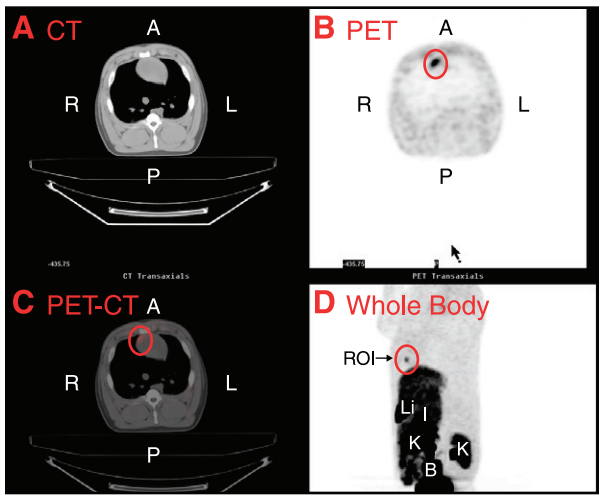


**FIGURE 18.** Example of molecular imaging study using reporter gene/reporter probe strategy to monitor cardiac therapeutic gene delivery in pigs. Computed tomography (CT) image (A), positron emission tomography (PET) image (B), fused PET/CT image (C), and whole body PET image (D) from pig study conducted using herpes simplex virus 1 thymidine kinase (HSV1-tk) reporter gene system and <sup>18</sup>F-radiolabeled 9-[4-fluoro-3-(hydroxymethyl)butyl]guanine ([<sup>18</sup>F]FHBG) as a PET reporter probe. PET/CT imaging revealed that there was [<sup>18</sup>F]FHBG accumulation in regions that received the gene therapy. A, anterior; B, bladder; CL, contralateral; I, intestines; K, kidney; L, left; Li, liver; LV, left ventricular; P, posterior; R, right. [From Rodriguez-Porcel et al. (357), with permission from Elsevier.]

moral injection of an adenoviral vector encoding the HSV1-tk enzyme, the PET/CT imaging was conducted, as this was believed to be the time point when expression of the reporter gene would be highest (judging from previous animal studies). The results showed there was significantly more accumulation of the reporter probe in the viable nodule compared with the surrounding tissue. Moreover, the images demonstrated that the reporter gene expression was contained to the liver tumor and that the transfected lesion was most clearly identifiable at 6.5 h postinjection of reporter probe. Although these studies involved intratumoral injection (which is suboptimal for clinical translation), they demonstrate the promise of using a highly sensitive technique like PET for monitoring reporter gene expression in HCC patients.

These preclinical and clinical studies have set the stage for using these techniques for assessing gene therapy strategies, hopefully aiding in their development and clinical translation (332).

### E. Cell Tracking

An important application of molecular imaging is the labeling of specific cell populations so their trafficking, proliferation, and fate can be monitored noninvasively over time; this technique is known as "cell tracking." This is particularly pertinent for monitoring the behavior of static cell populations (e.g., tumor xenografts) (463), and for investigating the bio-

distribution, underlying mechanisms, and functional benefits of cell-based therapies, thus expediting the clinical translation of these promising treatment strategies.

Molecular imaging will likely play a key role in the clinical translation of cell-based therapies. The two main areas of cell therapy are 1) tissue repair (renewal), pertaining to the treatment of cardiac infarctions, neurodegeneration, and stroke; and 2) reprogramming the body's own immune system to fight disease (e.g., in cancer and immunological diseases).

Cell therapy strategies have been evaluated for treatment of stroke (involving stereotactically injected human neuronal cells into the brains of patients with motor deficits due to stroke) (228), Parkinson's disease (intrastriatal transplantation of fetal mesencephalic tissue) (251), and cancer (via the in vitro loading of dendritic cells with tumor antigens and then readministering the cells to the subject) (207, 278). Most cell therapies have only demonstrated limited success, partly due to transplanted cells failing to differentiate into the functioning cells of interest (207), and also due to the long list of unanswered questions concerning these therapies. Such questions include the following: Where do the cells go following administration? How many cells localize in various regions of body? What is the optimal route of administration? What is the most suitable cell type for each application? Do transplanted cells differentiate into functional cells in the region of interest? What are the conditions necessary for this? Due to their currently limited success, the routine use of cell therapies is not yet on the horizon. A means of tracking cells noninvasively over time is required to better understand their mechanisms and what happens after their administration. This will ultimately lead to cell therapy techniques with greater specificities and thus increase the likelihood of clinical translation.

## 1. Characteristics of an ideal molecular imaging technique for cell tracking

The ideal molecular imaging method for tracking cells would enable noninvasive visualization of a specific cell population (or multiple populations) of interest in living subjects over time in a repeated fashion. The whole body distribution, exact numbers of cells, their viability, and potential interactions with other cells should be quantifiable at all times. Furthermore, the labeling of cells should not significantly perturb the cells, and long-term traceability should be possible. Lastly, the signaling component used to track the cells should not dissociate from (or leak out of) cells, and single cell sensitivity should be achievable.

### 2. Examples of cell tracking using molecular imaging

The imaging modalities most commonly used for cell tracking include the following: 1) MRI, via directly labeling cells with SPIOs/gadolinium chelates or via reporter genes (see

sect. IVD); 2) optical, either by directly labeling cells with fluorescent dyes/Qdots or via reporter gene methods for either fluorescent (GFP/RFP) or bioluminescence (luciferase) imaging (see sect. IVD); and 3) radionuclide (PET/SPECT), either by directly labeling cells with PET/SPECT imaging agents or via reporter gene methods (see sect. IVD).

Due to its high spatial resolution, MRI is the most frequently used modality for short-term tracking of stem or progenitor cells (SPCs) (168). Specific examples include the labeling of human mesenchymal stem cells with the gadolinium hexanedione nanoparticle T1 imaging agent (420) and the long-term tracking of transplanted human neural stem cells loaded with SPIOs (T2 contrast) in the rodent brain (138). In terms of optical imaging, NIR fluorescent dyes (93), Qdots (224), and reporter gene strategies (129, 302, 407) have been used to track cells.

SPECT radioligands [111In]oxyquinoline (oxine) or [99mTc]hexamethylpropyleneamine-oxine (HMPAO) can be used in a technique called leukocyte scintography, the oldest cell tracking method and the only one being routinely used in the clinic (406). This technique involves removing leukocytes from the blood of a patient, directly labeling the recovered cells with one of the above radioligands, and subsequently administering these labeled cells back into the same patient, via intravenous injection. The accumulation of these cells in regions of the patient containing inflammation or infection can then be visualized and tracked over time. A similar cell tracking technique is used for PET studies whereby [18F]FDG is loaded into a patient's cells that are then retransferred into the patient and tracked; this method (using [18F]FDG) has been used to noninvasively visualize many different types of cells including leukocytes for tracking infection (354), natural killer cells for tracking specific types of cancer (287), and circulating progenitor cells used in the treatment of acute myocardial infarction (90).

A clinical example of cell tracking using PET was described by our laboratory, whereby the location of therapeutic cytolytic T cells (CTLs) in a patient with glioma were tracked using the [18F]FHBG HSV1-tk reporter gene system (472) (FIGURE 19). This study involved treating a glioma patient with genetically modified CTLs that expressed HSV1-tk (to serve as the PET reporter gene) and interleukin 13 zetakine (which encodes a receptor protein that targets these T cells to tumor cells), followed by imaging with [18F]FHBG. This case was the first documented study to report the use of reporter gene technology to visualize and track therapeutic cells in a human. The patient received an approximate total of  $1 \times 10^9$  CTLs within a 5-wk period of infusions. PET imaging performed 3 days after the 5-wk infusion period demonstrated that [18F]FHBG accumulated within the region where the tumor was resected, where CTLs had been infused, and also close to the patient's corpus callosum, where a secondary tumor had formed. These results indi-

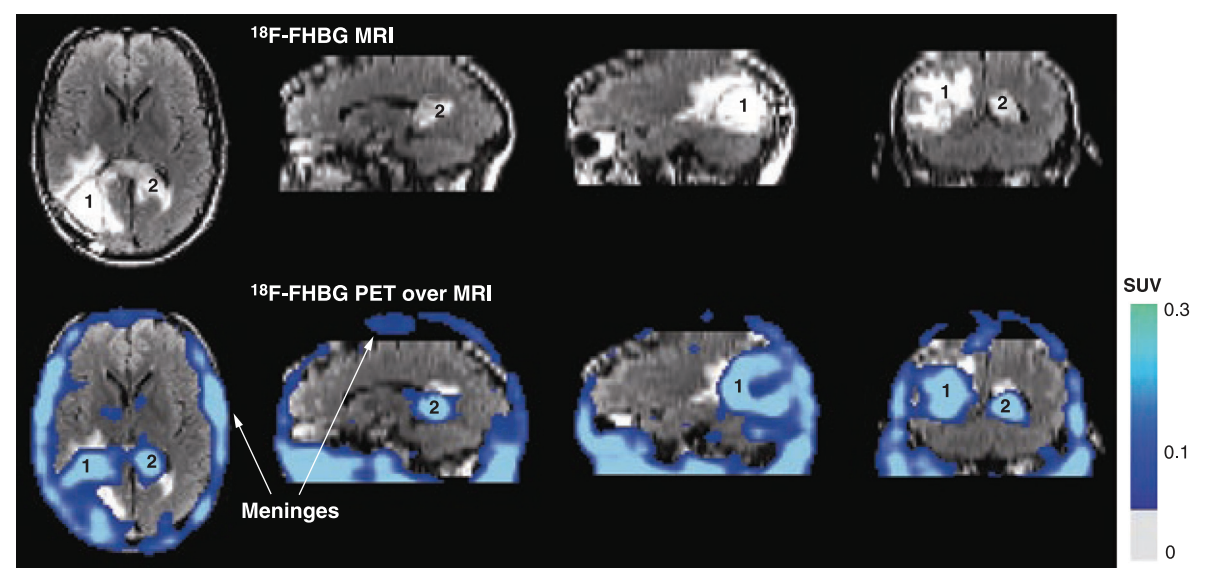


**FIGURE 19.** Example of cell tracking via molecular imaging. This figure shows the results from a clinical study, whereby a glioma patient received ex vivo expanded infusions of autologous cytolytic T cells (CTLs) containing interleukin-13 zetakine and herpes simplex virus 1 thymidine kinase (HSV1-tk) genes. Interleukin-13 zetakine encodes a receptor protein that can target T cells to tumor cells, whilst HSV1-tk encodes a PET reporter protein. *Top panel* shows magnetic resonance (MR) brain images of the patient, whereas *bottom panel* displays positron emission tomography (PET) brain images superimposed over MR images. PET imaging was conducted to detect the engineered CTLs within the patient's body 3 days after completion of a 5-wk cycle of CTL infusions. The CTLs were imaged with the PET reporter probe <sup>18</sup>F-radiolabeled 9-[4-fluoro-3-(hydroxymethyl)butyl]guanine ([<sup>18</sup>F]FHBG). The PET/MR images demonstrate [<sup>18</sup>F]FHBG accumulation within the region where the tumor was resected (1), and also close to the patient's corpus callosum (2), indicating that infused CTLs trafficked to the remote corpus callosum tumor. This was the first documented case to report the use of reporter gene technology for imaging therapeutic cells in a patient over time (473). [From Yaghoubi et al. (473), with permission from Nature Publishing Group.]

cated that infused CTLs trafficked to the remote corpus callosum tumor, and hence proved that [18F]FHBG was able to detect therapeutic CTLs expressing HSV1-tk within glioblastoma tumors. These results suggest that long-term monitoring of therapeutic cells via reporter gene imaging strategies for predicting the long-term efficacy of treatments has the potential to be useful in the future.

The challenges involved in cell tracking via molecular imaging are mainly due to the limitations of each modality (discussed in sect. II and summarized in FIGS. 3-12), and also the weaknesses of each labeling technique (i.e., direct compared with reporter gene). While direct labeling is relatively simple and does not involve any genetic manipulation, the signal can easily be diluted due to the label not being replicated when cells divide. In addition, it is also possible for the signaling component to leak out of the cells and potentially transfer to other cell populations, thus decreasing the specificity of the signal. The reporter gene strategy (if the reporter gene is stably integrated) does not suffer from the problem of dilution with cell division; however, there may be challenges concerning clinical translation due to the need for an exogenous substrate (in the case of bioluminescence imaging) and ex vivo genetic manipulation, which may lead to modification of cell characteristics and possible unwanted effects. Moreover, reporter gene expression can decrease over time (150, 324) as discussed in section IVD.

Another challenge with cell tracking via molecular imaging is the overall safety and/or cellular toxicity of the imaging agent used. For example, when deciding on a radionuclide for direct labeling of cells (for PET/SPECT imaging), there is always a tradeoff between time of traceability and safety profile (i.e., if a radionuclide with a long half-life is chosen it will enable longer traceability at the cost of higher exposure to ionizing radiation). Additionally, the labeling of cells with certain fluorescent probes (e.g., Qdots) can affect cell viability.

## Future directions for molecular imaging of cell tracking

Future directions for molecular imaging of cell tracking include the following: 1) the development of more multimodality-based approaches for imaging cell location(s), 2) further efforts to enable imaging of cell status and precise location(s), 3) additional research concerning rigorous quantification issues, 4) direct comparisons of different cell-tracking strategies so meaningful conclusions can be made concerning which techniques are better suited for different applications, and 5) optimization of strategies for clinical translation.

Cell-based therapy holds great potential in treating conditions such as stroke, myocardial infarction, neurodegeneration, cancer, and immunological diseases. Although there are many unresolved questions concerning

the underlying mechanisms of these therapies, molecular imaging is beginning to shed light on these unknowns and, in doing so, is catalyzing the design of new strategies. The partnering of molecular imaging with cell-based therapy research and development is helping make clinical translation of these treatments a real possibility.

#### F. Theranostics

Theranostics may be described as a marriage between diagnostics and therapeutics, wherein the detection and treatment of pathological phenomena are combined in one integrated approach (185). This emerging field of research has two distinct branches that aim to bring to fruition the dream of personalized medicine. In the first, diagnostic and therapeutic techniques are used hand-in-hand in clinical decision-making (e.g., PET imaging with [18F]FDG can be used to monitor and predict response to anti-cancer therapeutics, aiding the selection of suitable treatment strategies; see sect. IVA). The second branch involves the design, development, and use of agents that have both diagnostic and therapeutic capabilities, with the hope of creating a safer, more efficient, and efficacious means of simultaneously diagnosing, monitoring, and treating disease (185). There are various different types of imaging agents currently being investigated for their "theranostic potential," including peptides (76), QDots (157), microbubbles (391), and a range of nanoparticles (185) compatible with MRI, optical, radionuclide, and/or CT-based imaging techniques.

A specific example of an imaging agent developed as a theranostic agent is QDot nanoparticles functionalized with RNA aptamers (specific for PSMA) intercalated with the anthracycline drug doxorubicin (Dox) (14). These QDot-Apt(Dox) theranostic particles cannot be visualized prior to delivering Dox as the fluorescence of Qdots is quenched by Dox and the fluorescence of Dox is quenched by the aptamers. However, once Dox is released from the QDot-Apt, both QDot and Dox components can be traced via imaging. An in vitro study using these particles showed they increased therapeutic specificity towards LNCaP cells (containing PSMA) compared with PC3 cells (devoid of PSMA).

Theranostic imaging agents have enormous potential and are demonstrating promise with respect to simultaneous noninvasive imaging of biochemical processes, drug delivery, and response to the therapy over time. While there are issues with safety (toxicity and off-target accumulation), clearance (depending on the type of imaging agent used), difficulties associated with marrying/combining therapeutic molecules with imaging agents (due to different requirements of therapeutics drugs vs. diagnostic agents) (185), and their overall complexity, they are demonstrating measurable improvements in sensitivity and specificity (mostly shown in vitro at this stage) of simultaneously detecting and treating disease (compared with using therapeutic or diagnostic procedures as separate plat-

forms). Theranostics is an exciting area with much progress and growth likely yet to come.

## V. GUIDE TO PERFORMING A MOLECULAR IMAGING STUDY

The following is a general guide for performing a molecular imaging study (and validating molecular imaging agents) with the goal of visualizing a particular biochemical process or pathology in a clinical, preclinical, or basic research setting. Please refer to **FIGURE 20** throughout this section for a flowchart outlining some of the key steps involved in a molecular imaging study.

1. Define biochemical process, and/or pathology, to be investigated, and plan molecular imaging-based research strategy

As described throughout this review, one can use the principles of molecular imaging to visualize and study various molecular/cellular events and disease states noninvasively, in living subjects. For example, one can visualize the dimerization of a particular receptor, or the involvement of a certain protein in different stages of breast cancer. Once a biochemical process or pathology of interest has been selected, one needs to perform a thorough literature search and ask oneself some important questions, including (but not limited to): What is the significance of investigating this process/pathology via molecular imaging? What has been done in the past? Has anyone visualized this phenomenon via molecular imaging strategies? What has worked? What has failed, and why? Are there opportunities for improvement? And what remains unknown? After considering these points, one needs to carefully define their research question and molecular imaging strategy.

### 2. Identify appropriate molecular target(s)

As with in vitro approaches, one should begin by examining all relevant targets/biomarkers and determine which is most suitable for visualizing the phenomena of interest. It can be helpful to generate a list of potential targets for direct and/or indirect imaging approaches (see sect. III). One can also consider whether they want to image a specific molecular target (e.g., EGF receptors) or a molecular process (e.g., apoptosis) to gain information about the pathology and/or biochemical phenomena of interest. By choosing to image a particular molecular target, one can obtain very specific information; however, due to committing to one target, one might be limited in terms of the applications of the imaging strategy. On the other hand, by choosing a process (e.g., apoptosis), one can image an event that is a combination of multiple underlying targets and thus may be more generalizable to different applications; however, it may not be as specific. There is always a tradeoff, and this needs to be considered on a case-by-case basis. When identifying suit-

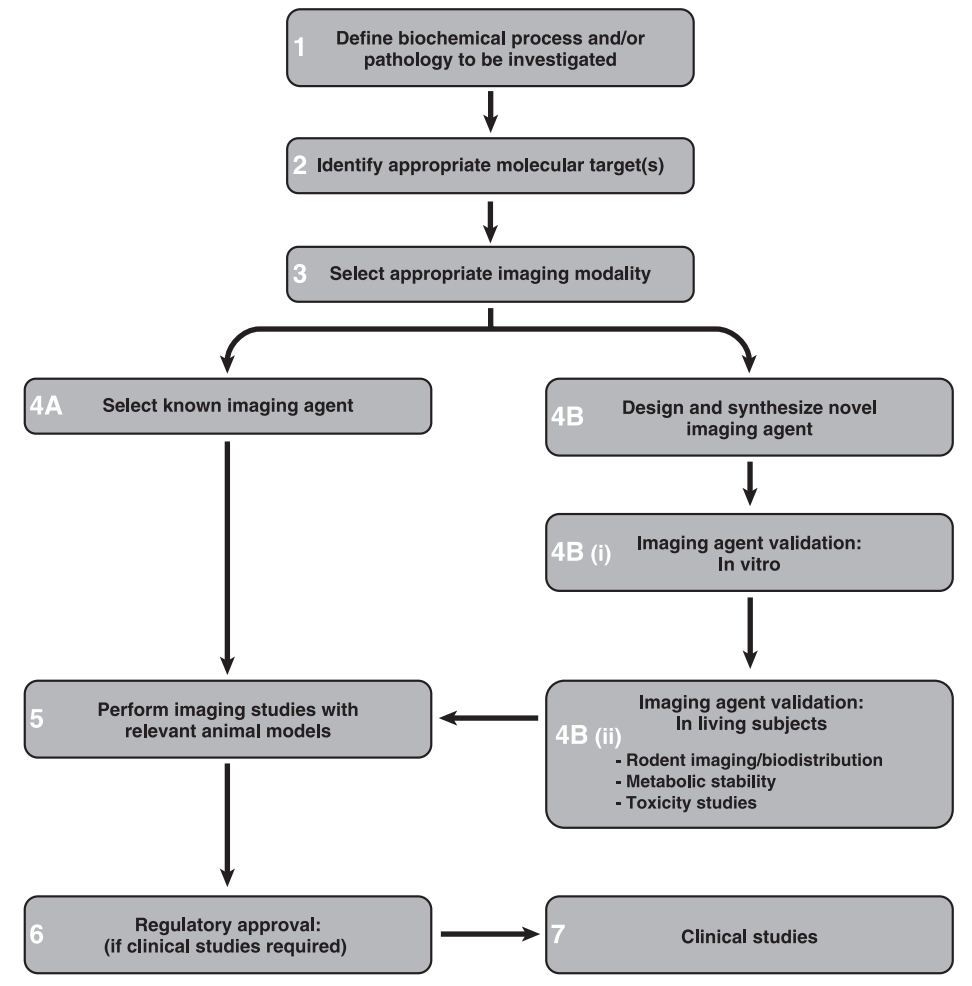


**FIGURE 20.** Flowchart demonstrating key steps involved in conducting a molecular imaging study (see text in sect. V for a description and key considerations).

able targets, one needs to keep a number of points in mind. If one wants to image breast cancer, it is usually important that the potential targets are not present in high levels in "normal" breast tissue (e.g., a 2-fold higher target level in cancerous breast tissue compared with normal breast tissue is likely insufficient for obtaining a high contrast image). Furthermore, the target needs to be "imageable" via the use of available or proposed techniques.

Steps 1 and 2 (FIGURE 20) are extremely important. Both the research question and proposed target(s) need to be thoroughly researched, discussed, and scrutinized. The significance of the research question and rationale behind target choice need to be clear.

#### 3. Select appropriate imaging modality or modalities

Once suitable molecular target(s) are decided upon, the next step is to decide which imaging modality, or combination thereof, is most suited to address the research question. Ultimately, this decision depends on the location of the target of interest and the eventual purpose of the research.

For example, if your ultimate goal is to image cancer metastases of unknown location in a clinical setting, whole body imaging is likely preferred, and an imaging modality with limitless depth of penetration and no restrictions concerning imaging large fields of view would be desirable (e.g., MRI, CT, PET, or SPECT). The strengths and limitations of each modality, and their corresponding imaging agents, need to be considered. As described in section II and FIGURES 3-12, the main considerations include the following: spatial resolution, depth of penetration, temporal resolution, cost, sensitivity (i.e., what mass of imaging agent needs to be administered to achieve detectable signal), clinical utility/translatability, safety profile, and how often a subject can be imaged. Optical imaging for example is a relatively cost effective way to evaluate reporter gene/reporter probe systems (276), as well as preclinical models; however, it is not suitable for many clinical applications.

## 4. Select a molecular imaging agent

If a molecular imaging agent is required, one can either *A*) select a known molecular imaging agent or *B*) design and

synthesize a completely new entity. The selected/proposed imaging agent must be able to bind to, or be converted by, the target of interest whilst enabling interrogation of the biochemical process(es) of interest via a detectable imaging signal. Whether deciding upon an available imaging agent, or designing one from first principles, there are numerous points to consider.

A) SELECT KNOWN MOLECULAR IMAGING AGENT. If the selected imaging agent is already known and has been extensively used for imaging your target of interest (e.g., [<sup>18</sup>F]FDG, for imaging glucose transport/hexokinase II activity), there is little need to assess its mechanism or kinetics prior to use; one can go directly to step 5 **(FIGURE 20)**. If, however, the imaging agent is known but has not been used to image the target of interest, one must first conduct a number of in vitro and in vivo studies (see *steps 4Bi* and *4Bii*) to assess specificity and selectivity.

B) DESIGN AND SYNTHESIZE NOVEL MOLECULAR IMAGING AGENT. When designing a new imaging agent, it is wise to thoroughly research what has been attempted in the past (for imaging the target of interest), and to consider the characteristics of an "ideal imaging agent" (see sect. III). After the novel imaging agent has been synthesized, it must go through a series of in vitro and in vivo tests to assess its specificity and selectivity for the target/process of interest. These tests should only be performed after the identity and purity of the newly synthesized imaging agent has been confirmed via appropriate QC methods. Depending on the type of imaging agent, QC procedures might involve NMR, high-performance liquid chromatography (HPLC), thin-layer chromatography (TLC), transmission electron microscopy (TEM), amongst others.

*I) Imaging agent validation: in vitro.* One of the first steps in validating an imaging agent is the assessment of its specificity and selectivity for the target site/process of interest in vitro. These properties can be investigated through binding/ accumulation studies, using the purified target and/or cell assays. For example, if one wants to perform cell assays for in vitro validation of an imaging agent for EGFR (a cellsurface receptor), one first needs to identify appropriate positive and negative cell lines. If one selects a cell line containing high levels of EGFR as a positive control, the same cell line can also be transfected with siRNA to knockdown levels of EGFR to create a negative control cell line. Alternatively, if a cell line devoid of EGFR is selected as the negative control, one can transfect this cell line with cDNA for EGFR to induce high levels of this target, to create a positive control cell line. After selecting appropriate positive and negative control cell lines, one can incubate the imaging agent with these cell lines to determine the kinetics of the imaging agent for the given process of interest. This is followed by a series of washing steps, and measurement of the imaging signal. It is a good idea to normalize the imaging signal to the amount of protein in each sample (e.g., through general protein assays) and to evaluate whether the imaging signal correlates with the levels of target of interest (e.g., via western blot, qPCR etc.). Evaluation of new imaging agents in positive and negative cell lines can provide information on binding specificity and also whether your agent can cross cell membranes. Assays can also be designed to assess extent of protein plasma binding, efflux of imaging agent, affinity, and selectivity of binding (via blocking and competition studies with known selective compounds for the chosen target). If the imaging agent binds to, or is converted by, targets other than the target of interest, the associated imaging signal will not provide information solely indicative of the process/site of interest. It is important that the imaging agent is highly specific and selective for the target of interest. In addition, depending on the type of imaging agent, other in vitro properties may need to be assessed. For example, when designing a CNS imaging agent that is intended to cross the intact blood-brain barrier, it is important to assess lipophilicity.

III) Imaging agent validation: in living subjects. If the imaging agent binds to, or is converted by, the target of interest, with sufficiently high specificity and selectivity in vitro, the next stage is to validate the imaging agent in living subjects. In general, a greater than threefold higher level of binding/interaction/accumulation of the imaging agent in a cell line/assay containing the target of interest, compared with a cell line/assay that is devoid of target of interest, is encouraging and warrants investigation in living subjects.

Evaluation of an imaging agent in small animals can provide invaluable information regarding its in vivo binding properties, biodistribution, and pharmacokinetics. For example, one can take blood samples at various time points following administration of imaging agent to evaluate its metabolism (by analyzing processed plasma samples via techniques such as HPLC). Ex vivo samples (e.g., liver, brain, or other organs) can also be processed and analyzed for metabolites at various time points of interest. It is preferred that metabolites of an imaging agent be more polar than their parent compound and that they do not accumulate in regions of interest. Ex vivo biodistribution studies are usually performed during initial evaluation of imaging agents in living subjects. These studies involve sacrificing animals at predetermined time points postinjection of imaging agent, harvesting organs of interest, followed by an analysis of imaging signal in individual organ samples. These studies can afford information about the percentage of injected dose (%ID) of imaging agent that accumulates in certain organs (typically one is interested in determining the %ID/g in organs at different times, to understand the kinetics and accumulation of an imaging agent).

At this stage, it might be useful to conduct acute and/or chronic toxicity studies to ascertain any potential toxic ef-

fects of the imaging agent, and to locate target organs of toxicity. Such toxicity studies may include radiation dosimetry, if working with a PET or SPECT radioligand, and can involve administering a dose of up to three orders of magnitude greater than the maximum expected dose for human use (464). Dosimetry studies are performed to obtain data concerning the safety of the imaging agent for use in human studies, provided clinical translation is the end goal of your studies. The results from dosimetry studies can ultimately limit the allowed amount of imaging agent to be administered in humans, thereby defining the success of a particular agent (336); it can be a make or break point for some molecular imaging probes.

If necessary, the imaging agent can be evaluated in larger animals, depending on the application of the imaging agent. For example, agents for clinical imaging of cardiovascular targets/processes will typically be assessed in pigs, as their cardiovascular system is comparable to that of a human. Likewise, imaging agents for CNS imaging are typically assessed in non-human primates due to the similarity of their brain structures to humans. Rodent organ systems, brain structures, and metabolic pathways are somewhat different from those in other species. Thus one must be mindful that imaging results from rodent experiments are not always predictive of what will be observed in larger animals, or humans, due to potential species differences in binding and/or metabolism of the imaging agent. It is therefore important to assess imaging agents in a few different in vivo models if possible. Likewise, it is important to consider evaluating the imaging agent in humans (after obtaining regulatory approval) even if unfavorable metabolism is observed in animals. Anesthesia used in animal studies may adversely affect imaging results. If this is thought to be the case, it may be worthwhile to conduct studies in animals that have been trained to remain stationary while being imaged, or moving the imaging probe into humans (where anesthesia is not required).

Importantly, one should validate whether the imaging signal reflects the underlying biological process of interest in living subjects (even if this has already been proven in vitro). This may involve western blots, immunohistochemistry (IHC), autoradiography (ARG), qPCR, mathematical modeling, and dynamic imaging data to relate the imaging signal to the actual levels of molecular target(s) of interest. One should also study the ability to reproduce the signal for a given level of molecular target to understand factors that lead to changes in the measured imaging signal. These quantitation issues are very important to validate an imaging agent and/or imaging strategy (122).

## 5. Perform imaging studies with relevant small animal models

The biological research question of interest (from *step 1*) can now be addressed using either a known imaging agent

(4A), or a novel agent that has been validated according to steps 4Bi-4Bii (for its ability to bind to, or interact with, the target of interest). Depending on the research question defined in step 1, one can select relevant animal models, for example, models of myocardial infarction, brain injury, cancer, inflammation, etc. Once again, one must carefully validate whether the imaging signal accurately reflects the underlying biological process of interest. For example, if one is interested in imaging EGFR overexpression in different cancers, one may choose to work with mice bearing xenografts or orthotopic tumors known to overexpress (or not express as a control) EGFR to validate their imaging strategy. Imaging studies can be followed by IHC and/or western blot analysis to determine levels of target.

## 6. Regulatory approval

If the research question is of a clinical nature, the imaging agent and/or imaging strategy must be tested for safety prior to pilot testing in humans. This process usually involves submission of animal data for approval of the imaging agent for human use by the FDA (159). For certain imaging agents, one can obtain an exploratory investigational new drug (eIND) approval from the FDA to proceed with pilot studies in human volunteers or patients (10 patients/application). To apply for an eIND, one must have appropriate toxicity data from testing in at least one species (e.g., rodent) and radiation dosimetry estimates based on animal studies (if the agent is radioactive). The eIND can be converted to a full IND based on the results in the pilot patient studies to proceed to additional patient studies. For most imaging agents, it is also currently possible to directly file for a full IND from the beginning with toxicity testing in two species.

### 7. Clinical studies

Initial clinical studies conducted via the eIND or IND mechanism can help to identify the potential application(s) of the imaging agent of interest. Some of the key important goals of the initial pilot human studies include 1) evaluation of the imaging agent's biodistribution in humans as a function of time following its administration, 2) proof that there is no toxicity in humans at the doses being used for producing a useful imaging signal, and 3) radiation dosimetry for whole body and each key organ (only in the case of a radioactive imaging agent). The need for human dosimetry data is becoming a common requirement for advancing a molecular imaging agent from phase I to phase II clinical trials (464). Another goal of human imaging studies is to provide information about whether the imaging results correlate with the levels of target(s) the imaging agent was designed to interact with. This is typically assessed by obtaining tissue samples from patients following imaging studies.

Design of the appropriate clinical trials, including control groups, is critical to understanding the true utility of an

imaging agent. Although the process of eventually obtaining clinical data is not entirely straightforward, human studies are extremely valuable when determining key applications of the imaging agent in the diagnosis and management of various diseases.

# VI. THE FUTURE OF MOLECULAR IMAGING

## A. Grand Challenges of the Field

Molecular imaging has revolutionized the way we study fundamental biological processes, and how we diagnose, stage, and monitor certain diseases. Although molecular imaging has enormous potential for a range of applications (see sect. IV), there remain challenges to overcome so that the potential of the field can be fully realized. Listed below are some of the key challenges/bottlenecks.

## 1. Imaging agents

The Achilles' heal of most molecular imaging techniques is undoubtedly the need to administer an exogenous imaging agent for interrogation of biochemical processes. The discovery of such imaging agents is a relatively long, arduous, and expensive investment that rarely affords a successful (clinically useful and reimbursed) imaging tool. Some imaging techniques, such as MRS and RS, do not require the use of an imaging agent; however, they are typically restricted by the types of biochemical targets/processes they can image and/or the depth and spatial resolution they can achieve. In the future, more emphasis needs to be placed on developing new molecular imaging strategies whereby imaging agents are not required, yet a large diversity of targets can be interrogated. However, if we cannot avoid using imaging agents, more collaborative efforts are needed to automate their discovery and synthesis, to expedite their production. Microfluidics, "lab-on-a-chip platforms," and phage display are already being implemented for these purposes.

### 2. Biomarker discovery

Unfortunately, therapeutic biomarkers do not necessarily translate into successful diagnostic imaging biomarkers. As a result, the molecular imaging community cannot simply rely on the pharmaceutical industry for their biomarker needs. The requirements for a successful "imaging biomarker" are quite different from those of a therapeutic biomarker. For example, a therapeutic biomarker needs to lead to a pharmacological effect when modulated by a therapeutic drug; however, this is not the case for an imaging biomarker. Due to the different needs of molecular imaging, researchers in this field should not necessarily overlook biomarkers that pharmaceutical companies ignore. More efforts should be focused on improving the high-throughput discovery of biomarkers suitable for imaging purposes.

If one ignores the types of biomarkers that pharmaceutical companies do (due to their different specific needs), one misses out on the potential to markedly improve the field of molecular imaging.

## 3. Chemistry

As mentioned above, imaging agent development is an inefficient and time-consuming process. One of the rate-limiting factors in this process is the chemistry required to synthesize these agents. This is mainly due to the amount of time, effort, and resources poured into devising "one off" solutions (i.e., strategies to synthesize one imaging agent). Rather, designs should be geared toward general solutions so that multiple imaging agents can be constructed using a near-identical strategy. This is currently being addressed through examples such as protein engineering-based generalizable scaffolds (see Sect. VIB5). In addition to improving the way synthetic strategies are approached, there is an enormous need for high-throughput platforms for expediting development of imaging agents and also for screening them in cell culture.

#### 4. Instrumentation

Although there are numerous useful molecular imaging instruments, they are not without their limitations. For example, PET is clinically useful but suffers from somewhat poor spatial resolution. At best, it enables the visualization of  $\sim 1$  million cells, whereas ideally we would like to zoom-in on just a few cells anywhere in the body. In terms of imaging instrumentation, there should be a focus on refining and improving upon already known instrumentation, brainstorming novel ways to use the physical electromagnetic spectrum, and further efforts geared toward the merging of existing modalities so as to take advantage of different strengths of complimentary instruments.

## Number of people in the field who are multimodality trained

There are an extremely limited number of scientists and clinicians in the field of molecular imaging that are multimodality and multidisciplinary trained. Most have a solid background in one (or two) discipline(s) and are instrument- or technique-specialized. This means that the majority of molecular imagers are limited in the way they approach an imaging problem/research question. A new generation of multidisciplinary scientists that can approach a biological problem of interest through multimodality imaging strategies continues to be in need.

#### 6. Clinical translation

To expedite clinical translation of promising imaging agents and instruments, we need to prove clinical utility.

This should be accomplished by increasing the number of rapid first-in-man efforts and by demonstrating safety and reproducibility through standardization of techniques. Academic groups developing imaging agents need to collaborate with each other to accelerate clinical translation and to perform multicenter international clinical trials. Novel models that involve academia, industry (pharmaceutical and imaging companies), governments, and foundations need to be better explored. Without help from industry, academic groups will never be able to bring enough molecular imaging agents into pilot trials. Intellectual property issues related to novel imaging agents also need to be considered along with business models to show profitability for specific imaging agents and their clinical applications.

## 7. Multiplexing capabilities and sensitivity

At present, it is not possible to look at a large number of biochemical processes or targets simultaneously using most molecular imaging techniques. For molecular imaging to reach its full potential, we need to devise ways of visualizing multiple targets and signaling pathways, simultaneously, with ultra high sensitivity and specificity to gain a more complete picture of disease and normal physiology. A systems imaging approach must be married to a systems biology approach if we are to truly unravel the complexity of biological systems.

#### 8. Cost and availability of facilities

Many of the molecular imaging techniques are still relatively expensive compared with in vitro techniques. Molecular imaging will not survive as a field if everything is relatively costly. We must work towards next-generation solutions while optimizing many variables including costs. If we can make molecular imaging with inherently lower cost technologies (e.g., ultrasound, optical, photoacoustics) successful, then the technologies will be deployed worldwide and gain much more rapid acceptance. Additionally, the molecular imaging agents themselves need to become relatively low cost. This may be possible with nonradionuclide based agents.

#### **B.** Possible Future Directions

Looking to the future, there are a number of areas in which molecular imaging will likely advance dramatically. Some areas include the following.

## 1. Implementation of newer imaging agents and imaging techniques in standard practice

A number of the emerging imaging agents and imaging techniques described in this article will become standard practice in clinical environments and/or preclinical settings. Imaging agents for visualizing AD (e.g., [11C]PIB) will likely be used more frequently in the clinical arena during the next decade. Also, imaging agents/technologies for prostate cancer detection, and apoptosis imaging for monitoring tumor response to therapy will likely become available. It is important to realize that (as with drug discovery and development) only a handful of imaging agents that enter clinical trials will ever become truly clinically useful. We will fail often in our endeavors to design and implement new imaging strategies, and thus we need to learn from our mistakes and have realistic expectations. It is easy to get frustrated due to the iterative nature of all research; however, patience and persistence in the field of molecular imaging are critical.

## 2. More effective screening and personalized medicine

A combination of in vitro diagnostics and molecular imaging will likely enable screening of "at-risk" populations. Effective screening will result in early detection of disease, far before any clinical signs or symptoms manifest, ultimately leading to improved treatment strategies and patient outcomes. The merger of in vitro diagnostics and in vivo diagnostics will be critical to solving the limitations of each approach, and thus making personalized medicine a reality. Clinically, this will lead to a blurring of boundaries between radiology and pathology.

# 3. More dual-modality and multi-modality molecular imaging

When investigating disease states and biological phenomena, it is not favorable to restrict oneself to a single modality, as each modality has its limitations. Future efforts will be aimed at combining modalities so we can draw on the strengths of each individual instrument/approach. Ultimately, this will improve the way we study complex biological systems and disease states. Currently, there is no Swissarmy knife equivalent of imaging that is able to answer all questions for various applications, but by combining several imaging technologies, we can move closer to this idea. Upcoming clinical technologies, such as MRI-PET, are a perfect example of two modalities that when combined may lead to very useful clinical applications, including monitoring pediatric tumors, and brain imaging using both MRS and PET.

## 4. Improvements in imaging agent design and development

It is envisioned that much progress will be made in the area of imaging agent development. In particular, it is believed that more high-throughput platforms for screening and evaluating imaging agents prior to their investigation in animals will become available. Significant progress is also

expected in the areas of "smart" probe development and multi-modality probes. Moreover, improvements in reporterprobe pairs to facilitate molecular-genetic imaging are expected, resulting in more generalizable "indirect" imaging approaches. For the most part, our communication with imaging agents is one way, i.e., we can only receive information. However, in the near future, we will likely have access to imaging agents that not only provide us with information, but are also able to receive and respond to external input. Innovations such as this will allow true bidirectional communication with imaging agents, thereby allowing for better delivery of imaging agents that can then act as small nanomachines to accomplish tasks we give them to perform. The merger of diagnostics and therapeutics into the evolving field of theranostics (see sect. IVF) will then likely be possible. Since there are so many parallels between developing and using molecular drugs and molecular imaging agents, there is a strong likelihood that the two fields will merge to accomplish both diagnosis and therapy in a unified fashion.

## 5. Generalizable scaffolds for imaging agents

For reasons mentioned above, it is not usually wise to focus enormous effort into developing "one-off" chemistry solutions for development of imaging agents. Instead, a general scaffold for a molecular imaging agent that can be easily modified to adjust its in vivo behavior and pharmacokinetics, depending on the needs of a given imaging study, is desirable. This is becoming possible through identifying generalizable scaffolds to which different targeting components can be added, and the size, surface chemistry, and lipophilicity can be tuned to yield an imaging agent with customized capabilities, suitable for different imaging needs. This type of strategy is not necessarily straightforward for all types of imaging agents, such as small molecules; however, it is certainly worthwhile exploring before investing time and resources into novel imaging agent development. Progress in the areas of protein engineering and nanoparticle-platform production is already making these types of generalizable scaffolds a reality. Further efforts and progress in this area is anticipated in the future.

## C. Conclusion

The future of molecular imaging is indeed very promising. The continual development in the field is likely to lead to major breakthroughs in our understanding of in vivo biology, and also improvement in the clinical detection of disease and management of patients. Although many approaches will likely fail, we must accept this as part of the journey to success. As hard as it may be to believe for many, the field of molecular imaging is still only in its infancy, with many important discoveries around the corner.

### VII. SUPPLEMENTARY MATERIAL

#### A. Fluorescent Proteins

Fluorescent proteins (FPs) are proteins capable of fluorescing when exposed to an excitation light of a certain wavelength. The first discovered FP was green fluorescent protein (GFP). In 1962, Shimomura and colleagues reported the isolation of GFP from the jellyfish *Aequorea victoria* (385); however, it was not until 1994 that GFP was used for molecular imaging purposes (49).

The use of FPs in cell biology and in molecular imaging of living intact subjects is now standard practice. A FP is typically used as either 1) a reporter of gene expression or 2) a fluorescent tag so that a protein of interest can be tracked/ studied over time. The latter application involves genetically fusing the cDNA of a FP, to the gene of a second protein of interest. The resulting recombinant vector is then transferred into a host organism/subject so that one can study the location and intracellular dynamics/interactions of the protein of interest (125). Various cellular processes, biochemical pathways, and protein-protein interactions have been visualized using FPs and fluorescence microscopy/related imaging techniques. Some of the common FPs and their important applications in molecular imaging are detailed in the following key references (64, 160, 162, 163, 216, 380, 475).

Compared with fluorophores, FPs are relatively nontoxic, meaning one can observe processes over extended periods of time. This is important when longitudinal studies are required.

Genetic variants of the original GFP nucleotide sequence have been produced, including enhanced GFP (known as EGFP) and Emerald. In fact, there are a number of available spectral classes of FPs, including blue fluorescent proteins (emission  $\lambda$  $\sim$ 440–470 nm), cyan fluorescent proteins (emission  $\lambda \sim$ 470– 500 nm), green fluorescent protein (emission  $\lambda \sim 500-525$ nm), yellow fluorescent proteins (emission  $\lambda \sim 525-555$  nm), orange fluorescent proteins (emission  $\lambda \sim 555-590$  nm), and red fluorescent proteins. Each spectral class of FPs consists of a range of variants, for example, within the red fluorescent protein class there exists mCherry, mRFP1, tdTomato, mStrawberry, mRuby, mApple, and others. In total, there are over 40 different FPs, each with different spectral profiles, photostability, and brightness (125). It can therefore become overwhelming and confusing when choosing an appropriate FP variant for a particular study. It is typically recommended to stick with the variants that have been tried and tested, for example, EGFP (although some would argue the superiority of the variant Emerald). Please refer to the following review for a guide to selecting FPs (380).

Due to progress in protein engineering, FP variants have been tuned to improve their properties. Ideally, a FP should

have good photostability, sufficient brightness (so there is adequate signal compared with background autofluorescence), suitable spectral profile, and pH insensitivity. Unfortunately, no one FP is suitable for all applications, and no single FP combines the best features of all FPs, so no matter which FP is selected, there will always be a trade-off concerning brightness, photostability, and/or spectral profile (125).

It is important to note that the process of genetically fusing the FP to the second protein of interest can often alter the function (folding, normal localization, etc.) of either, or both, proteins. Please refer to Reference 125 for trouble-shooting concerning creating fusion fluorescent proteins and issues relating to unexpected low levels of fluorescence, improper folding of proteins, unstable expression, and/or poor localization.

The discovery of FPs and their use in imaging studies has forever changed the way we study biological systems. These fluorescing entities are invaluable research tools for studying biochemical processes and pathologies.

## **B. Stimulated Raman Scattering**

The amplification of Raman scattering can be afforded via the use of SRS, a phenomena first witnessed in 1962 (465). SRS requires the use of two laser beams and has far greater sensitivity compared with that of traditional spontaneous RS. When the Raman shift equals that of a certain molecular vibrational resonance, the Raman signal is amplified as a consequence of stimulated excitation (111). This three-dimensional multiphoton microscopy technique has been used in a variety of in vitro and ex vivo biomedical applications, including imaging living cells to decipher distributions of omega-3 fatty acids and saturated lipids, evaluation of brain and skin tissues according to intrinsic lipid contrast, and observing drug delivery (111). The main advantages of SRS are its high sensitivity, three-dimensional mapping capabilities, and the fact that no exogenous imaging agent is required.

SRS microscopy is a budding new technique for investigating biochemical processes and their dynamics in living cells and/or tissues based on the molecular specificity of Raman spectroscopy. Imaging studies still need to be performed in living subjects.

### **ACKNOWLEDGMENTS**

Address for reprint requests and other correspondence: S. S. Gambhir, Molecular Imaging Program, Dept. of Radiology, Bio-X Program, Stanford University, 318 Campus Dr., Palo Alto, CA 94305 (e-mail: sgambhir@stanford.edu).

#### **DISCLOSURES**

No conflicts of interest, financial or otherwise, are declared by the authors.

#### **REFERENCES**

- Abrams MJ, Murrer BA. Metal compounds in therapy and diagnosis. Science 261: 725–730, 1993
- Acton PD, Kung HF. Small animal imaging with high resolution single photon emission tomography. Nucl Med Biol 30: 889–895, 2003.
- Agostini D, Verberne HJ, Burchert W, Knuuti J, Povinec P, Sambuceti G, Unlu M, Estorch M, Banerjee G, Jacobson AF. I-123-mlBG myocardial imaging for assessment of risk for a major cardiac event in heart failure patients: insights from a retrospective European multicenter study. Eur J Nucl Med Mol Imaging 35: 535–546, 2008.
- Akimoto H, Kwon HJ, Ozaki M, Yasuda K, Honma K, Ohmiya Y. In vivo bioluminescence imaging of bone marrow-derived cells in brain inflammation. *Biochem Biophys Res Commun* 380: 844

  –849, 2009.
- Albers MJ, Bok R, Chen AP, Cunningham CH, Zierhut ML, Zhang VY, Kohler SJ, Tropp J, Hurd RE, Yen YF, Nelson SJ, Vigneron DB, Kurhanewicz J. Hyperpolarized <sup>13</sup>C lactate, pyruvate, and alanine: noninvasive biomarkers for prostate cancer detection and grading. *Cancer Res* 68: 8607–8615, 2008.
- Alford R, Ogawa M, Choyke PL, Kobayashi H. Molecular probes for the in vivo imaging of cancer. Mol Biosyst 5: 1279–1291, 2009.
- Allen HC Jr, Libby RL, Cassen B. The scintillation counter in clinical studies of human thyroid physiology using I<sup>131</sup>. J Clin Endocrinol Metab 11: 492–511, 1951.
- Allen-Auerbach M, Weber WA. Measuring response with FDG-PET: methodological aspects. Oncologist 14: 369–377, 2009.
- Alvarez-Curto E, Pediani JD, Milligan G. Applications of fluorescence and bioluminescence resonance energy transfer to drug discovery at G protein coupled receptors. *Anal Bioanal Chem* 398: 167–180, 2010.
- Amirbekian V, Lipinski MJ, Briley-Saebo KC, Amirbekian S, Aguinaldo JG, Weinreb DB, Vucic E, Frias JC, Hyafil F, Mani V, Fisher EA, Fayad ZA. Detecting and assessing macrophages in vivo to evaluate atherosclerosis noninvasively using molecular MRI. Proc Natl Acad Sci USA 104: 961–966, 2007.
- 10a. Ananias HJ, Yu Z, Dierckx RA, van der Wiele C, Helfrich W, Wang F, Yan Y, Chen X, de Jong IJ, Elsinga PH. (99m) Technetium-HYNIC (tricine/TPPTS)-Aca-bumbesin (7-14) as a targeted imaging agent with micro SPECT in a PC-3 prostate cancer xenograft model. Mol Pharm 8: 1165–1173, 2011.
- Ardenkjaer-Larsen JH, Fridlund B, Gram A, Hansson G, Hansson L, Lerche MH, Servin R, Thaning M, Golman K. Increase in signal-to-noise ratio of >10,000 times in liquid-state NMR. Proc Natl Acad Sci USA 100: 10158–10163, 2003.
- Arlicot N, Katsifis A, Garreau L, Mattner F, Vergote J, Duval S, Kousignian I, Bodard S, Guilloteau D, Chalon S. Evaluation of CLINDE as potent translocator protein (18 kDa) SPECT radiotracer reflecting the degree of neuroinflammation in a rat model of microglial activation. Eur J Nucl Med Mol Imaging 35: 2203–2211, 2008.
- Azulay H, Striem E, Amedi A. Negative BOLD in sensory cortices during verbal memory: a component in generating internal representations? *Brain Topogr* 21: 221– 231, 2009.
- Bagalkot V, Zhang L, Levy-Nissenbaum E, Jon S, Kantoff PW, Langer R, Farokhzad OC. Quantum dot-aptamer conjugates for synchronous cancer imaging, therapy, and sensing of drug delivery based on bi-fluorescence resonance energy transfer. *Nano Lett* 7: 3065–3070, 2007.
- Ballon D, Koutcher JA. Nuclear magnetic resonance: principles and applications to pathology. Clin Lab Med 8: 737–751, 1988.
- 16. Banati RB, Newcombe J, Gunn RN, Cagnin A, Turkheimer F, Heppner F, Price G, Wegner F, Giovannoni G, Miller DH, Perkin GD, Smith T, Hewson AK, Bydder G, Kreutzberg GW, Jones T, Cuzner ML, Myers R. The peripheral benzodiazepine binding site in the brain in multiple sclerosis: quantitative in vivo imaging of microglia as a measure of disease activity. Brain 123: 2321–2337, 2000.

- Baum RP, Swietaszczyk C, Prasad V. FDG-PET/CT in lung cancer: an update. Front Radiat Ther Oncol 42: 15–45, 2009.
- Beal MF. Mitochondria and neurodegeneration. Novartis Found Symp 287: 183–192, 2007
- Beekman FJ, van der Have F, Vastenhouw B, van der Linden AJ, van Rijk PP, Burbach JP, Smidt MP. U-SPECT-I: a novel system for submillimeter-resolution tomography with radiolabeled molecules in mice. J Nucl Med 46: 1194–1200, 2005.
- Beer AJ, Lorenzen S, Metz S, Herrmann K, Watzlowik P, Wester HJ, Peschel C, Lordick F, Schwaiger M. Comparison of integrin alphaVbeta3 expression and glucose metabolism in primary and metastatic lesions in cancer patients: a PET study using <sup>18</sup>F-galacto-RGD and <sup>18</sup>F-FDG. J Nucl Med 49: 22–29, 2008.
- Behm CZ, Lindner JR. Cellular and molecular imaging with targeted contrast ultrasound. Ultrasound Q 22: 67–72, 2006.
- Belhocine T, Steinmetz N, Hustinx R, Bartsch P, Jerusalem G, Seidel L, Rigo P, Green
   A. Increased uptake of the apoptosis-imaging agent (99m)Tc recombinant human
   Annexin V in human tumors after one course of chemotherapy as a predictor of tumor
   response and patient prognosis. Clin Cancer Res 8: 2766–2774, 2002.
- Belikova AM, Zarytova VF, Grineva NI. Synthesis of ribonucleosides and diribonucleoside phosphates containing 2-chloroethylamine and nitrogen mustard residues. Tetrahedron Lett 37: 3557–3562, 1967.
- Bell AG. Upon the production of sound by radiant energy. Philos Mag J Sci XI 510 528, 1880.
- Berthelot T, Lasne MC, Deleris G. New trends in molecular imaging of tumor angiogenesis. Anticancer Agents Med Chem 8: 497–522, 2008.
- Biju V, Itoh T, Anas A, Sujith A, Ishikawa M. Semiconductor quantum dots and metal nanoparticles: syntheses, optical properties, and biological applications. *Anal Bioanal Chem* 391: 2469–2495. 2008.
- Blake P, Johnson B, VanMeter JW. Positron emission tomography (PET) and single photon emission computed tomography (SPECT): clinical applications. J Neuroophthalmol 23: 34–41, 2003.
- 28. Blamire AM. The technology of MRI-the next 10 years? Br J Radiol 81: 601-617, 2008.
- Bleaney B. Edward Mills Purcell. 30 August 1912–7 March 1997: elected For Mem R S 1989. Biogr Mems Fell R Soc 45: 437–447, 1999.
- Boerman OC, Oyen WJ. Multimodality probes: amphibian cars for molecular imaging. J Nucl Med 49: 1213–1214, 2008.
- Bohdiewicz PJ. Indium-III satumomab pendetide: the first FDA-approved monoclonal antibody for tumor imaging. J Nucl Med Technol 26: 155–163, 1998.
- Bohndiek SE, Kettunen MI, Hu DE, Kennedy BW, Boren J, Gallagher FA, Brindle KM. Hyperpolarized [1-<sup>13</sup>C]-ascorbic and dehydroascorbic acid: vitamin C as a probe for imaging redox status in vivo. J Am Chem Soc 133: 11795–11801, 2011.
- Bohndiek SE, Kettunen MI, Hu DE, Witney TH, Kennedy BWC, Gallagher FA, Brindle KM. Detecting tumor response to a vascular disrupting agent using hyperpolarized <sup>13</sup>C magnetic resonance spectroscopy. Mol Cancer Ther 9: 3278–3288, 2010.
- Bouchard PR, Hutabarat RM, Thompson KM. Discovery and development of therapeutic aptamers. Annu Rev Pharmacol Toxicol 50: 237–257, 2010.
- Bremer C, Bredow S, Mahmood U, Weissleder R, Tung CH. Optical imaging of matrix metalloproteinase-2 activity in tumors: feasibility study in a mouse model. *Radiology* 221: 523–529, 2001.
- Bremer C, Tung CH, Weissleder R. In vivo molecular target assessment of matrix metalloproteinase inhibition. Nat Med 7: 743–748, 2001.
- Brink JA, Heiken JP, Wang G, McEnery KW, Schlueter FJ, Vannier MW. Helical CT: principles and technical considerations. Radiographics 14: 887–893, 1994.
- Bural GG, Torigian DA, Chamroonrat W, Alkhawaldeh K, Houseni M, El-Haddad G, Alavi A. Quantitative assessment of the atherosclerotic burden of the aorta by combined FDG-PET and CT image analysis: a new concept. *Nucl Med Biol* 33: 1037–1043, 2006.
- Buxton RB. Introduction to Functional Magnetic Resonance Imaging: Principles and Techniques. Cambridge, UK: Cambridge Univ. Press, 2002.

- Bystrom P, Berglund A, Garske U, Jacobsson H, Sundin A, Nygren P, Frodin JE, Glimelius B. Early prediction of response to first-line chemotherapy by sequential [<sup>18</sup>F]-2-fluoro-2-deoxy-D-glucose positron emission tomography in patients with advanced colorectal cancer. *Ann Oncol* 20: 1057–1061, 2009.
- Cagnin A, Brooks DJ, Kennedy AM, Gunn RN, Myers R, Turkheimer FE, Jones T, Banati RB. In-vivo measurement of activated microglia in dementia. *Lancet* 358: 461– 467, 2001
- 41a. Cagnin A, Gerhard A, Banati RB. In vivo imaging of neuroinflammation. Eur Neuropsychopharmacol 12: 581–586, 2002.
- Cagnin A, Myers R, Gunn RN, Lawrence AD, Stevens T, Kreutzberg GW, Jones T, Banati RB. In vivo visualization of activated glia by [¹¹C](R)-PK11195-PET following herpes encephalitis reveals projected neuronal damage beyond the primary focal lesion. *Brain* 124: 2014–2027, 2001.
- 43. Cai W, Chen X. Multimodality molecular imaging of tumor angiogenesis. J Nucl Med 49 Suppl 2: 113S–128S, 2008.
- Cai W, Olafsen T, Zhang X, Cao Q, Gambhir SS, Williams LE, Wu AM, Chen X. PET imaging of colorectal cancer in xenograft-bearing mice by use of an <sup>18</sup>F-labeled T84.66 anti-carcinoembryonic antigen diabody. J Nucl Med 48: 304–310, 2007.
- Cai W, Shin DW, Chen K, Gheysens O, Cao Q, Wang SX, Gambhir SS, Chen X. Peptide-labeled near-infrared quantum dots for imaging tumor vasculature in living subjects. Nano Lett 6: 669–676, 2006.
- Capala J, Barth RF, Bailey MQ, Fenstermaker RA, Marek MJ, Rhodes BA. Radiolabeling of epidermal growth factor with 99mTc and in vivo localization following intracerebral injection into normal and glioma-bearing rats. *Bioconjug Chem* 8: 289–295, 1997.
- 47. Capote HA. Neuroimaging in psychiatry. Neurol Clin 27: 237–249, 2009.
- Cassen B, Curtis L, Reed C, Libby R. Instrumentation for 1311 use in medical studies. Nucleonics 9: 46–50, 1951.
- Chalfie M, Tu Y, Euskirchen G, Ward WW, Prasher DC. Green fluorescent protein as a marker for gene expression. Science 263: 802–805, 1994.
- Chan CT, Paulmurugan R, Reeves RE, Solow-Cordero D, Gambhir SS. Molecular imaging of phosphorylation events for drug development. Mol Imaging Biol 11: 144– 158, 2009.
- 51. Chan MY, Cohen MG, Dyke CK, Myles SK, Aberle LG, Lin M, Walder J, Steinhubl SR, Gilchrist IC, Kleiman NS, Vorchheimer DA, Chronos N, Melloni C, Alexander JH, Harrington RA, Tonkens RM, Becker RC, Rusconi CP. Phase 1b randomized study of antidote-controlled modulation of factor IXa activity in patients with stable coronary artery disease. *Circulation* 117: 2865–2874, 2008.
- Charlton J, Sennello J, Smith D. In vivo imaging of inflammation using an aptamer inhibitor of human neutrophil elastase. Chem Biol 4: 809–816, 1997.
- Chatham JC, Blackband SJ. Nuclear magnetic resonance spectroscopy and imaging in animal research. *ILAR J* 42: 189–208, 2001.
- Chawla S, Kim S, Wang S, Poptani H. Diffusion-weighted imaging in head and neck cancers. Future Oncol 5: 959–975, 2009.
- Chen CM, Hou BL, Holodny Al. Effect of age and tumor grade on BOLD functional MR imaging in preoperative assessment of patients with glioma. *Radiology* 248: 971– 978, 2008.
- Chen IY, Wu JC. Cardiovascular molecular imaging: focus on clinical translation. Circulation. In press.
- Chen X, Conti PS, Moats RA. In vivo near-infrared fluorescence imaging of integrin alphavbeta3 in brain tumor xenografts. Cancer Res 64: 8009–8014, 2004.
- Chen Z, Chen H, Meng H, Xing G, Gao X, Sun B, Shi X, Yuan H, Zhang C, Liu R, Zhao F, Zhao Y, Fang X. Bio-distribution and metabolic paths of silica coated CdSeS quantum dots. *Toxicol Appl Pharmacol* 230: 364–371, 2008.
- Cheng JX, Xie S. Coherent anti-stokes raman scattering microscopy: instrumentation, theory, and applications. J Phys Chem B 108: 827–840, 2004.
- Cheng Z, De Jesus OP, Namavari M, De A, Levi J, Webster JM, Zhang R, Lee B, Syud FA, Gambhir SS. Small-animal PET imaging of human epidermal growth factor receptor type 2 expression with site-specific <sup>18</sup>F-labeled protein scaffold molecules. J Nucl Med 49: 804–813, 2008.

- Cheng Z, Levi J, Xiong Z, Gheysens O, Keren S, Chen X, Gambhir SS. Near-infrared fluorescent deoxyglucose analogue for tumor optical imaging in cell culture and living mice. *Bioconjug Chem* 17: 662–669, 2006.
- Chi Z, Melendez AJ. Role of cell adhesion molecules and immune-cell migration in the initiation, onset and development of atherosclerosis. Cell Adh Migr 1: 171–175, 2007.
- 63. Choi M, Heilbrun LK, Venkatramanamoorthy R, Lawhorn-Crews JM, Zalupski MM, Shields AF. Using <sup>18</sup>F-fluorodeoxyglucose positron emission tomography to monitor clinical outcomes in patients treated with neoadjuvant chemo-radiotherapy for locally advanced pancreatic cancer. Am J Clin Oncol 2009.
- Chudakov DM, Lukyanov S, Lukyanov KA. Fluorescent proteins as a toolkit for in vivo imaging. Trends Biotechnol 23: 605–613, 2005.
- Chudakov DM, Matz MV, Lukyanov S, Lukyanov KA. Fluorescent proteins and their applications in imaging living cells and tissues. *Physiol Rev* 90: 1103–1163, 2010.
- Clarke CE, Guttman M. Dopamine agonist monotherapy in Parkinson's disease. Lancet 360: 1767–1769, 2002.
- Contag CH, Contag PR, Mullins JI, Spilman SD, Stevenson DK, Benaron DA. Photonic detection of bacterial pathogens in living hosts. Mol Microbiol 18: 593–603, 1995.
- Costouros NG, Diehn FE, Libutti SK. Molecular imaging of tumor angiogenesis. J Cell Biochem Suppl 39: 72–78, 2002.
- Couillard-Despres S, Finkl R, Winner B, Ploetz S, Wiedermann D, Aigner R, Bogdahn U, Winkler J, Hoehn M, Aigner L. In vivo optical imaging of neurogenesis: watching new neurons in the intact brain. *Mol Imaging* 7: 28–34, 2008.
- Crawley EO, Evans WD, Owen GM. A theoretical analysis of the accuracy of singleenergy CT bone-mineral measurements. Phys Med Biol 33: 1113–1127, 1988.
- Day SE, Kettunen MI, Gallagher FA, Hu DE, Lerche M, Wolber J, Golman K, Ardenkjaer-Larsen JH, Brindle KM. Detecting tumor response to treatment using hyperpolarized <sup>13</sup>C magnetic resonance imaging and spectroscopy. *Nat Med* 13: 1382–1387, 2007.
- De A, Loening AM, Gambhir SS. An improved bioluminescence resonance energy transfer strategy for imaging intracellular events in single cells and living subjects. *Cancer Res* 67: 7175–7183, 2007.
- De Figueiredo EH, Borgonovi AF, Doring TM. Basic concepts of MR imaging, diffusion MR imaging, and diffusion tensor imaging. Magn Reson Imaging Clin N Am 19: 1–22.
- De Goeij JM, Bonardi ML. How do we define the concepts specific activity, radioactive concentration, carrier, carrier-free and no-carrier-added? J Radioanal Nucl Chem 263: 13–18, 2005
- De Graaf RA. In Vivo NMR Spectroscopy: Principles and Techniques. New York: Wiley, 2007.
- De Jong M, Breeman WA, Kwekkeboom DJ, Valkema R, Krenning EP. Tumor imaging and therapy using radiolabeled somatostatin analogues. Acc Chem Res 42: 873–880, 2009.
- De la Zerda A, Liu Z, Bodapati S, Teed R, Vaithilingam S, Khuri-Yakub BT, Chen X, Dai H, Gambhir SS. Ultrahigh sensitivity carbon nanotube agents for photoacoustic molecular imaging in living mice. *Nano Lett* 10: 2168–2172, 2010.
- De la Zerda A, Zavaleta C, Keren S, Vaithilingam S, Bodapati S, Liu Z, Levi J, Smith BR, Ma TJ, Oralkan O, Cheng Z, Chen X, Dai H, Khuri-Yakub BT, Gambhir SS. Carbon nanotubes as photoacoustic molecular imaging agents in living mice. *Nat Nanotechnol* 3: 557–562, 2008.
- De Leon-Rodriguez LM, Lubag AJ, Malloy CR, Martinez GV, Gillies RJ, Sherry AD. Responsive MRI agents for sensing metabolism in vivo. Acc Chem Res 42: 948–957, 2009.
- Debbage P, Jaschke W. Molecular imaging with nanoparticles: giant roles for dwarf actors. Histochem Cell Biol 130: 845–875, 2008.
- Debruyne JC, Versijpt J, Van Laere KJ, De Vos F, Keppens J, Strijckmans K, Achten E, Slegers G, Dierckx RA, Korf J, De Reuck JL. PET visualization of microglia in multiple sclerosis patients using [11C]PK11195. Eur J Neurol 10: 257–264, 2003.
- Decristoforo C, Melendez-Alafort L, Sosabowski JK, Mather SJ. 99mTc-HYNIC-[Tyr3]-octreotide for imaging somatostatin-receptor-positive tumors: preclinical evaluation and comparison with <sup>111</sup>In-octreotide. J Nucl Med 41: 1114–1119, 2000.

- DeNardo SJ, DeNardo GL, Miers LA, Natarajan A, Foreman AR, Gruettner C, Adamson GN, Ivkov R. Development of tumor targeting bioprobes [(111)In-chimeric L6 monoclonal antibody nanoparticles] for alternating magnetic field cancer therapy. Clin Cancer Res 11: 7087s–7092s, 2005.
- 84. Deshpande N, Needles A, Willmann JK. Molecular ultrasound imaging: current status and future directions. *Clin Radiol* 65: 567–581, 2010.
- Deshpande N, Pysz MA, Willmann JK. Molecular ultrasound assessment of tumor angiogenesis. Angiogenesis 13: 175–188.
- Ding AA, Chen YY, Wang CC, Li PC, Shieh DB. HER-2 antibody conjugated gold nano rod for in vivo photothermal therapy. *Nanotechnology*, *NANO '08 8th IEEE Conference* 882, 2008.
- 87. Divgi CR, Pandit-Taskar N, Jungbluth AA, Reuter VE, Gonen M, Ruan S, Pierre C, Nagel A, Pryma DA, Humm J, Larson SM, Old LJ, Russo P. Preoperative characterisation of clear-cell renal carcinoma using iodine-124-labeled antibody chimeric G250 (124-G250) and PET in patients with renal masses: a phase I trial. *Lancet Oncol* 8: 304–310, 2007.
- Doggrell SA. Pegaptanib: the first antiangiogenic agent approved for neovascular macular degeneration. Expert Opin Pharmacother 6: 1421–1423, 2005.
- Douma K, Prinzen L, Slaaf DW, Reutelingsperger CP, Biessen EA, Hackeng TM, Post MJ, van Zandvoort MA. Nanoparticles for optical molecular imaging of atherosclerosis. Small 5: 544–557, 2009.
- Doyle B, Kemp BJ, Chareonthaitawee P, Reed C, Schmeckpeper J, Sorajja P, Russell S, Araoz P, Riederer SJ, Caplice NM. Dynamic tracking during intracoronary injection of <sup>18</sup>F-FDG-labeled progenitor cell therapy for acute myocardial infarction. J Nucl Med 48: 1708–1714, 2007.
- Drew SC, Haigh CL, Klemm HM, Masters CL, Collins SJ, Barnham KJ, Lawson VA.
   Optical imaging detects apoptosis in the brain and peripheral organs of prion-infected mice. J Neuropathol Exp Neurol 70: 143–150, 2011.
- Drzezga A. Basic pathologies of neurodegenerative dementias and their relevance for state-of-the-art molecular imaging studies. Eur J Nucl Med Mol Imaging 35 Suppl 1: S4–S11, 2008.
- Du XM, Yan Y, Bai ZL, Zhang JP, Wang Z, Liu LL, Feng LJ. Evaluation of the cytotoxicity of a two photon absorbing fluorescence compound on human HepG2 cells and its application to tracking human hepatic cancer cells in mice. *Biotech Histochem* 85: 107–113, 2009.
- Dubroff JG, Newberg A. Neuroimaging of traumatic brain injury. Semin Neurol 28: 548–557, 2008.
- Edgington LE, Berger AB, Blum G, Albrow VE, Paulick MG, Lineberry N, Bogyo M. Noninvasive optical imaging of apoptosis by caspase-targeted activity-based probes. Nat Med 15: 967–973, 2009.
- Edwards WB, Xu B, Akers W, Cheney PP, Liang K, Rogers BE, Anderson CJ, Achilefu S. Agonist-antagonist dilemma in molecular imaging: evaluation of a monomolecular multimodal imaging agent for the somatostatin receptor. *Bioconjug Chem* 19: 192– 200, 2008.
- Elias A, Tsourkas A. Imaging circulating cells and lymphoid tissues with iron oxide nanoparticles. Hematology Am Soc Hematol Educ Program 720–726, 2009.
- Endo K, Oriuchi N, Higuchi T, Iida Y, Hanaoka H, Miyakubo M, Ishikita T, Koyama K. PET and PET/CT using <sup>18</sup>F-FDG in the diagnosis and management of cancer patients. Int J Clin Oncol 11: 286–296, 2006.
- Endres CJ, Pomper MG, James M, Uzuner O, Hammoud DA, Watkins CC, Reynolds A, Hilton J, Dannals RF, Kassiou M. Initial evaluation of <sup>11</sup>C-DPA-713, a novel TSPO PET ligand, in humans. J Nucl Med 50: 1276–1282, 2009.
- Farokhzad OC, Langer R. Nanomedicine: developing smarter therapeutic and diagnostic modalities. Adv Drug Deliv Rev 58: 1456–1459, 2006.
- Faulds K, Barbagallo RP, Keer JT, Smith WE, Graham D. SERRS as a more sensitive technique for the detection of labelled oligonucleotides compared with fluorescence. Analyst 129: 567–568, 2004.
- 102. Faulkner W. Basic Principles of MRI. OutSource, 1996.

- 103. Felicio AC, Shih MC, Godeiro-Junior C, Andrade LA, Bressan RA, Ferraz HB. Molecular imaging studies in Parkinson disease: reducing diagnostic uncertainty. *Neurologist* 15: 6–16, 2009.
- 104. Fero M, Pogliano K. Automated quantitative live cell fluorescence microscopy. Cold Spring Harb Perspect Biol 2: a000455, 2010.
- 105. Fink GR. Functional MR imaging: from the BOLD effect to higher motor cognition. Suppl Clin Neurophysiol 57: 458–468, 2004.
- Flohr T, Stierstorfer K, Bruder H, Simon J, Schaller S. New technical developments in multislice CT. Part 1: Approaching isotropic resolution with sub-millimeter 16-slice scanning. Rofo 174: 839–845, 2002.
- Flotats A, Carrio I. Radionuclide noninvasive evaluation of heart failure beyond left ventricular function assessment. J Nucl Cardiol 16: 304–315, 2009.
- 108. Forster BB, MacKay AL, Whittall KP, Kiehl KA, Smith AM, Hare RD, Liddle PF. Functional magnetic resonance imaging: the basics of blood-oxygen-level dependent (BOLD) imaging. Can Assoc Radiol J 49: 320–329, 1998.
- Franc BL, Acton PD, Mari C, Hasegawa BH. Small-animal SPECT and SPECT/CT: important tools for preclinical investigation. J Nucl Med 49: 1651–1663, 2008.
- 110. Frasco MF, Chaniotakis N. Bioconjugated quantum dots as fluorescent probes for bioanalytical applications. Anal Bioanal Chem 396: 229–240.
- 111. Freudiger CW, Min W, Saar BG, Lu S, Holtom GR, He C, Tsai JC, Kang JX, Xie XS. Label-free biomedical imaging with high sensitivity by stimulated Raman scattering microscopy. Science 322: 1857–1861, 2008.
- Friedlander M, Brooks PC, Shaffer RW, Kincaid CM, Varner JA, Cheresh DA. Definition of two angiogenic pathways by distinct alpha v integrins. Science 270: 1500–1502, 1995.
- Friedman M, Stahl S. Engineered affinity proteins for tumour-targeting applications. Biotechnol Appl Biochem 53: 1–29, 2009.
- 114. Fujii N, Inamoto Y, Saitoh E, Baba M, Okada S, Yoshioka S, Nakai T, Ida Y, Katada K, Palmer JB. Evaluation of swallowing using 320-detector-row multislice CT. Part I: Single- and multiphase volume scanning for three-dimensional morphological and kinematic analysis. Dysphagia 2010.
- 115. Fujimura Y, Ikoma Y, Yasuno F, Suhara T, Ota M, Matsumoto R, Nozaki S, Takano A, Kosaka J, Zhang MR, Nakao R, Suzuki K, Kato N, Ito H. Quantitative analyses of <sup>18</sup>F-FEDAA1106 binding to peripheral benzodiazepine receptors in living human brain. *J Nucl Med* 47: 43–50, 2006.
- 116. Furusawa M, Onomichi M, Morishita S, Hamatake S, Takahashi M, Ito YH. Carbon-13 magnetic resonance spectroscopy of glucose metabolism in SCC-VII tumors. *Radiat Med* 15: 149–153, 1997.
- Gaa J, Rummeny EJ, Seemann MD. Whole-body imaging with PET/MRI. Eur J Med Res
   309–312, 2004.
- 118. Gallagher FA, Bohndiek SE, Kettunen MI, Lewis DY, Soloviev D, Brindle KM. Hyper-polarized <sup>13</sup>C MRI and PET: in vivo tumor biochemistry. J Nucl Med 52: 1333–1336, 2011.
- Gallagher FA, Kettunen MI, Brindle KM. Imaging pH with hyperpolarized (13)C. NMR Biomed 24: 1006–1015, 2011.
- 120. Gallagher FA, Kettunen MI, Hu DE, Jensen PR, Zandt RI, Karlsson M, Gisselsson A, Nelson SK, Witney TH, Bohndiek SE, Hansson G, Peitersen T, Lerche MH, Brindle KM. Production of hyperpolarized [1,4-13C2]malate from [1,4-13C2]fumarate is a marker of cell necrosis and treatment response in tumors. Proc Natl Acad Sci USA 106: 19801–19806, 2009.
- Gambhir SS. Molecular imaging of cancer with positron emission tomography. Nat Rev Cancer 2: 683

  –693, 2002.
- Gambhir SS. Quantitative assay development for PET. In: PET: Molecular Imaging and Its Biological Applications, edited by Phelps M. New York: Springer, 2004, p. 195–201.
- 123. Gambhir SS, Barrio JR, Phelps ME, Iyer M, Namavari M, Satyamurthy N, Wu L, Green LA, Bauer E, MacLaren DC, Nguyen K, Berk AJ, Cherry SR, Herschman HR. Imaging adenoviral-directed reporter gene expression in living animals with positron emission tomography. Proc Natl Acad Sci USA 96: 2333–2338, 1999.

- 124. Gambhir SS, Herschman HR, Cherry SR, Barrio JR, Satyamurthy N, Toyokuni T, Phelps ME, Larson SM, Balatoni J, Finn R, Sadelain M, Tjuvajev J, Blasberg R. Imaging transgene expression with radionuclide imaging technologies. *Neoplasia* 2: 118–138, 2000
- Gambhir SS, Yaghoubi S. Molecular Imaging With Reporter Genes. Cambridge, UK: Cambridge Univ. Press, 2010.
- 126. Gammon ST, Villalobos VM, Roshal M, Samrakandi M, Piwnica-Worms D. Rational design of novel red-shifted BRET pairs: platforms for real-time single-chain protease biosensors. *Biotechnol Prog* 25: 559–569, 2009.
- 127. Gao X, Cui Y, Levenson RM, Chung LW, Nie S. In vivo cancer targeting and imaging with semiconductor quantum dots. *Nat Biotechnol* 22: 969–976, 2004.
- 128. Ge J, Erickson SJ, Godavarty A. Fluorescence tomographic imaging using a handheld-probe-based optical imager: extensive phantom studies. *Appl Opt* 48: 6408–6416, 2009.
- 129. Geuze RE, Prins HJ, Oner FC, van der Helm YJ, Schuijff LS, Martens AC, Kruyt MC, Alblas J, Dhert WJ. Luciferase labeling for multipotent stromal cell tracking in spinal fusion versus ectopic bone tissue engineering in mice and rats. Tissue Eng Part A 2010.
- Girgis MD, Kenanova V, Olafsen T, McCabe KE, Wu AM, Tomlinson JS. Anti-CA19-9 diabody as a PET imaging probe for pancreas cancer. J Surg Res 170: 169–178, 2011.
- Glasspool RM, Evans TR. Clinical imaging of cancer metastasis. Eur J Cancer 36: 1661– 1670, 2000.
- 132. Glunde K, Artemov D, Penet MF, Jacobs MA, Bhujwalla ZM. Magnetic resonance spectroscopy in metabolic and molecular imaging and diagnosis of cancer. Chem Rev 110: 3043–3059.
- 133. Goldman ER, Balighian ED, Mattoussi H, Kuno MK, Mauro JM, Tran PT, Anderson GP. Avidin: a natural bridge for quantum dot-antibody conjugates. J Am Chem Soc 124: 6378–6382, 2002.
- 134. Graser A, Becker CR, Staehler M, Clevert DA, Macari M, Arndt N, Nikolaou K, Sommer W, Stief C, Reiser MF, Johnson TR. Single-phase dual-energy CT allows for characterization of renal masses as benign or malignant. *Invest Radiol* 45: 399–405, 2010
- Grierson JR, Shields AF. Radiosynthesis of 3'-deoxy-3'-[(18)F]fluorothymidine:
   [(18)F]FLT for imaging of cellular proliferation in vivo. Nucl Med Biol 27: 143–156,
   2000
- 136. Guhlke S, Wester HJ, Bruns C, Stocklin G. (2-[¹8F]fluoropropionyl-(D)phe1)-octreotide, a potential radiopharmaceutical for quantitative somatostatin receptor imaging with PET: synthesis, radiolabeling, in vitro validation and biodistribution in mice. Nucl Med Biol 21: 819–825, 1994.
- 137. Gulec SA, Hoenie E, Hostetter R, Schwartzentruber D. PET probe-guided surgery: applications and clinical protocol. World J Surg Oncol 5: 65, 2007.
- 138. Guzman R, Uchida N, Bliss TM, He D, Christopherson KK, Stellwagen D, Capela A, Greve J, Malenka RC, Moseley ME, Palmer TD, Steinberg GK. Long-term monitoring of transplanted human neural stem cells in developmental and pathological contexts with MRI. Proc Natl Acad Sci USA 104: 10211–10216. 2007.
- Haberkorn U, Altmann A, Mier W, Eisenhut M. Molecular imaging of tumor metabolism and apoptosis. Ernst Schering Found Symp Proc 125–152, 2007.
- 140. Hadjipanayis CG, Machaidze R, Kaluzova M, Wang L, Schuette AJ, Chen H, Wu X, Mao H. EGFRvIII antibody-conjugated iron oxide nanoparticles for magnetic resonance imaging-guided convection-enhanced delivery and targeted therapy of glioblastoma. *Cancer Res* 70: 6303–6312, 2010.
- Hakumaki JM, Liimatainen T. Molecular imaging of apoptosis in cancer. Eur J Radiol 56: 143–153. 2005.
- 142. Halldin C, Gulyas B, Farde L. PET studies with carbon-11 radioligands in neuropsychopharmacological drug development. Curr Pharm Res 7: 1907–1929, 2001.
- 143. Halldin C, Gulyas B, Langer O, Farde L. Brain radioligands–state of the art and new trends. Q J Nucl Med 45: 139–152, 2001.
- 144. Haller J, Hyde D, Deliolanis N, de Kleine R, Niedre M, Ntziachristos V. Visualization of pulmonary inflammation using noninvasive fluorescence molecular imaging. J Appl Physiol 104: 795–802, 2008.

- Hamaguchi N, Ellington A, Stanton M. Aptamer beacons for the direct detection of proteins. Anal Biochem 294: 126–131, 2001.
- 146. Hammoud DA, Hoffman JM, Pomper MG. Molecular neuroimaging: from conventional to emerging techniques. *Radiology* 245: 21–42, 2007.
- 147. Hanahan D, Weinberg RA. The hallmarks of cancer. Cell 100: 57-70, 2000.
- 148. Hancu I, Dixon WT, Woods M, Vinogradov E, Sherry AD, Lenkinski RE. CEST and PARACEST MR contrast agents. Acta Radiol 51: 910–923, 2010.
- 149. Hausner SH, Marik J, Gagnon MK, Sutcliffe JL. In vivo positron emission tomography (PET) imaging with an alphavbeta6 specific peptide radiolabeled using <sup>18</sup>F-"click" chemistry: evaluation and comparison with the corresponding 4-[<sup>18</sup>F]fluorobenzoyl-and 2-[<sup>18</sup>F]fluoropropionyl-peptides. J Med Chem 51: 5901–5904, 2008.
- 150. He YX, Guo QY. Clinical applications and advances of positron emission tomography with fluorine-18-fluorodeoxyglucose (<sup>18</sup>F-FDG) in the diagnosis of liver neoplasms. Postgrad Med J 84: 246–251, 2008.
- Heckl S. Future contrast agents for molecular imaging in stroke. Curr Med Chem 14: 1713–1728, 2007.
- 152. Heiken JP, Brink JA, Vannier MW. Spiral (helical) CT. Radiology 189: 647-656, 1993.
- Hennigan A, O'Callaghan RM, Kelly AM. Neurotrophins and their receptors: roles in plasticity, neurodegeneration and neuroprotection. *Biochem Soc Trans* 35: 424–427, 2007.
- 154. Herman B, Krishnan RV, Centonze VE. Microscopic analysis of fluorescence resonance energy transfer (FRET). Methods Mol Biol 261: 351–370, 2004.
- 155. Hicke BJ, Stephens AW, Gould T, Chang YF, Lynott CK, Heil J, Borkowski S, Hilger CS, Cook G, Warren S, Schmidt PG. Tumor targeting by an aptamer. J Nucl Med 47: 668–678. 2006.
- 156. Hiona A, Wu JC. Noninvasive radionuclide imaging of cardiac gene therapy: progress and potential. Nat Clin Pract Cardiovasc Med 5 Suppl 2: S87–S95, 2008.
- 157. Ho YP, Leong KW. Quantum dot-based theranostics. Nanoscale 2: 60-68, 2010.
- 158. Hodgson RJ, O'Connor P, Moots R. MRI of rheumatoid arthritis image quantitation for the assessment of disease activity, progression and response to therapy. Rheumatology 47: 13–21, 2008.
- Hoffman JM, Gambhir SS, Kelloff GJ. Regulatory and reimbursement challenges for molecular imaging. Radiology 245: 645–660, 2007.
- 160. Hoffman RM. The multiple uses of fluorescent proteins to visualize cancer in vivo. Nat Rev Cancer 5: 796–806, 2005.
- Hoffman RM. Visualization of GFP-expressing tumors and metastasis in vivo. Biotechniques 30: 1016–1022, 2001.
- Hoffman RM, Yang M. Subcellular imaging in the live mouse. Nat Protoc 1: 775–782, 2006.
- 163. Hoffman RM, Yang M. Whole-body imaging with fluorescent proteins. Nat Protoc 1: 1429–1438. 2006.
- 164. Hom RK, Katzenellenbogen JA. Technetium-99m-labeled receptor-specific small-molecule radiopharmaceuticals: recent developments and encouraging results. Nucl Med Biol 24: 485–498, 1997.
- 165. Hong H, Sun J, Cai W. Radionuclide-based cancer imaging targeting the carcinoembryonic antigen. Biomark Insights 3: 435–451, 2008.
- Hong H, Zhang Y, Sun J, Cai W. Positron emission tomography imaging of prostate cancer. Amino Acids 39: 11–27, 2010.
- 167. Hoshida T, Isaka N, Hagendoorn J, di Tomaso E, Chen YL, Pytowski B, Fukumura D, Padera TP, Jain RK. Imaging steps of lymphatic metastasis reveals that vascular endothelial growth factor-C increases metastasis by increasing delivery of cancer cells to lymph nodes: therapeutic implications. Cancer Res 66: 8065–8075, 2006.
- Hoshino K, Ly HQ, Frangioni JV, Hajjar RJ. In vivo tracking in cardiac stem cell-based therapy. Prog Cardiovasc Dis 49: 414–420, 2007.
- 169. Hossain MK, Kitahama Y, Huang GG, Han X, Ozaki Y. Surface-enhanced Raman scattering: realization of localized surface plasmon resonance using unique substrates and methods. Anal Bioanal Chem 394: 1747–1760, 2009.

- 170. Hsiung PL, Hardy J, Friedland S, Soetikno R, Du CB, Wu AP, Sahbaie P, Crawford JM, Lowe AW, Contag CH, Wang TD. Detection of colonic dysplasia in vivo using a targeted heptapeptide and confocal microendoscopy. Nat Med 14: 454–458, 2008.
- 171. Hu H. Multi-slice helical CT: scan and reconstruction. Med Phys 26: 5-18, 1999.
- 172. Hu S, Balakrishnan A, Bok RA, Anderton B, Larson PE, Nelson SJ, Kurhanewicz J, Vigneron DB, Goga A. <sup>13</sup>C-pyruvate imaging reveals alterations in glycolysis that precede c-Myc-induced tumor formation and regression. *Cell Metab* 14: 131–142, 2011
- 173. Huang WS, Lin SZ, Lin JC, Wey SP, Ting G, Liu RS. Evaluation of early-stage Parkinson's disease with 99mTc-TRODAT-I imaging. J Nucl Med 42: 1303–1308, 2001.
- 174. Hyafil F, Cornily JC, Feig JE, Gordon R, Vucic E, Amirbekian V, Fisher EA, Fuster V, Feldman LJ, Fayad ZA. Noninvasive detection of macrophages using a nanoparticulate contrast agent for computed tomography. Nat Med 13: 636–641, 2007.
- 175. Ide AG, Baker NH, Warren SL. Vascularization of the Brown-Pearce rabbit epithelioma transplant as seen in the transplant ear chamber. Am J Roentgenol 42: 891–899, 1939.
- 176. Ido T, Wan CN, Casella V, Fowler JS, Wolf AP, Reivich M, Kuhl DE. Labeled 2-deoxy-D-glucose analogs. <sup>18</sup>F-labeled 2-deoxy-2-fluoro-D-mannose and <sup>14</sup>C-2-deoxy-2-fluoro-D-glucose. J Labelled Comp Radiopharm 14: 175–183, 1978.
- 177. Indrevoll B, Kindberg GM, Solbakken M, Bjurgert E, Johansen JH, Karlsen H, Mendizabal M, Cuthbertson A. NC-100717: a versatile RGD peptide scaffold for angiogenesis imaging. Bioorg Med Chem Lett 16: 6190-6193, 2006.
- 178. Isasi CR, Moadel RM, Blaufox MD. A meta-analysis of FDG-PET for the evaluation of breast cancer recurrence and metastases. Breast Cancer Res Treat 90: 105–112, 2005.
- 179. Jacobs AH, Li H, Winkeler A, Hilker R, Knoess C, Ruger A, Galldiks N, Schaller B, Sobesky J, Kracht L, Monfared P, Klein M, Vollmar S, Bauer B, Wagner R, Graf R, Wienhard K, Herholz K, Heiss WD. PET-based molecular imaging in neuroscience. Eur J Nucl Med Mol Imaging 30: 1051–1065, 2003.
- 180. Jacobs AH, Winkeler A, Dittmar C, Hilker R, Heiss WD. Prospects of molecular imaging in neurology. J Cell Biochem Suppl 39: 98–109, 2002.
- 181. Jacobson AF, Lombard J, Banerjee G, Camici PG. <sup>123</sup>I-mIBG scintigraphy to predict risk for adverse cardiac outcomes in heart failure patients: design of two prospective multicenter international trials. *J Nucl Cardiol* 16: 113–121, 2009.
- 182. Jain RK. Angiogenesis and lymphangiogenesis in tumors: insights from intravital microscopy. Cold Spring Harb Symp Quant Biol 67: 239–248, 2002.
- Jain RK, Munn LL, Fukumura D. Dissecting tumour pathophysiology using intravital microscopy. Nat Rev Cancer 2: 266–276, 2002.
- 184. James ML, Fulton RR, Henderson DJ, Eberl S, Meikle SR, Thomson S, Allan RD, Dolle F, Fulham MJ, Kassiou M. Synthesis and in vivo evaluation of a novel peripheral benzodiazepine receptor PET radioligand. *Bioorg Med Chem* 13: 6188–6194, 2005.
- Janib SM, Moses AS, MacKay JA. Imaging and drug delivery using theranostic nanoparticles. Adv Drug Deliv Rev 62: 1052–1063, 2010.
- 186. Jayasena SD. Aptamers: an emerging class of molecules that rival antibodies in diagnostics. Clin Chem 45: 1628–1650, 1999.
- 187. Jiang T, Olson ES, Nguyen QT, Roy M, Jennings PA, Tsien RY. Tumor imaging by means of proteolytic activation of cell-penetrating peptides. *Proc Natl Acad Sci USA* 101: 17867–17872, 2004.
- 188. Jin AY, Tuor UI, Rushforth D, Filfil R, Kaur J, Ni F, Tomanek B, Barber PA. Magnetic resonance molecular imaging of post-stroke neuroinflammation with a P-selectin targeted iron oxide nanoparticle. Contrast Media Mol Imaging 4: 305–311, 2009.
- Johnson TR, Weckbach S, Kellner H, Reiser MF, Becker CR. Clinical image: dualenergy computed tomographic molecular imaging of gout. Arthritis Rheum 56: 2809, 2007.
- 190. Jokerst J, Gambhir SS. Small silica particles are an alternative to microbubbles for ultrasound tracking of stem cells in vivo. In: World Molecular Imaging Congress 2011.
- Jokerst JV, Lobovkina T, Zare RN, Gambhir SS. Nanoparticle PEGylation for imaging and therapy. Nanomed. In press.

- Jokerst JV, Miao Z, Zavaleta C, Cheng Z, Gambhir SS. Affibody-functionalized goldsilica nanoparticles for Raman molecular imaging of the epidermal growth factor receptor. Small 7: 625–633, 2011.
- Jones GJ, Barsby NL, Cohen EA, Holden J, Harris K, Dickie P, Jhamandas J, Power C.
   HIV-I Vpr causes neuronal apoptosis and in vivo neurodegeneration. J Neurosci 27: 3703–3711, 2007.
- 194. Kai H. Novel non-invasive approach for visualizing inflamed atherosclerotic plaques using fluorodeoxyglucose-positron emission tomography. Geriatr Gerontol Int 10: 1–8, 2010.
- 195. Kang JH, Chung JK. Molecular-genetic imaging based on reporter gene expression. J Nucl Med 49 Suppl 2: 164S–179S, 2008.
- 196. Kaufmann BA, Sanders JM, Davis C, Xie A, Aldred P, Sarembock IJ, Lindner JR. Molecular imaging of inflammation in atherosclerosis with targeted ultrasound detection of vascular cell adhesion molecule-1. Circulation 116: 276–284, 2007.
- 197. Ke S, Wen X, Gurfinkel M, Charnsangavej C, Wallace S, Sevick-Muraca EM, Li C. Near-infrared optical imaging of epidermal growth factor receptor in breast cancer xenografts. Cancer Res 63: 7870–7875, 2003.
- Keefe AD, Pai S, Ellington A. Aptamers as therapeutics. Nat Rev Drug Discov 9: 537–550.
- 199. Kelly KA, Allport JR, Tsourkas A, Shinde-Patil VR, Josephson L, Weissleder R. Detection of vascular adhesion molecule-1 expression using a novel multimodal nanoparticle. Circ Res 96: 327–336, 2005.
- Kennel SJ, Davis IA, Branning J, Pan H, Kabalka GW, Paulus MJ. High resolution computed tomography and MRI for monitoring lung tumor growth in mice undergoing radioimmunotherapy: correlation with histology. Med Phys 27: 1101–1107, 2000.
- Kenny LM, Aboagye EO, Price PM. Positron emission tomography imaging of cell proliferation in oncology. Clin Oncol 16: 176–185, 2004.
- Kepe V, Huang SC, Small GW, Satyamurthy N, Barrio JR. Visualizing pathology deposits in the living brain of patients with Alzheimer's disease. *Methods Enzymol* 412: 144–160, 2006.
- Keren S, Gheysens O, Levin CS, Gambhir SS. A comparison between a time domain and continuous wave small animal optical imaging system. *IEEE Trans Med Imaging* 27: 58–63. 2008.
- Keren S, Zavaleta C, Cheng Z, de la Zerda A, Gheysens O, Gambhir SS. Noninvasive molecular imaging of small living subjects using Raman spectroscopy. *Proc Natl Acad Sci* USA 105: 5844–5849, 2008.
- 205. Keshari KR, Wilson DM, Chen AP, Bok R, Larson PE, Hu S, Van Criekinge M, Macdonald JM, Vigneron DB, Kurhanewicz J. Hyperpolarized [2-13C]-fructose: a hemiketal DNP substrate for in vivo metabolic imaging. J Am Chem Soc 131: 17591–17596, 2009.
- $206. \ \ Keyes JWJr, Orlandea N, Heetderks WJ, Leonard PF, Rogers WL. The Humongotron: a scintillation-camera transaxial tomograph. J Nucl Med 18: 381–387, 1977.$
- 207. Kiessling F. Noninvasive cell tracking. Handb Exp Pharmacol 305–321, 2008.
- Kietselaer BL, Reutelingsperger CP, Heidendal GA, Daemen MJ, Mess WH, Hofstra L, Narula J. Noninvasive detection of plaque instability with use of radiolabeled annexin A5 in patients with carotid-artery atherosclerosis. N Engl J Med 350: 1472–1473, 2004.
- 209. Kim C, Cho EC, Chen J, Song KH, Au L, Favazza C, Zhang Q, Cobley CM, Gao F, Xia Y, Wang LV. In vivo molecular photoacoustic tomography of melanomas targeted by bioconjugated gold nanocages. ACS Nano 4: 4559–4564, 2010.
- Kim D, Jeong YY, Jon S. A drug-loaded aptamer-gold nanoparticle bioconjugate for combined CT imaging and therapy of prostate cancer. ACS Nano 4: 3689–3696, 2010.
- 211. Kim EM, Park EH, Cheong SJ, Lee CM, Kim DW, Jeong HJ, Lim ST, Sohn MH, Kim K, Chung J. Characterization, biodistribution and small-animal SPECT of I-125-labeled c-Met binding peptide in mice bearing c-Met receptor tyrosine kinase-positive tumor xenografts. Nucl Med Biol 36: 371–378, 2009.
- 212. Kinoshita M, Yoshioka Y, Okita Y, Hashimoto N, Yoshimine T. MR molecular imaging of HER-2 in a murine tumor xenograft by SPIO labeling of anti-HER-2 affibody. Contrast Media Mol Imaging 5: 18–22, 2010.

- 213. Kircher MF, de la Zerda A, Jokerst JV, Zavaleta C, Kempen P, Mittra E, Habte F, Sinclair R, Gambhir SS. A brain tumor molecular imaging strategy using a novel triple-modality nanoparticle. Nat Med. In press.
- 214. Kirsch DG, Grimm J, Guimaraes AR, Wojtkiewicz GR, Perez BA, Santiago PM, Anthony NK, Forbes T, Doppke K, Weissleder R, Jacks T. Imaging primary lung cancers in mice to study radiation biology. *Int J Radiat Oncol Biol Phys* 76: 973–977, 2010.
- 215. Kirsch DG, Grimm J, Guimaraes AR, Wojtkiewicz GR, Perez BA, Santiago PM, Anthony NK, Forbes T, Doppke K, Weissleder R, Jacks T. Imaging primary lung cancers in mice to study radiation biology. *Int J Radiat Oncol Biol Phys* 76: 973–977.
- Kishimoto H, Zhao M, Hayashi K, Urata Y, Tanaka N, Fujiwara T, Penman S, Hoffman RM. In vivo internal tumor illumination by telomerase-dependent adenoviral GFP for precise surgical navigation. *Proc Natl Acad Sci USA* 106: 14514–14517, 2009.
- Kitching AR, Kuligowski MP, Hickey MJ. In vivo imaging of leukocyte recruitment to glomeruli in mice using intravital microscopy. Methods Mol Biol 466: 109–117, 2009.
- 218. Klibanov AL, Rasche PT, Hughes MS, Wojdyla JK, Galen KP, Wible JH Jr, Brandenburger GH. Detection of individual microbubbles of ultrasound contrast agents: imaging of free-floating and targeted bubbles. *Invest Radiol* 39: 187–195, 2004.
- 219. Klunk WE, Engler H, Nordberg A, Wang Y, Blomqvist G, Holt DP, Bergstrom M, Savitcheva I, Huang GF, Estrada S, Ausen B, Debnath ML, Barletta J, Price JC, Sandell J, Lopresti BJ, Wall A, Koivisto P, Antoni G, Mathis CA, Langstrom B. Imaging brain amyloid in Alzheimer's disease with Pittsburgh Compound-B. Ann Neurol 55: 306–319, 2004.
- 220. Klussmann S. The Aptamer Handbook Functional Oligonucleotides and Their Applications. Weinheim, Germany: Wiley-VCH, 2006.
- 221. Kneipp K, Kneipp H, Itzkan I, Dasari RR, Feld MS. Ultrasensitive chemical analysis by Raman spectroscopy. *Chem Rev* 99: 2957–2976, 1999.
- Kobayashi H, Choyke PL. Target-cancer-cell-specific activatable fluorescence imaging probes: rational design and in vivo applications. Acc Chem Res 44: 83–90, 2010.
- Kobayashi H, Longmire MR, Ogawa M, Choyke PL, Kawamoto S. Multiplexed imaging in cancer diagnosis: applications and future advances. *Lancet Oncol* 11: 589–595, 2010
- 224. Kobayashi H, Ogawa M, Kosaka N, Choyke PL, Urano Y. Multicolor imaging of lymphatic function with two nanomaterials: quantum dot-labeled cancer cells and dendrimer-based optical agents. *Nanomedicine* 4: 411–419, 2009.
- 225. Koehl GE, Gaumann A, Geissler EK. Intravital microscopy of tumor angiogenesis and regression in the dorsal skin fold chamber: mechanistic insights and preclinical testing of therapeutic strategies. Clin Exp Metastasis 26: 329–344, 2009.
- Koenig W, Khuseyinova N. Biomarkers of atherosclerotic plaque instability and rupture. Arterioscler Thromb Vasc Biol 27: 15–26, 2007.
- 227. Kohler SJ, Yen Y, Wolber J, Chen AP, Albers MJ, Bok R, Zhang V, Tropp J, Nelson S, Vigneron DB, Kurhanewicz J, Hurd RE. In vivo 13 carbon metabolic imaging at 3T with hyperpolarized <sup>13</sup>C-I-pyruvate. *Magn Reson Med* 58: 65–69, 2007.
- 228. Kondziolka D, Steinberg GK, Wechsler L, Meltzer CC, Elder E, Gebel J, Decesare S, Jovin T, Zafonte R, Lebowitz J, Flickinger JC, Tong D, Marks MP, Jamieson C, Luu D, Bell-Stephens T, Teraoka J. Neurotransplantation for patients with subcortical motor stroke: a phase 2 randomized trial. J Neurosurg 103: 38–45, 2005.
- Koyama Y, Hama Y, Urano Y, Nguyen DM, Choyke PL, Kobayashi H. Spectral fluorescence molecular imaging of lung metastases targeting HER2/neu. *Clin Cancer Res* 13: 2936–2945, 2007.
- 230. Krohn KA, Link JM, Mason RP. Molecular imaging of hypoxia. J Nucl Med 49 Suppl 2: 1295–148S, 2008.
- 231. Kumar A, Kumar R, Seenu V, Gupta SD, Chawla M, Malhotra A, Mehta SN. The role of <sup>18</sup>F-FDG PET/CT in evaluation of early response to neoadjuvant chemotherapy in patients with locally advanced breast cancer. *Eur Radiol* 19: 1347–1357, 2009.
- 232. Kung HF, Kung MP, Choi SR. Radiopharmaceuticals for single-photon emission computed tomography brain imaging. Semin Nucl Med 33: 2–13, 2003.
- 233. Kurhanewicz J, Vigneron DB, Brindle K, Chekmenev EY, Comment A, Cunningham CH, Deberardinis RJ, Green GG, Leach MO, Rajan SS, Rizi RR, Ross BD, Warren WS, Malloy CR. Analysis of cancer metabolism by imaging hyperpolarized nuclei: prospects for translation to clinical research. *Neoplasia* 13: 81–97, 2011.

- 234. Laitinen I, Saraste A, Weidl E, Poethko T, Weber AW, Nekolla SG, Leppanen P, Yla-Herttuala S, Holzlwimmer G, Walch A, Esposito I, Wester HJ, Knuuti J, Schwaiger M. Evaluation of alphavbeta3 integrin-targeted positron emission tomography tracer <sup>18</sup>F-galacto-RGD for imaging of vascular inflammation in atherosclerotic mice. *Circ Cardiovasc Imaging* 2: 331–338, 2009.
- 235. Lancelot E, Amirbekian V, Brigger I, Raynaud JS, Ballet S, David C, Rousseaux O, Le Greneur S, Port M, Lijnen HR, Bruneval P, Michel JB, Ouimet T, Roques B, Amirbekian S, Hyafil F, Vucic E, Aguinaldo JG, Corot C, Fayad ZA. Evaluation of matrix metalloproteinases in atherosclerosis using a novel noninvasive imaging approach. Arterioscler Thromb Vasc Biol 28: 425–432, 2008.
- Lecchi M, Ottobrini L, Martelli C, Del Sole A, Lucignani G. Instrumentation and probes for molecular and cellular imaging. Q J Nucl Med Mol Imaging 51: 111–126, 2007
- 237. Lee S, Chon H, Lee M, Choo J, Shin SY, Lee YH, Rhyu JJ, Son SW, Oh CH. Surface-enhanced Raman scattering imaging of HER2 cancer markers overexpressed in single MCF7 cells using antibody conjugated hollow gold nanospheres. *Biosens Bioelectron* 24: 2260–2263. 2009.
- 238. Lee S, Xie J, Chen X. Peptides and peptide hormones for molecular imaging and disease diagnosis. Chem Rev 110: 3087–3111, 2010.
- Leong-Poi H, Christiansen J, Klibanov AL, Kaul S, Lindner JR. Noninvasive assessment of angiogenesis by ultrasound and microbubbles targeted to alpha(v)-integrins. Circulation 107: 455–460, 2003.
- Leu AJ, Berk DA, Lymboussaki A, Alitalo K, Jain RK. Absence of functional lymphatics within a murine sarcoma: a molecular and functional evaluation. *Cancer Res* 60: 4324– 4327, 2000.
- 241. Levine HA, Nilsen-Hamilton M. A mathematical analysis of SELEX. *Comput Biol Chem* 31: 11–35, 2007.
- Levitt MH. Spin Dynamics: Basics of Nuclear Magnetic Resonance. New York: Wiley, 2008, p. 744.
- 243. Lewis MA. Multislice CT: opportunities and challenges. Br J Radiol 74: 779-781, 2001.
- 244. Li J, Chaudhary A, Chmura SJ, Pelizzari C, Rajh T, Wietholt C, Kurtoglu M, Aydogan B. A novel functional CT contrast agent for molecular imaging of cancer. *Phys Med Biol* 55: 4389–4397, 2010.
- Liang F, Chen B. A review on biomedical applications of single-walled carbon nanotubes. Curr Med Chem 17: 10–24, 2010.
- 246. Liang HD, Blomley MJ. The role of ultrasound in molecular imaging. *Br J Radiol* 76: S140–150, 2003.
- 247. Liang Q, Satyamurthy N, Barrio JR, Toyokuni T, Phelps MP, Gambhir SS, Herschman HR. Noninvasive, quantitative imaging in living animals of a mutant dopamine D2 receptor reporter gene in which ligand binding is uncoupled from signal transduction. Gene Ther 8: 1490–1498, 2001.
- 248. Lijowski M, Caruthers S, Hu G, Zhang H, Scott MJ, Williams T, Erpelding T, Schmieder AH, Kiefer G, Gulyas G, Athey PS, Gaffney PJ, Wickline SA, Lanza GM. High sensitivity: high-resolution SPECT-CT/MR molecular imaging of angiogenesis in the Vx2 model. *Invest Radiol* 44: 15–22, 2009.
- Lin TJ, Huang CC, Wang IJ, Lin JW, Hung KS, Fan L, Tsao HH, Yang NS, Lin KJ.
   Validation of an animal FDG PET imaging system for study of glioblastoma xenografted mouse and rat models. Ann Nucl Med Sci 23: 77–83, 2010.
- Lindner JR, Song J, Christiansen J, Klibanov AL, Xu F, Ley K. Ultrasound assessment of inflammation and renal tissue injury with microbubbles targeted to P-selectin. Circulation 104: 2107–2112, 2001.
- Lindvall O, Bjorklund A. Cell therapy in Parkinson's disease. NeuroRx 1: 382–393, 2004
- 252. Liu H, Ren G, Miao Z, Zhang X, Tang X, Han P, Gambhir SS, Cheng Z. Molecular optical imaging with radioactive probes. *PLoS One* 5: e9470, 2010.
- 253. Liu JT, Mandella MJ, Ra H, Wong LK, Solgaard O, Kino GS, Piyawattanametha W, Contag CH, Wang TD. Miniature near-infrared dual-axes confocal microscope utilizing a two-dimensional microelectromechanical systems scanner. Opt Lett 32: 256– 258, 2007.

- 254. Liu Z, Zhao M, Zhu X, Furenlid LR, Chen YC, Barrett HH. In vivo dynamic imaging of myocardial cell death using 99mTc-labeled C2A domain of synaptotagmin I in a rat model of ischemia and reperfusion. Nucl Med Biol 34: 907–915, 2007.
- Loening AM, Dragulescu-Andrasi A, Gambhir SS. A red-shifted Renilla luciferase for transient reporter-gene expression. Nat Methods 7: 5–6, 2010.
- Loening AM, Wu AM, Gambhir SS. Red-shifted Renilla reniformis luciferase variants for imaging in living subjects. Nat Methods 4: 641–643, 2007.
- Longmire M, Choyke PL, Kobayashi H. Clearance properties of nano-sized particles and molecules as imaging agents: considerations and caveats. *Nanomedicine* 3: 703–717. 2008.
- Lorincz A, Haddad D, Naik R, Naik V, Fung A, Cao A, Manda P, Pandya A, Auner G, Rabah R, Langenburg SE, Klein MD. Raman spectroscopy for neoplastic tissue differentiation: a pilot study. J Pediatr Surg 39: 953–956, 2004.
- Louie A. Multimodality imaging probes: design and challenges. Chem Rev 110: 3146–3195, 2010.
- Lucignani G. Monitoring cancer therapy with PET: probably effective, but more research is needed. Eur J Nucl Med Mol Imaging 36: 1520–1525, 2009.
- Luker GD, Luker KE. Optical imaging: current applications and future directions. J Nucl Med 49: 1–4. 2008.
- Luker KE, Gupta M, Luker GD. Imaging chemokine receptor dimerization with firefly luciferase complementation. FASEB J 23: 823–834, 2009.
- Luker KE, Hutchens M, Schultz T, Pekosz A, Luker GD. Bioluminescence imaging of vaccinia virus: effects of interferon on viral replication and spread. Virology 341: 284– 300, 2005.
- 264. Lusis AJ. Atherosclerosis. Nature 407: 233-241, 2000.
- 265. Mading P, Fuchtner F, Wust F. Module-assisted synthesis of the bifunctional labelling agent N-succinimidyl 4-[(18)F]fluorobenzoate ([(18)F]SFB). Appl Radiat Isot 63: 329 332, 2005.
- Mahadevan-Jansen A, Richards-Kortum A. Raman spectroscopy for the detection of cancers and precancers. J Biomed Opt 1: 31–70, 1996.
- Mahmood U, Weissleder R. Near-infrared optical imaging of proteases in cancer. Mol Cancer Ther 2: 489–496, 2003.
- Mallidi S, Larson T, Tam J, Joshi PP, Karpiouk A, Sokolov K, Emelianov S. Multiwavelength photoacoustic imaging and plasmon resonance coupling of gold nanoparticles for selective detection of cancer. *Nano Lett* 9: 2825–2831, 2009.
- Mallo RD, Salem L, Lalani T, Flum DR. Computed tomography diagnosis of ischemia and complete obstruction in small bowel obstruction: a systematic review. J Gastrointest Surg 9: 690–694, 2005.
- 270. Malviya G, Conti F, Chianelli M, Scopinaro F, Dierckx RA, Signore A. Molecular imaging of rheumatoid arthritis by radiolabelled monoclonal antibodies: new imaging strategies to guide molecular therapies. Eur J Nucl Med Mol Imaging 37: 386–398.
- Mansson S, Johansson E, Magnusson P, Chai CM, Hansson G, Petersson JS, Stahlberg F, Golman K. <sup>13</sup>C imaging-a new diagnostic platform. Eur Radiol 16: 57–67, 2006.
- Manyak MJ. Indium-111 capromab pendetide in the management of recurrent prostate cancer. Expert Rev Anticancer Ther 8: 175–181, 2008.
- Marik J, Sutcliffe JL. Fully automated preparation of nca 4-[<sup>18</sup>F]fluorobenzoic acid and N-succinimidyl 4-[<sup>18</sup>F]fluorobenzoate using a Siemens/CTI chemistry process control unit (CPCU). Appl Radiat Isot 65: 199–203, 2007.
- Marshall V, Grosset D. Role of dopamine transporter imaging in routine clinical practice. Mov Disord 18: 1415–1423, 2003.
- Masdeu JC, Bakshi R. Neuroimaging: anything to do with neurotherapeutics? NeuroRx
   163–166, 2005.
- Massoud TF, Gambhir SS. Molecular imaging in living subjects: seeing fundamental biological processes in a new light. Genes Dev 17: 545–580, 2003.
- Massoud TF, Paulmurugan R, De A, Ray P, Gambhir SS. Reporter gene imaging of protein-protein interactions in living subjects. Curr Opin Biotechnol 18: 31–37, 2007.

- Matera L. The choice of the antigen in the dendritic cell-based vaccine therapy for prostate cancer. Cancer Treat Rev 36: 131–141, 2009.
- 279. Matter CM, Stuber M, Nahrendorf M. Imaging of the unstable plaque: how far have we got? Eur Heart J 30: 2566–2574, 2009.
- Matthews JC, Hori K, Cormier MJ. Purification and properties of Renilla reniformis luciferase. *Biochemistry* 16: 85–91, 1977.
- 281. Matyus L. Fluorescence resonance energy transfer measurements on cell surfaces. A spectroscopic tool for determining protein interactions. J Photochem Photobiol B 12: 323–337, 1992.
- 282. McAllister SS, Weinberg RA. Tumor-host interactions: a far-reaching relationship. *J Clin Oncol* 28: 4022–4028. 2010.
- McDevitt MR, Chattopadhyay D, Jaggi JS, Finn RD, Zanzonico PB, Villa C, Rey D, Mendenhall J, Batt CA, Njardarson JT, Scheinberg DA. PET imaging of soluble yttrium-86-labeled carbon nanotubes in mice. PLoS One 2: e907, 2007.
- McNeil SE. Nanoparticle therapeutics: a personal perspective. Wiley Interdiscip Rev Nanomed Nanobiotechnol 1: 264–271, 2009.
- 285. Medarova Z, Moore A. Imaging of pancreatic cancer: a promise for early diagnosis through targeted strategies. *Cancer Therapy* 2: 329–344, 2004.
- 286. Mees G, Dierckx R, Vangestel C, Van de Wiele C. Molecular imaging of hypoxia with radiolabelled agents. Eur J Nucl Med Mol Imaging 36: 1674–1686, 2009.
- 287. Meier R, Piert M, Piontek G, Rudelius M, Oostendorp RA, Senekowitsch-Schmidtke R, Henning TD, Wels WS, Uherek C, Rummeny EJ, Daldrup-Link HE. Tracking of [18F]FDG-labeled natural killer cells to HER2/neu-positive tumors. *Nucl Med Biol* 35: 579–588, 2008.
- 288. Meikle SR, Kench P, Kassiou M, Banati RB. Small animal SPECT and its place in the matrix of molecular imaging technologies. *Phys Med Biol* 50: R45–61, 2005.
- 289. Menger MD, Laschke MW, Vollmar B. Viewing the microcirculation through the window: some twenty years experience with the hamster dorsal skinfold chamber. Eur Surg Res 34: 83–91, 2002.
- Miller MJ, Wei SH, Cahalan MD, Parker I. Autonomous T cell trafficking examined in vivo with intravital two-photon microscopy. *Proc Natl Acad Sci USA* 100: 2604–2609, 2003
- 291. Milligan G. Applications of bioluminescence- and fluorescence resonance energy transfer to drug discovery at G protein-coupled receptors. Eur J Pharm Sci 21: 397– 405, 2004.
- Min JJ, Gambhir SS. Molecular imaging of PET reporter gene expression. Handb Exp Pharmacol 277–303, 2008.
- Mishra A, Pfeuffer J, Mishra R, Engelmann J, Mishra AK, Ugurbil K, Logothetis NK. A new class of Gd-based DO3A-ethylamine-derived targeted contrast agents for MR and optical imaging. Bioconjug Chem 17: 773–780, 2006.
- 294. Mittra E, Goris M, lagaru A, Kardan A, Liu S, Shen B, Chin FT, Chen X, Gambhir SS. First in man studies of [ $^{18}$ F]FPRGD2: a novel PET radiopharmaceutical for imaging  $\alpha \nu \beta 3$  integrin levels. *J Nucl Med* 51: 1433, 2010.
- 295. Moffat BA, Chenevert TL, Lawrence TS, Meyer CR, Johnson TD, Dong Q, Tsien C, Mukherji S, Quint DJ, Gebarski SS, Robertson PL, Junck LR, Rehemtulla A, Ross BD. Functional diffusion map: a noninvasive MRI biomarker for early stratification of clinical brain tumor response. Proc Natl Acad Sci USA 102: 5524–5529, 2005.
- 296. Moffat FL Jr, Pinsky CM, Hammershaimb L, Petrelli NJ, Patt YZ, Whaley FS, Goldenberg DM. Clinical utility of external immunoscintigraphy with the IMMU-4 technetium-99m Fab' antibody fragment in patients undergoing surgery for carcinoma of the colon and rectum: results of a pivotal, phase III trial, The Immunomedics Study Group. J Clin Oncol 14: 2295–2305, 1996.
- 297. Morinaga A, Ono K, Ikeda T, Ikeda Y, Shima K, Noguchi-Shinohara M, Samuraki M, Yanase D, Yoshita M, Iwasa K, Mastunari I, Yamada M. A comparison of the diagnostic sensitivity of MRI, CBF-SPECT, FDG-PET and cerebrospinal fluid biomarkers for detecting Alzheimer's Disease in a memory clinic. Dement Geriatr Cogn Disord 30: 285–292.
- 298. Mountford CE, Stanwell P, Lin A, Ramadan S, Ross B. Neurospectroscopy: the past, present and future. *Chem Rev* 110: 3060–3086.

- 299. Mullins ME. MR spectroscopy: truly molecular imaging; past, present and future. Neuroimaging Clin N Am 16: 605–618, 2006.
- 300. Mumprecht V, Detmar M. Lymphangiogenesis and cancer metastasis. *J Cell Mol Med* 13: 1405–1416. 2009.
- 301. Muzzey D, van Oudenaarden A. Quantitative time-lapse fluorescence microscopy in single cells. *Annu Rev Cell Dev Biol* 25: 301–327, 2009.
- Narsinh KH, Cao F, Wu JC. Molecular imaging of human embryonic stem cells. Methods Mol Biol 515: 13–32, 2009.
- Naumov GN, Wilson SM, MacDonald IC, Schmidt EE, Morris VL, Groom AC, Hoffman RM, Chambers AF. Cellular expression of green fluorescent protein, coupled with high-resolution in vivo videomicroscopy, to monitor steps in tumor metastasis. J Cell Sci 112: 1835–1842, 1999.
- 304. Nielson CH, Kimura RH, Withofs N, Tran PT, Miao Z, Cochran JR, Cheng Z, Felsher D, Kjær A, Willmann JK, Gambhir SS. PET imaging of tumor neovascularization in a transgenic mouse model with a novel 64Cu-DOTA-Knottin peptide. *Cancer Res* 70: 9020–9030, 2010.
- Nieman K. Noninvasive stent imaging with MSCT. EuroIntervention 5 Suppl D: D107– 111, 2009.
- Niidome T, Yamagata M, Okamoto Y, Akiyama Y, Takahashi H, Kawano T, Katayama Y, Niidome Y. PEG-modified gold nanorods with a stealth character for in vivo applications. J Control Release 114: 343–347, 2006.
- 307. Nikolaus S, Wirrwar A, Antke C, Arkian S, Schramm N, Muller HW, Larisch R. Quantitation of dopamine transporter blockade by methylphenidate: first in vivo investigation using [123] FP-CIT and a dedicated small animal SPECT. Eur J Nucl Med Mol Imaging 32: 308–313, 2005.
- Nimmagadda S, Shields AF. The role of DNA synthesis imaging in cancer in the era of targeted therapeutics. Cancer Metastasis Rev 27: 575–587, 2008.
- Ntziachristos V, Bremer C, Weissleder R. Fluorescence imaging with near-infrared light: new technological advances that enable in vivo molecular imaging. Eur Radiol 13: 195–208, 2003.
- Ogawa M, Ishino S, Mukai T, Asano D, Teramoto N, Watabe H, Kudomi N, Shiomi M, Magata Y, Iida H, Saji H. (18)F-FDG accumulation in atherosclerotic plaques: immunohistochemical and PET imaging study. J Nucl Med 45: 1245–1250, 2004.
- 311. Ogawa M, Kosaka N, Choyke PL, Kobayashi H. In vivo molecular imaging of cancer with a quenching near-infrared fluorescent probe using conjugates of monoclonal antibodies and indocyanine green. *Cancer Res* 69: 1268–1272, 2009.
- 312. Ogawa M, Regino CA, Seidel J, Green MV, Xi W, Williams M, Kosaka N, Choyke PL, Kobayashi H. Dual-modality molecular imaging using antibodies labeled with activatable fluorescence and a radionuclide for specific and quantitative targeted cancer detection. *Bioconjug Chem* 20: 2177–2184, 2009.
- Oghabian MA, Farahbakhsh NM. Potential use of nanoparticle based contrast agents in MRI: a molecular imaging perspective. J Biomed Nanotechnol 6: 203–213, 2010.
- Okarvi SM. Peptide-based radiopharmaceuticals: future tools for diagnostic imaging of cancers and other diseases. Med Res Rev 24: 357–397, 2004.
- Okouchi M, Ekshyyan O, Maracine M, Aw TY. Neuronal apoptosis in neurodegeneration. Antioxid Redox Signal 9: 1059–1096, 2007.
- 317. Olafsen T, Wu AM. Antibody vectors for imaging. Semin Nucl Med 40: 167–181, 2010.
- Osborn EA, Jaffer FA. Advances in molecular imaging of atherosclerotic vascular disease. Curr Opin Cardiol 23: 620–628, 2008.
- 319. Pachiappan A, Thwin MM, Manikandan J, Gopalakrishnakone P. Glial inflammation and neurodegeneration induced by candoxin, a novel neurotoxin from Bungarus candidus venom: global gene expression analysis using microarray. *Toxicon* 46: 883–899, 2005.
- 320. Padera TP, Stoll BR, So PT, Jain RK. Conventional and high-speed intravital multiphoton laser scanning microscopy of microvasculature, lymphatics, and leukocyte-endothelial interactions. *Mol Imaging* 1: 9–15, 2002.
- Padhani AR, Husband JE. Dynamic contrast-enhanced MRI studies in oncology with an emphasis on quantification, validation and human studies. *Clin Radiol* 56: 607–620,

- Palm D, Lang K, Brandt B, Zaenker KS, Entschladen F. In vitro and in vivo imaging of cell migration: two interdepending methods to unravel metastasis formation. Semin Cancer Biol 15: 396–404, 2005.
- 323. Papadopoulos V, Baraldi M, Guilarte TR, Knudsen TB, Lacapere JJ, Lindemann P, Norenberg MD, Nutt D, Weizman A, Zhang MR, Gavish M. Translocator protein (18 kDa): new nomenclature for the peripheral-type benzodiazepine receptor based on its structure and molecular function. Trends Pharmacol Sci 27: 402–409, 2006.
- 324. Park DS, Obeidat A, Giovanni A, Greene LA. Cell cycle regulators in neuronal death evoked by excitotoxic stress: implications for neurodegeneration and its treatment. Neurobiol Aging 21: 771–781, 2000.
- Paulmurugan R, Gambhir SS. Combinatorial library screening for developing an improved split-firefly luciferase fragment-assisted complementation system for studying protein-protein interactions. *Anal Chem* 79: 2346–2353, 2007.
- Paulmurugan R, Gambhir SS. Firefly luciferase enzyme fragment complementation for imaging in cells and living animals. Anal Chem 77: 1295–1302, 2005.
- Paulmurugan R, Gambhir SS. Monitoring protein-protein interactions using split synthetic renilla luciferase protein-fragment-assisted complementation. Anal Chem 75: 1584–1589, 2003.
- Paulmurugan R, Gambhir SS. Novel fusion protein approach for efficient highthroughput screening of small molecule-mediating protein-protein interactions in cells and living animals. *Cancer Res* 65: 7413–7420, 2005.
- Paulmurugan R, Umezawa Y, Gambhir SS. Noninvasive imaging of protein-protein interactions in living subjects by using reporter protein complementation and reconstitution strategies. *Proc Natl Acad Sci USA* 99: 15608–15613, 2002.
- Payne CK. Imaging gene delivery with fluorescence microscopy. Nanomedicine 2: 847–860, 2007.
- 331. Pearson DA, Lister-James J, McBride WJ, Wilson DM, Martel LJ, Civitello ER, Taylor JE, Moyer BR, Dean RT. Somatostatin receptor-binding peptides labeled with technetium-99m: chemistry and initial biological studies. J Med Chem 39: 1361–1371, 1996.
- 332. Penuelas I, Mazzolini G, Boan JF, Sangro B, Marti-Climent J, Ruiz M, Ruiz J, Satyamurthy N, Qian C, Barrio JR, Phelps ME, Richter JA, Gambhir SS, Prieto J. Positron emission tomography imaging of adenoviral-mediated transgene expression in liver cancer patients. Gastroenterology 128: 1787–1795, 2005.
- Phelps ME. Inaugural article: positron emission tomography provides molecular imaging of biological processes. Proc Natl Acad Sci USA 97: 9226–9233, 2000.
- Pichler BJ, Judenhofer MS, Pfannenberg C. Multimodal imaging approaches: PET/CT and PET/MRI. Handb Exp Pharmacol 109–132, 2008.
- Pike VW. Positron-emitting radioligands for studies in vitro: probes for human psychopharmacology. J Psychopharmacol 7: 139–158, 1993.
- Pimlott SL. Radiotracer development in psychiatry. Nucl Med Commun 26: 183–188, 2005.
- Piwnica-Worms D, Luker KE. Imaging protein-protein interactions in whole cells and living animals. Ernst Schering Res Found Workshop 35–41, 2005.
- 338. Plathow C, Weber WA. Tumor cell metabolism imaging. J Nucl Med 49 Suppl 2: 43S-63S, 2008.
- Pomper MG, Lee JS. Small animal imaging in drug development. Curr Pharm Des 11: 3247–3272, 2005.
- Popovtzer R, Agrawal A, Kotov NA, Popovtzer A, Balter J, Carey TE, Kopelman R. Targeted gold nanoparticles enable molecular CT imaging of cancer. *Nano Lett* 8: 4593–4596, 2008.
- Prehn JH. Mitochondrial transmembrane potential and free radical production in excitotoxic neurodegeneration. *Naunyn-Schmiedebergs Arch Pharmacol* 357: 316–322, 1998.
- 342. Primak AN, Fletcher JG, Vrtiska TJ, Dzyubak OP, Lieske JC, Jackson ME, Williams JC Jr, McCollough CH. Noninvasive differentiation of uric acid versus non-uric acid kidney stones using dual-energy CT. Acad Radiol 14: 1441–1447, 2007.
- 343. Prokop M. General principles of MDCT. Eur J Radiol 45 Suppl 1: S4–S10, 2003.

- Provenzano PP, Eliceiri KW, Keely PJ. Multiphoton microscopy and fluorescence lifetime imaging microscopy (FLIM) to monitor metastasis and the tumor microenvironment. Clin Exp Metastasis 26: 357–370, 2009.
- 345. Pysz MA, Gambhir SS, Willmann JK. Molecular imaging: current status and emerging strategies. Clin Radiol 65: 500–516, 2010.
- 346. Qian X, Peng XH, Ansari DO, Yin-Goen Q, Chen GZ, Shin DM, Yang L, Young AN, Wang MD, Nie S. In vivo tumor targeting and spectroscopic detection with surface-enhanced Raman nanoparticle tags. Nat Biotechnol 26: 83–90, 2008.
- Ray P, Bauer E, Iyer M, Barrio JR, Satyamurthy N, Phelps ME, Herschman HR, Gambhir SS. Monitoring gene therapy with reporter gene imaging. Semin Nucl Med 31: 312–320. 2001.
- Raymond SB, Skoch J, Hills ID, Nesterov EE, Swager TM, Bacskai BJ. Smart optical probes for near-infrared fluorescence imaging of Alzheimer's disease pathology. Eur J Nucl Med Mol Imaging 35 Suppl 1: S93–S98, 2008.
- 349. Ren G, Zhang R, Liu Z, Webster JM, Miao Z, Gambhir SS, Syud FA, Cheng Z. A 2-helix small protein labeled with 68Ga for PET imaging of HER2 expression. J Nucl Med 50: 1492–1499, 2009.
- Reshef A, Shirvan A, Akselrod-Ballin A, Wall A, Ziv I. Small-molecule biomarkers for clinical PET imaging of apoptosis. J Nucl Med 51: 837–840, 2010.
- 351. Reuning U, Sperl S, Kopitz C, Kessler H, Kruger A, Schmitt M, Magdolen V. Urokinase-type plasminogen activator (uPA) and its receptor (uPAR): development of antagonists of uPA/uPAR interaction and their effects in vitro and in vivo. Curr Pharm Des 9: 1529–1543, 2003.
- Ribi W, Senden TJ, Sakellariou A, Limaye A, Zhang S. Imaging honey bee brain anatomy with micro-X-ray-computed tomography. J Neurosci Methods 171: 93–97, 2008.
- 353. Rice BW, Cable MD, Nelson MB. In vivo imaging of light-emitting probes. *J Biomed Opt* 6: 432–440, 2001.
- Rini JN, Palestro CJ. Imaging of infection and inflammation with <sup>18</sup>F-FDG-labeled leukocytes. QJ Nucl Med Mol Imaging 50: 143–146, 2006.
- 355. Rizi RR. A new direction for polarized carbon-13 MRI. *Proc Natl Acad Sci USA* 106: 5453–5454, 2009.
- Robertson R, Germanos MS, Li C, Mitchell GS, Cherry SR, Silva MD. Optical imaging of Cerenkov light generation from positron-emitting radiotracers. *Phys Med Biol* 54: N355–N365, 2009.
- 357. Rodriguez-Porcel M, Brinton TJ, Chen IY, Gheysens O, Lyons J, Ikeno F, Willmann JK, Wu L, Wu JC, Yeung AC, Yock P, Gambhir SS. Reporter gene imaging following percutaneous delivery in swine moving toward clinical applications. J Am Coll Cardiol 51: 595–597, 2008.
- 358. Rowland DJ, Lewis JS, Welch MJ. Molecular imaging: the application of small animal positron emission tomography. *J Cell Biochem Suppl* 39: 110–115, 2002.
- 359. Rudd JH, Warburton EA, Fryer TD, Jones HA, Clark JC, Antoun N, Johnstrom P, Davenport AP, Kirkpatrick PJ, Arch BN, Pickard JD, Weissberg PL. Imaging atherosclerotic plaque inflammation with [18F]-fluorodeoxyglucose positron emission tomography. Circulation 105: 2708–2711, 2002.
- Sadikot RT, Blackwell TS. Bioluminescence imaging. Proc Am Thorac Soc 2: 537–540, 511–532. 2005.
- Sahai E, Wyckoff J, Philippar U, Segall JE, Gertler F, Condeelis J. Simultaneous imaging of GFP, CFP and collagen in tumors in vivo using multiphoton microscopy. BMC Biotechnol 5: 14. 2005.
- Sajja HK, East MP, Mao H, Wang YA, Nie S, Yang L. Development of multifunctional nanoparticles for targeted drug delivery and noninvasive imaging of therapeutic effect. Curr Drug Discov Technol 6: 43–51, 2009.
- 363. Sandison JD. The transparent chamber of the rabbit's ear giving a complete description of improved techniques of construction and introduction and general account of growth and behavior of living cells and tissues seen with the microscope. Am J Anat 41: 447–472, 1928.
- Saraste A, Nekolla SG, Schwaiger M. Cardiovascular molecular imaging: an overview. Cardiovasc Res 83: 643–652, 2009.

- Sato AK, Viswanathan M, Kent RB, Wood CR. Therapeutic peptides: technological advances driving peptides into development. Curr Opin Biotechnol 17: 638

  –642, 2006.
- 366. Schaefer PW, Copen WA, Lev MH, Gonzalez RG. Diffusion-weighted imaging in acute stroke. Neuroimaging Clin N Am 15: 503–530, 2005.
- Scheer KE, Winkel KZ. The use of a scintillation camera in clinical diagnostic studies. *Minerya Nucl* 9: 386–390. 1965.
- 368. Schipper ML, Nakayama-Ratchford N, Davis CR, Kam NW, Chu P, Liu Z, Sun X, Dai H, Gambhir SS. A pilot toxicology study of single-walled carbon nanotubes in a small sample of mice. Nat Nanotechnol 3: 216–221, 2008.
- 369. Schmidt MM, Wittrup KD. A modeling analysis of the effects of molecular size and binding affinity on tumor targeting. *Mol Cancer Ther* 8: 2861–2871, 2009.
- Schmolze DB, Standley C, Fogarty KE, Fischer AH. Advances in microscopy techniques. Arch Pathol Lab Med 135: 255–263.
- Schottelius M, Wester HJ. Molecular imaging targeting peptide receptors. Methods 48: 161–177, 2009.
- 372. Schuhmacher J, Zhang H, Doll J, Macke HR, Matys R, Hauser H, Henze M, Haberkorn U, Eisenhut M. GRP receptor-targeted PET of a rat pancreas carcinoma xenograft in nude mice with a 68Ga-labeled bombesin(6–14) analog. J Nucl Med 46: 691–699, 2005
- 373. Seddon BM, Workman P. The role of functional and molecular imaging in cancer drug discovery and development. *Br J Radiol* 76: S128–S138, 2003.
- Seliger HH, McElroy WD. The colors of firefly bioluminescence: enzyme configuration and species specificity. Proc Natl Acad Sci USA 52: 75–81, 1964.
- Senaratne R, Milne AM, MacQueen GM, Hall GB. Increased choline-containing compounds in the orbitofrontal cortex and hippocampus in euthymic patients with bipolar disorder: a proton magnetic resonance spectroscopy study. *Psychiatry Res* 172: 205– 209, 2009.
- Senft C, Hattingen E, Pilatus U, Franz K, Schanzer A, Lanfermann H, Seifert V, Gasser T. Diagnostic value of proton magnetic resonance spectroscopy in the noninvasive grading of solid gliomas: comparison of maximum and mean choline values. *Neurosur*gery 65: 908–913, 2009.
- Serganova I, Mayer-Kukuck P, Huang R, Blasberg R. Molecular imaging: reporter gene imaging. Handb Exp Pharmacol 167–223, 2008.
- Serkova NJ, Renner B, Larsen BA, Stoldt CR, Hasebroock KM, Bradshaw-Pierce EL, Holers VM, Thurman JM. Renal inflammation: targeted iron oxide nanoparticles for molecular MR imaging in mice. *Radiology* 255: 517–526, 2010.
- 379. Seton-Rogers S. Cancer code cracked? Nat Rev Cancer 10: 80, 2010.
- Shaner NC, Steinbach PA, Tsien RY. A guide to choosing fluorescent proteins. Nat Methods 2: 905–909, 2005.
- Sherry AD, Woods M. Chemical exchange saturation transfer contrast agents for magnetic resonance imaging. Annu Rev Biomed Eng 10: 391–411, 2008.
- Sheth RA, Josephson L, Mahmood U. Evaluation and clinically relevant applications of a fluorescent imaging analog to fluorodeoxyglucose positron emission tomography. J Biomed Opt 14: 064014, 2009.
- Shim MG, Song LM, Marcon NE, Wilson BC. In vivo near-infrared Raman spectroscopy: demonstration of feasibility during clinical gastrointestinal endoscopy. *Pho*tochem Photobiol 72: 146–150, 2000.
- 384. Shim MG, Wilson BC. Development of an in vivo Raman spectroscopic system for diagnostic applications. J Raman Spectrosc 28: 131–142, 1997.
- Shimomura O, Johnson FH, Saiga Y. Extraction, purification and properties of aequorin, a bioluminescent protein from the luminous hydromedusan, Aequorea. J Cell Comp Physiol 59: 223–239, 1962.
- Shirani J, Dilsizian V. Molecular imaging in heart failure. Curr Opin Biotechnol 18: 65–72, 2007.
- 387. Siegle GJ, Thompson W, Carter CS, Steinhauer SR, Thase ME. Increased amygdala and decreased dorsolateral prefrontal BOLD responses in unipolar depression: related and independent features. *Biol Psychiatry* 61: 198–209, 2007.

- 388. Siphanto RI, Kolkman RG, Huisjes A, Pilatou MC, de Mul FF, Steenbergen W, van Adrichem LN. Imaging of small vessels using photoacoustics: an in vivo study. Lasers Surg Med 35: 354–362, 2004.
- 389. Sipkins DA, Cheresh DA, Kazemi MR, Nevin LM, Bednarski MD, Li KC. Detection of tumor angiogenesis in vivo by alphaVbeta3-targeted magnetic resonance imaging. Nat Med 4: 623–626, 1998.
- Sirk SJ, Olafsen T, Barat B, Bauer KB, Wu AM. Site-specific, thiol-mediated conjugation of fluorescent probes to cysteine-modified diabodies targeting CD20 or HER2. *Bioconjug Chem* 19: 2527–2534, 2008.
- Sirsi S, Borden M. Microbubble compositions, properties and biomedical applications. Bubble Sci Eng Technol 1: 3–17, 2009.
- Smith BR, Cheng Z, De A, Koh AL, Sinclair R, Gambhir SS. Real-time intravital imaging of RGD-quantum dot binding to luminal endothelium in mouse tumor neovasculature. Nano Lett 8: 2599–2606, 2008.
- 393. So MK, Xu C, Loening AM, Gambhir SS, Rao J. Self-illuminating quantum dot conjugates for in vivo imaging. *Nat Biotechnol* 24: 339–343, 2006.
- 394. Song KH, Kim C, Cobley CM, Xia Y, Wang LV. Near-infrared gold nanocages as a new class of tracers for photoacoustic sentinel lymph node mapping on a rat model. *Nano Lett* 9: 183–188. 2009.
- 395. Sosnovik DE, Nahrendorf M, Panizzi P, Matsui T, Aikawa E, Dai G, Li L, Reynolds F, Dorn GW, 2nd Weissleder R, Josephson L, Rosenzweig A. Molecular MRI detects low levels of cardiomyocyte apoptosis in a transgenic model of chronic heart failure. Circ Cardiovasc Imaging 2: 468–475, 2009.
- Sossi V, Ruth TJ. Micropet imaging: in vivo biochemistry in small animals. J Neural Transm 112: 319–330, 2005.
- Stein PD, Hull RD. Multidetector computed tomography for the diagnosis of acute pulmonary embolism. Curr Opin Pulm Med 13: 384–388, 2007.
- Stephen RM, Gillies RJ. Promise and progress for functional and molecular imaging of response to targeted therapies. *Pharm Res* 24: 1172–1185, 2007.
- 399. Stephens DJ, Allan VJ. Light microscopy techniques for live cell imaging. Science 300:
- 400. Stoll G, Bendszus M. Inflammation and atherosclerosis: novel insights into plaque formation and destabilization. Stroke 37: 1923–1932, 2006.
- 401. Stoll G, Bendszus M. New approaches to neuroimaging of central nervous system inflammation. *Curr Opin Neurol* 23: 282–286, 2010.
- Sumen C, Mempel TR, Mazo IB, von Andrian UH. Intravital microscopy: visualizing immunity in context. *Immunity* 21: 315–329, 2004.
- 402a.Sun C, Veiseh O, Gunn J, Fang C, Hansen S, Lec D, Sze R, Ellenbogen RG, Olson J, Zhang M. In vivo MRI detection of gliomas by chlorotoxin-conjugated superparamagnetic nanoprobes. Small 4: 372–379, 2008.
- Sun Z, Ng KH. Multislice CT angiography in cardiac imaging. Part II: clinical applications in coronary artery disease. Singapore Med J 51: 282–289, 2010.
- 404. Sundaresan G, Yazaki PJ, Shively JE, Finn RD, Larson SM, Raubitschek AA, Williams LE, Chatziioannou AF, Gambhir SS, Wu AM. <sup>124</sup>I-labeled engineered anti-CEA minibodies and diabodies allow high-contrast, antigen-specific small-animal PET imaging of xenografts in athymic mice. *J Nucl Med* 44: 1962–1969, 2003.
- Tada H, Higuchi H, Wanatabe TM, Ohuchi N. In vivo real-time tracking of single quantum dots conjugated with monoclonal anti-HER2 antibody in tumors of mice. Cancer Res 67: 1138–1144, 2007.
- 406. Tagliabue L, Majoli C, Pajoro U, Musarra M, Di Leo C, Del Sole A, Bestetti A, Tarolo GL. Labelled leukocytes for diagnosis of infectious diseases. Our experience in labelling and clinical usefulness. *Minerva Med* 91: 267–274, 2000.
- 407. Tam JM, Upadhyay R, Pittet MJ, Weissleder R, Mahmood U. Improved in vivo wholeanimal detection limits of green fluorescent protein-expressing tumor lines by spectral fluorescence imaging. Mol Imaging 6: 269–276, 2007.
- 408. Tan CH, Wang J, Kundra V. Diffusion weighted imaging in prostate cancer. Eur Radiol 21: 593–603, 2011.

- 409. Tannous BA, Kim DE, Fernandez JL, Weissleder R, Breakefield XO. Codon-optimized Gaussia luciferase cDNA for mammalian gene expression in culture and in vivo. Mol Ther. 11: 435–443. 2005.
- Tavitian B. In vivo imaging with oligonucleotides for diagnosis and drug development. Gut 52 Suppl 4: iv40-iv47, 2003.
- 411. Tavitian B, Duconge F, Boisgard R, Dolle F. In vivo imaging of oligonucleotidic aptamers. *Methods Mol Biol* 535: 241–259, 2009.
- 412. Tearney GJ, Waxman S, Shishkov M, Vakoc BJ, Suter MJ, Freilich MI, Desjardins AE, Oh WY, Bartlett LA, Rosenberg M, Bouma BE. Three-dimensional coronary artery microscopy by intracoronary optical frequency domain imaging. *Cardiovasc Imaging* 1: 752–761, 2008.
- Theron J, Tyler JL. Takayasu's arteritis of the aortic arch: endovascular treatment and correlation with positron emission tomography. Am J Neuroradiol 8: 621–626, 1987.
- 414. Thibon A, Pierre VC. Principles of responsive lanthanide-based luminescent probes for cellular imaging. *Anal Bioanal Chem* 394: 107–120, 2009.
- Thiel KW, Giangrande PH. Therapeutic applications of DNA and RNA aptamers. Oligonucleotides 19: 209–222, 2009.
- Thorek DL, Chen AK, Czupryna J, Tsourkas A. Superparamagnetic iron oxide nanoparticle probes for molecular imaging. Ann Biomed Eng 34: 23–38, 2006.
- Tong L, Cheng JX. Gold nanorod-mediated photothermolysis induces apoptosis of macrophages via damage of mitochondria. Nanomed 4: 265–276, 2009.
- 418. Torchilin VP. Handbook of Targeted Delivery of Imaging Agents. Boca Raton, FL: CRC, 1995
- Troyer JK, Beckett ML, Wright GL Jr. Location of prostate-specific membrane antigen in the LNCaP prostate carcinoma cell line. *Prostate* 30: 232–242, 1997.
- 420. Tseng CL, Shih IL, Stobinski L, Lin FH. Gadolinium hexanedione nanoparticles for stem cell labeling and tracking via magnetic resonance imaging. *Biomaterials* 31: 5427–5435, 2010.
- 421. Turkbey B, Kobayashi H, Ogawa M, Bernardo M, Choyke PL. Imaging of tumor angiogenesis: functional or targeted? *Am J Roentgenol* 193: 304–313, 2009.
- 422. Ullrich RT, Kracht LW, Jacobs AH. Neuroimaging in patients with gliomas. Semin Neurol 28: 484–494, 2008.
- Vaccarili M, Lococo A, Fabiani F, Staffilano A. Clinical diagnostic application of 111In-DTPA-octreotide scintigraphy in small cell lung cancer. *Tumori* 86: 224–228, 2000.
- Valotassiou V, Wozniak G, Sifakis N, Demakopoulos N, Georgoulias P. Radiopharmaceuticals in neurological and psychiatric disorders. *Curr Clin Pharmacol* 3: 99–107, 2008.
- 425. Van De Ven SMWY, Elias SG, Chan CT, Miao Z, Cheng Z, De A, Gambhir SS. Optical imaging with HER2-targeted affibody molecules can monitor Hsp90 treatment response in a xenograft mouse model. *Clin Cancer Res.* In Press.
- 427. Van de Wiele C, Dumont F, Vanden Broecke R, Oosterlinck W, Cocquyt V, Serreyn R, Peers S, Thornback J, Slegers G, Dierckx RA. Technetium-99m RP527, a GRP analogue for visualisation of GRP receptor-expressing malignancies: a feasibility study. Eur J Nucl Med 27: 1694–1699, 2000.
- 428. Van de Wiele C, Phonteyne P, Pauwels P, Goethals I, Van den Broecke R, Cocquyt V, Dierckx RA. Gastrin-releasing peptide receptor imaging in human breast carcinoma versus immunohistochemistry. J Nucl Med 49: 260–264, 2008.
- 429. Van den Hoff J. Principles of quantitative positron emission tomography. *Amino Acids* 29: 341–353, 2005.
- Van der Have F, Vastenhouw B, Ramakers RM, Branderhorst W, Krah JO, Ji C, Staelens SG, Beekman FJ. U-SPECT-II: an ultra-high-resolution device for molecular small-animal imaging. J Nucl Med 50: 599–605, 2009.
- 431. Van der Meel R, Gallagher WM, Oliveira S, O'Connor AE, Schiffelers RM, Byrne AT. Recent advances in molecular imaging biomarkers in cancer: application of bench to bedside technologies. Drug Discov Today 2009.
- 432. Van Dongen GA, Visser GW, Lub-de Hooge MN, de Vries EG, Perk LR. Immuno-PET: a navigator in monoclonal antibody development and applications. *Oncologist* 12: 1379–1389, 2007.

- 433. Van Haren RM, Fitzgerald TL. Intraoperative hand held gamma probe detection of a recurrent nonfunctional neuroendocrine tumor. JOP 9: 704–707, 2008.
- Veiseh O, Gunn JW, Kievit FM, Sun C, Fang C, Lee JS, Zhang M. Inhibition of tumorcell invasion with chlorotoxin-bound superparamagnetic nanoparticles. Small 5: 256 – 264. 2009.
- Veiseh O, Sun C, Gunn J, Kohler N, Gabikian P, Lee D, Bhattarai N, Ellenbogen R, Sze R, Hallahan A, Olson J, Zhang M. Optical and MRI multifunctional nanoprobe for targeting gliomas. *Nano Lett* 5: 1003–1008, 2005.
- 436. Venisnik KM, Olafsen T, Loening AM, Iyer M, Gambhir SS, Wu AM. Bifunctional antibody-Renilla luciferase fusion protein for in vivo optical detection of tumors. Protein Eng Des Sel 19: 453–460, 2006.
- 437. Venneti S, Lopresti BJ, Wang G, Hamilton RL, Mathis CA, Klunk WE, Apte UM, Wiley CA. PK11195 labels activated microglia in Alzheimer's disease and in vivo in a mouse model using PET. Neurobiol Aging 30: 1217–1226, 2009.
- 438. Venneti S, Lopresti BJ, Wiley CA. The peripheral benzodiazepine receptor (Translocator protein 18kDa) in microglia: from pathology to imaging. *Prog Neurobiol* 80: 308–322, 2006.
- 439. Versijpt JJ, Dumont F, Van Laere KJ, Decoo D, Santens P, Audenaert K, Achten E, Slegers G, Dierckx RA, Korf J. Assessment of neuroinflammation and microglial activation in Alzheimer's disease with radiolabelled PK11195 and single photon emission computed tomography. A pilot study. Eur Neurol 50: 39–47, 2003.
- Villalobos V, Naik S, Piwnica-Worms D. Detection of protein-protein interactions in live cells and animals with split firefly luciferase protein fragment complementation. Methods Mol Biol 439: 339–352, 2008.
- 441. Vlieghe P, Lisowski V, Martinez J, Khrestchatisky M. Synthetic therapeutic peptides: science and market. *Drug Discov Today* 15: 40–56.
- 442. Vlychou M, Athanasou NA. Radiological and pathological diagnosis of paediatric bone tumours and tumour-like lesions. *Pathology* 40: 196–216, 2008.
- 443. Von Andrian UH. Intravital microscopy of the peripheral lymph node microcirculation in mice. *Microcirculation* 3: 287–300, 1996.
- 444. Von Maltzahn G, Park JH, Agrawal A, Bandaru NK, Das SK, Sailor MJ, Bhatia SN. Computationally guided photothermal tumor therapy using long-circulating gold nanorod antennas. *Cancer Res* 69: 3892–3900, 2009.
- 445. Wachsmann-Hogiu S, Weeks T, Huser T. Chemical analysis in vivo and in vitro by Raman spectroscopy–from single cells to humans. Curr Opin Biotechnol 20: 63–73, 2009.
- 446. Walling MA, Novak JA, Shepard JR. Quantum dots for live cell and in vivo imaging. *Int J Mol Sci* 10: 441–491, 2009.
- 447. Wallis de Vries BM, Hillebrands JL, van Dam GM, Tio RA, de Jong JS, Slart RH, Zeebregts CJ. Images in cardiovascular medicine. Multispectral near-infrared fluorescence molecular imaging of matrix metalloproteinases in a human carotid plaque using a matrix-degrading metalloproteinase-sensitive activatable fluorescent probe. Circulation 119: e534–e536, 2009.
- 448. Wallis de Vries BM, van Dam GM, Tio RA, Hillebrands JL, Slart RH, Zeebregts CJ. Current imaging modalities to visualize vulnerability within the atherosclerotic carotid plaque. J Vasc Surg 48: 1620–1629, 2008.
- 449. Wang K, Shen B, Huang T, Sun X, Li W, Jin G, Li L, Bu L, Li R, Wang D, Chen X. MR reporter gene imaging of endostatin expression and therapy. *Mol Imaging Biol* 2009.
- 450. Wang X, Yang L, Chen ZG, Shin DM. Application of nanotechnology in cancer therapy and imaging. *Cancer J Clin* 58: 97–110, 2008.
- 451. Weissleder R. Molecular imaging in cancer. Science 312: 1168-1171, 2006.
- 452. Weissleder R, Pittet MJ. Imaging in the era of molecular oncology. *Nature* 452: 580 589, 2008.
- Welsh JP, Patel KG, Manthiram K, Swartz JR. Multiply mutated Gaussia luciferases provide prolonged and intense bioluminescence. *Biochem Biophys Res Commun* 389: 563–568. 2009.
- Werle M, Bernkop-Schnurch A. Strategies to improve plasma half life time of peptide and protein drugs. Amino Acids 30: 351–367, 2006.

- 455. Wernick MN, Aarsvold JN. Emission Tomography: The Fundamentals of PET and SPECT. Orlando, FL: Academic, 2004.
- Willets KA. Surface-enhanced Raman scattering (SERS) for probing internal cellular structure and dynamics. Anal Bioanal Chem 394: 85–94, 2009.
- 457. Williams LE. Anniversary paper: nuclear medicine: fifty years and still counting. *Med Phys* 35: 3020–3029, 2008.
- 458. Willmann JK, Chen K, Wang H, Paulmurugan R, Rollins M, Cai W, Wang DS, Chen IY, Gheysens O, Rodriguez-Porcel M, Chen X, Gambhir SS. Monitoring of the biological response to murine hindlimb ischemia with <sup>64</sup>Cu-labeled vascular endothelial growth factor-121 positron emission tomography. *Circulation* 117: 915–922, 2008.
- 459. Willmann JK, Cheng Z, Davis C, Lutz AM, Schipper ML, Nielsen CH, Gambhir SS. Targeted microbubbles for imaging tumor angiogenesis: assessment of whole-body biodistribution with dynamic micro-PET in mice. *Radiology* 249: 212–219, 2008.
- Willmann JK, Lutz AM, Paulmurugan R, Patel MR, Chu P, Rosenberg J, Gambhir SS.
   Dual-targeted contrast agent for US assessment of tumor angiogenesis in vivo. Radiology 248: 936–944, 2008.
- 461. Willmann JK, Paulmurugan R, Chen K, Gheysens O, Rodriguez-Porcel M, Lutz AM, Chen IY, Chen X, Gambhir SS. US imaging of tumor angiogenesis with microbubbles targeted to vascular endothelial growth factor receptor type 2 in mice. *Radiology* 246: 508–518. 2008.
- 462. Willmann JK, van Bruggen N, Dinkelborg LM, Gambhir SS. Molecular imaging in drug development. *Nat Rev Drug Discov* 7: 591–607, 2008.
- 463. Winnard PT Jr, Kluth JB, Raman V. Noninvasive optical tracking of red fluorescent protein-expressing cancer cells in a model of metastatic breast cancer. *Neoplasia* 8: 796–806, 2006.
- 464. Wong DF, Pomper MG. Predicting the success of a radiopharmaceutical for in vivo imaging of central nervous system neuroreceptor systems. Mol Imaging Biol 5: 350– 362, 2003.
- 465. Woodbury EJ, Ng WK. Ruby laser operation in the near IR. Proc IRE 50: 2367, 1962.
- Wu AM. Antibodies and antimatter: the resurgence of immuno-PET. J Nucl Med 50: 2–5. 2009.
- Wu JC, Bengel FM, Gambhir SS. Cardiovascular molecular imaging. Radiology 244: 337–355, 2007.
- 468. Wu X, Liu H, Liu J, Haley KN, Treadway JA, Larson JP, Ge N, Peale F, Bruchez MP. Immunofluorescent labeling of cancer marker Her2 and other cellular targets with semiconductor quantum dots. Nat Biotechnol 21: 41–46, 2003.
- 469. Xia Y. Nanomaterials at work in biomedical research. Nat Mater 7: 758-760, 2008.
- 470. Xiao Y, Gao X, Taratula O, Treado S, Urbas A, Holbrook RD, Cavicchi RE, Avedisian CT, Mitra S, Savla R, Wagner PD, Srivastava S, He H. Anti-HER2 IgY antibody-functionalized single-walled carbon nanotubes for detection and selective destruction of breast cancer cells. BMC Cancer 9: 351, 2009.

- 471. Yaghoubi S, Barrio JR, Dahlbom M, Iyer M, Namavari M, Satyamurthy N, Goldman R, Herschman HR, Phelps ME, Gambhir SS. Human pharmacokinetic and dosimetry studies of [(18)F]FHBG: a reporter probe for imaging herpes simplex virus type-I thymidine kinase reporter gene expression. J Nucl Med 42: 1225–1234, 2001.
- 472. Yaghoubi SS, Jensen MC, Satyamurthy N, Budhiraja S, Paik D, Czernin J, Gambhir SS. Noninvasive detection of therapeutic cytolytic T cells with <sup>18</sup>F-FHBG PET in a patient with glioma. *Nat Clin Pract Oncol* 6: 53–58, 2008.
- 473. Yaghoubi SS, Jensen MC, Satyamurthy N, Budhiraja S, Paik D, Czernin J, Gambhir SS. Noninvasive detection of therapeutic cytolytic T cells with <sup>18</sup>F-FHBG PET in a patient with glioma. *Nat Clin Pract Oncol* 6: 53–58, 2009.
- 474. Yang L, Mao H, Cao Z, Wang YA, Peng X, Wang X, Sajja HK, Wang L, Duan H, Ni C, Staley CA, Wood WC, Gao X, Nie S. Molecular imaging of pancreatic cancer in an animal model using targeted multifunctional nanoparticles. *Gastroenterology* 136: 1514–1525, 2009.
- Yang M, Jiang P, Hoffman RM. Whole-body subcellular multicolor imaging of tumorhost interaction and drug response in real time. Cancer Res 67: 5195–5200, 2007.
- Yano Y, Matsuzaki K. Tag-probe labeling methods for live-cell imaging of membrane proteins. Biochim Biophys Acta 1788: 2124–2131, 2009.
- 477. Younes CK, Boisgard R, Tavitian B. Labelled oligonucleotides as radiopharmaceuticals: pitfalls, problems and perspectives. *Curr Pharm Des* 8: 1451–1466, 2002.
- 478. Yuan F, Salehi HA, Boucher Y, Vasthare US, Tuma RF, Jain RK. Vascular permeability and microcirculation of gliomas and mammary carcinomas transplanted in rat and mouse cranial windows. *Cancer Res* 54: 4564–4568, 1994.
- 479. Zavaleta C, de la Zerda A, Liu Z, Keren S, Cheng Z, Schipper M, Chen X, Dai H, Gambhir SS. Noninvasive Raman spectroscopy in living mice for evaluation of tumor targeting with carbon nanotubes. *Nano Lett* 8: 2800–2805, 2008.
- 480. Zavaleta CL, Kircher MF, Gambhir SS. Raman's "effect" on molecular imaging. J Nucl Med. In press.
- Zhang J, Yan CH, Chui CK, Ong SH. Accurate measurement of bone mineral density using clinical CT imaging with single energy beam spectral intensity correction. *IEEE Trans Med Imaging* 29: 1382–1389, 2010.
- Zhang S, Merritt M, Woessner DE, Lenkinski RE, Sherry AD. PARACEST agents: modulating MRI contrast via water proton exchange. Acc Chem Res 36: 783–790, 2003.
- 483. Zhao H, Cui K, Muschenborn A, Wong STC. Progress of engineered antibody-targeted molecular imaging for solid tumors. *Mol Med Rep* 1: 131–134, 2008.
- 484. Ziemus B, Baumann O, Luerding R, Schlosser R, Schuierer G, Bogdahn U, Greenlee MW. Impaired working-memory after cerebellar infarcts paralleled by changes in BOLD signal of a cortico-cerebellar circuit. Neuropsychologia 45: 2016–2024, 2007.
- Zwanziger D, Khan IU, Neundorf I, Sieger S, Lehmann L, Friebe M, Dinkelborg L, Beck-Sickinger AG. Novel chemically modified analogues of neuropeptide Y for tumor targeting. Bioconjug Chem 19: 1430–1438, 2008.